IN SITU CHARACTERIZATION OF ADSORBED SPECIES ON METHANOL SYNTHESIS CATALYSTS BY FT-IR SPECTROSCOPY

AMES LAB., IA

JUN 1984

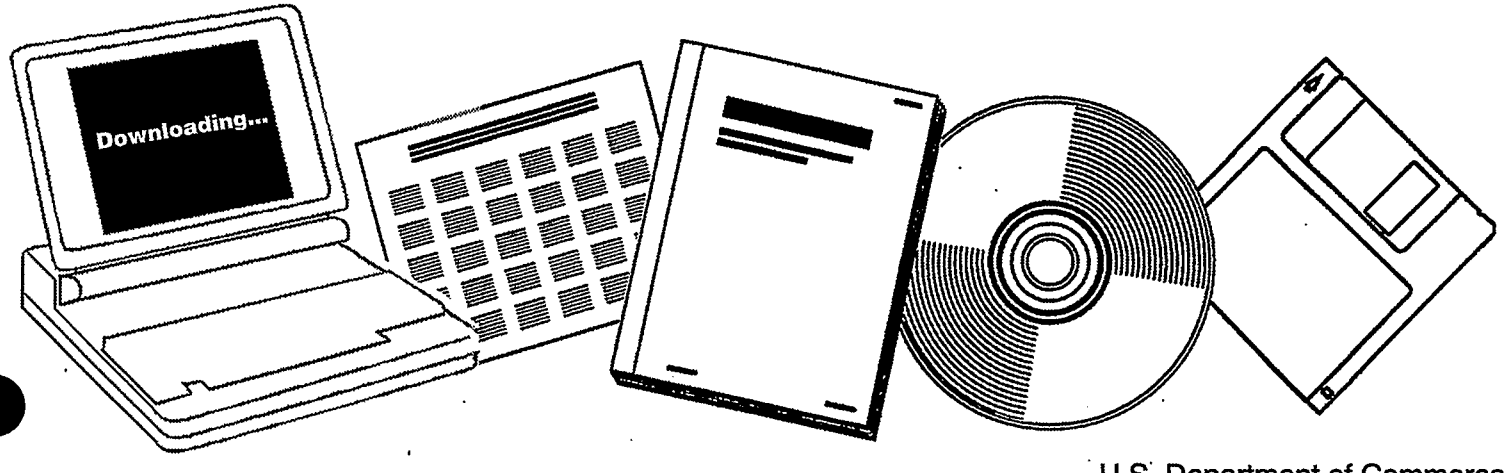

One Source. One Search. One Solution.

NTIS

Providing Permanent, Easy Access to U.S. Government Information

National Technical Information Service is the nation's largest repository and disseminator of government-initiated scientific, technical, engineering, and related business information. The NTIS collection includes almost 3,000,000 information products in a variety of formats: electronic download, online access, CD-ROM, magnetic tape, diskette, multimedia, microfiche and paper.

Search the NTIS Database from 1990 forward

NTIS has upgraded its bibliographic database system and has made all entries since 1990 searchable on **www.ntis.gov.** You now have access to information on more than 600,000 government research information products from this web site.

Link to Full Text Documents at Government Web Sites

Because many Government agencies have their most recent reports available on their own web site, we have added links directly to these reports. When available, you will see a link on the right side of the bibliographic screen.

Download Publications (1997 - Present)

NTIS can now provides the full text of reports as downloadable PDF files. This means that when an agency stops maintaining a report on the web, NTIS will offer a downloadable version. There is a nominal fee for each download for most publications.

For more information visit our website:

www.ntis.gov

U.S. DEPARTMENT OF COMMERCE
Technology Administration
National Technical Information Service
Springfield, VA 22161

IS-T 1121

IS-T--1121

DE84 014105

In situ characterization of adsorbed species on methanol synthesis catalysts by FT-IR spectroscopy

by

James Francis Edwards

PhD Thesis submitted to Iowa State University

Ames Laboratory, U.S. DOE
Iowa State University
Ames, Iowa 50011

Date Transmitted: June 1984

PREPARED FOR THE U. S. DEPARTMENT OF ENERGY
UNDER CONTRACT NO. W-7405-Eng-82.

DISCLAIMER

Printed in the United States of America

Available from
National Technical Information Service
U.S. Department of Commerce
5265 Port Royal Road
Springfield, VA 22161

In situ characterization of adsorbed species on methanol synthesis catalysts by FT-IR spectroscopy[1]

by

James Francis Edwards

Under the Supervision of Glenn L. Schrader
From the Department of Chemical Engineering
Iowa State University

Transmission infrared spectroscopy was used to characterize adsorbed species on methanol synthesis catalysts during reaction conditions. A copper carbonyl, bidentate formate, and methoxy species were identified as stable surface groups. An adsorbed formaldehyde species was unstable at the reaction temperature, but could be observed on the catalyst surface at the beginning of the reaction. Surface species were very similar for feed mixtures of 1) carbon monoxide and hydrogen, 2) carbon monoxide, carbon dioxide, and hydrogen, and 3) formic acid and hydrogen. The role of copper in methanol synthesis catalysts was to increase the adsorption of carbon monoxide to form a linear carbonyl species. This carbonyl promoted the hydrogenation of formate groups. The formate species was adsorbed on a zinc site (Zn_β) different from the zinc site (Zn_γ) on which formaldehyde and methoxy groups were adsorbed. The rate-determining step in methanol synthesis was determined to be the reaction of hydrogen from a hydroxyl species adsorbed on another zinc site (Zn_α) with a methoxy group to yield methanol. It was established that at the experimental conditions used in this study, the methanol synthesis reaction was

---

[1]DOE Report IS-T-1121. This work was performed under Contract No. W-7405-Eng-82 with the U.S. Department of Energy.

far from equilibrium while the water-gas shift reaction was near equilibrium.

In situ characterization of adsorbed species on methanol synthesis catalysts by FT-IR spectroscopy

by

James Francis Edwards

A Dissertation Submitted to the
Graduate Faculty in Partial Fulfillment of the
Requirements for the Degree of
DOCTOR OF PHILOSOPHY

Major: Chemical Engineering

Approved:

_____
In Charge of Major Work

_____
For the Major Department

_____
For the Graduate College

Iowa State University
Ames, Iowa

1984

TABLE OF CONTENTS

LIST OF TABLES

LIST OF FIGURES

NOMENCLATURE

a, b, c	lattice parameters, Å
c_p	heat capacity
$d_{h,k,l}$	interplanar distance, Å
E	energy, eV
f	fugacity
ΔG	free energy of formation
ΔH	heat of formation
H	dead-space pressure, mmHg
K	equilibrium constant
M	molecular weight; modulus of rupture
P	pressure
r	radius; reaction rate
R	ideal gas constant
S	surface area
t	thickness
T	temperature, °K
V	volume, cm^3
W	weight, g
y	mole fraction
α, β, γ	lattice angles, degrees
α	perfect gas law correction factor
γ	fugacity coefficient
θ	diffraction angle, degrees; contact angle condensate
λ	radiation wavelength, Å

ρ	density
σ	surface tension
ν	vibrational frequency, cm^{-1}
ϕ	correction term in XPS, eV

INTRODUCTION

One of the great challenges facing the chemical industry as the 21st century approaches will be making the adjustments in fuel and raw material sources as petroleum and natural gas reserves diminish. Coal is expected to become a major source for chemical feedstocks in this country because of its availability and abundance, but economic considerations have thus far restricted the development of coal-based industries for organic synthesis. There are two major approaches for coal utilization: 1) coal gasification to produce light hydrocarbons, carbon oxides, hydrogen, and water, and 2) coal liquefaction to produce heavier organics, especially aromatics. The technology involved in coal gasification is well-developed, e.g., the Winkler, Koppers-Totzek, or Lurgi processes, and has been used for many years on a large industrial scale in South Africa. Although the synthesis gas produced by gasification can be used in various processes for manufacturing organic compounds, this discussion will be limited to the use of synthesis gas to produce methanol. Coal gasification on a commercial scale for methanol synthesis is under development in North Dakota (Great Plains Coal Gasification Project) to make 17.5 tons/d of methanol for cleaning the raw-gas product, and in Tennessee (Tennessee Eastman Co.) to make acetic anhydride which involves methanol synthesis as an intermediate step. The Tennessee Valley Authority plans to construct a coal-to-methanol facility (North Alabama Coal Gasification Project) to produce 1 million gal/d of fuel-grade methanol.

Currently most methanol is produced from synthesis gas obtained

by steam reforming of natural gas:

$$CH_4 + H_2O \rightleftharpoons 3H_2 + CO$$

The CO/H_2 ratio is adjusted to 1/2 by adding carbon dioxide to the natural g: (combination of steam reforming and water-gas shift reactions):

$$CO_2 + CH_4 \rightleftharpoons 2CO + 2H_2$$

The synthesis gas is reacted over a highly selective mixed metal oxide catalyst at elevated pressures and temperatures to produce methanol:

$$CO + 2H_2 \rightleftharpoons CH_3OH$$

The initial technology for methanol synthesis was developed by Badische Anilin und Soda Fabrik in 1923 using a zinc chromite catalyst at pressures of several hundred atmospheres and temperatures between 300 and 450°C. During the 1960s, Imperial Chemical Industries developed a low-pressure process using a copper-zinc chromite catalyst at pressures of 50-100 atmospheres and temperatures of 250-300°C. The only significant change in catalyst composition since 1960 has been the substitution of alumina for chromia.

Annual methanol demand in this country has been projected to double during the 1980s to 8 million metric tons due mainly to rapid expansion in several developing applications (Weismantel, 1980). Major uses for methanol are the production of formaldehyde, dimethyl terephthalate (DMT), methyl methacrylate, methyl halides, methyl amines, and acetic acid. Large quantities of methanol are used as a gasoline blending

agent and as a solvent. Legislated reductions in the amount of tetraethyl lead allowed in gasoline have increased the demand for octane boosters such as methyl tert-butyl ether (MTBE) which is made from methanol and isobutylene. The recent development of a single-step catalytic distillation process (MTBE plus), which eliminates the methanol recovery section of the conventional process, provides an economically attractive alternative to isobutylene alkylation for octane enhancement (Lander et al., 1983). Methanol by itself can be used as an octane booster, but there are problems with methanol/gasoline mixtures due to their higher affinity for water, higher evaporative losses, and the need to modify the engine. Despite these problems, the TVA and ARCO will be testing a 6-7% methanol/gasoline mixture in 150 automobiles as part of the North Alabama Coal Gasification Project; West Germany has pursued a more ambitious program testing more than 1000 vehicles with a 15% methanol/gasoline mixture with only minor adjustments to the engines (Parkinson et al., 1982).

Future demand for methanol could expand multifold as coal assumes a greater proportion of our energy needs. Although methanol is presently economically unattractive as a substitute for gasoline, the State of California has begun a program to operate 550 vehicles with methanol because it produces fewer pollutants than gasoline. More than 300 privately-owned vehicles, converted by Future Fuels of America, Inc., are running on methanol in the Sacramento, San Francisco, and Los Angeles areas. Even if gasoline remains the major automotive fuel into the next century, methanol production could increase significantly if technology such as Mobil Oil's M-Gasoline process is used to produce gasoline. This

process uses a zeolite catalyst (ZSM-5) to convert methanol into a blend of paraffins, cycloparaffins, and aromatics with a research octane number of 93, i.e., an unleaded premium gasoline (Berry, 1980). New Zealand will use this technology to convert natural gas into approximately 12,500 bbl/d of gasoline. Utilities using coal gasification technology for power generation will probably also manufacture methanol. During off-peak hours, part of the syngas would be converted to methanol and stored; during peak hours, the methanol would be used as fuel in gas turbines to meet the high electrical demand. And finally, there is great potential for future development of methanol as a primary feedstock in the chemical industry, especially as supplies of ethylene and propylene decrease. An example is the manufacture of acetic acid, where methanol has replaced ethylene as the primary feedstock in new technologies by BASF and Monsanto (Kohn, 1979).

The key development in methanol synthesis technology has been the catalyst. Improvements in catalyst performance are usually obtained by trial-and-error methods: variations in composition or preparation techniques are tried until a catalyst is found having greater activity, selectivity, or stability. Characterization of physical and chemical properties is often incomplete, and the reasons for the superiority of a particular catalyst are frequently unclear. Although methanol synthesis as a commercial process is fully developed, the specific function of the catalyst and the fundamentals of the elementary surface reactions are still highly speculative. The main objective of this investigation has been to prepare several different compositions of methanol synthesis catalysts and characterize these catalysts by physical

and chemical techniques, placing emphasis on the use of Fourier transform infrared (FT-IR) spectroscopy to identify the chemical species adsorbed on the catalyst surfaces under methanol synthesis conditions. Part I of this thesis describes the properties of the catalysts during the various stages of preparation (i.e., precursor, oxide, and reduced states) using the techniques of X-ray diffraction, atomic absorption, ESCA, surface area, and pore distribution measurements. Part II examines the adsorption of various organic molecules such as carbon monoxide, formic acid, formaldehyde, and methanol on oxidized and reduced catalysts to identify intermediate surface species and to observe the behavior of adsorbed species under various conditions using FT-IR spectroscopy. Part III evaluates the relative activities and selectivities of several catalysts for methanol synthesis and identifies the adsorbed species under reaction conditions. It should be emphasized that this study has focused on the FT-IR characterization of adsorbed surface species under in situ conditions with the objective of obtaining a better understanding of the molecular interactions occurring on the catalyst surface.

PART I.

PREPARATION AND CHARACTERIZATION OF METHANOL SYNTHESIS CATALYSTS

LITERATURE REVIEW

The development of an inorganic catalyst for the synthesis of methanol from hydrogen and carbon monoxide occurred during the early part of this century when catalysis was just beginning to play an important role in the chemical industry. This development was important because it enabled methanol to be produced on a larger scale and at a lower cost compared to synthesis by the destructive distillation of wood. Although there have been many improvements in the preparation of methanol catalysts during the succeeding years, the basic components — zinc oxide, copper oxide, and a promoter such as chromia or alumina — are unchanged. Methanol catalysts may be divided into two groups: (1) the high-pressure zinc catalysts composed of zinc oxide and a promoter, and (2) the low-pressure copper catalysts composed of zinc oxide, copper oxide, and a promoter. The developments in methanol catalysts are summarized in Table 1. Supported-metal catalysts for methanol synthesis have been developed in recent years but have not been applied commercially. Excellent reviews of methanol catalysts have been provided by Natta (1955) and Klier (1982).

Zinc Catalysts

The catalyst developed by BASF in 1923 for methanol synthesis was a highly selective, mixed metal oxide containing zinc oxide and chromia in a ratio of 9/1, respectively (BASF, 1923). Zinc oxide by itself is a fairly good catalyst for methanol synthesis, but it is quite susceptible to aging (crystallite growth) under reaction conditions

Table 1. Developments in methanol catalysts

Year	Inventor/assignee	Catalyst
1913	BASF G.P. 293,787	Oxides of Cr, Co, Mn, Mo, Pd, Ti, Zn
1923	BASF G.P. 415,686	90% ZnO - 10% Cr_2O_3
1923	Patart	90% CuO - 10% ZnO
1923	BASF F.P. 571,356	Oxides of Cu, Cr, Zn, Mn
1933	Dodge U.S. 1,908,696	ZnO - CuO (Cu)
1936	Larson U.S. 2,061,470	CuO-MnO_2; CuO-ZnO plus Cr_2O_3, Al_2O_3, ZrO_2, V_2O_3, TiO_2, ThO_2, SiO_2, or CeO_2
1967	ICI U.S. 3,326,956	ZnO - CuO - Cr_2O_3
1967	ICI F.P. 1,489,682	ZnO - CuO - Al_2O_3
1971	Metallgesellschaft F.P. 2,049,193	Oxides of Zn, Cu, Mn, V
1978	Stiles U.S. 4,111,847	ZnO - CuO

which reduces the catalytic activity. Chromia, a very poor hydrogenation catalyst which is also difficult to reduce, is added to zinc oxide to prevent aging. X-ray (Williams and Cunningham, 1974) and ESR (Rálek et al., 1968) studies of the mixed oxides have established that the active catalyst contains a mixture of zinc oxide and zinc chromite spinel, $ZnCr_2O_4$. The spinel is not catalytically active, but serves as a stabilizer for zinc oxide. The effect of chromia is mainly physical, as evident by comparing the activation energies of a ZnO-Cr_2O_3 catalyst with pure zinc oxide: both have a value of about 30 kcal/mol.

The optimum composition for a mixed ZnO-Cr_2O_3 catalyst depends greatly on the preparation method. Various values for the optimum Cr/Zn ratio have been determined by conversion tests to be 0.3-0.5 (Molstad and Dodge, 1935), 1.0 (Natta, 1955), 1.0-1.5 (Oba, 1965), 0.4-0.5 (Oba, 1965), and 0.5-1.4 (Vlasenko, 1966). The amount of chromia required appears to depend on the homogeneity of the catalyst components; less chromia is needed for catalysts which have small crystallites of each component in intimate contact with each other. The catalytic activity is poor below a Cr/Zn ratio of 0.3 because of crystallite growth, and is also poor at high ratios because of the decrease in the amount of the active component, zinc oxide. Lower amounts of chromia improve the catalyst selectivity. A catalyst with a Cr/Zn ratio of 0.1 produces methanol of greater than 99% purity (Natta et al., 1953).

Other metal oxides have been investigated as possible promoters for zinc oxide or zinc oxide-chromia catalysts. Alumina forms a spinel with zinc oxide (Kauffe and Pschera, 1950), but is less desirable as a stabilizer than chromia because alumina enhances the dehydration of

methanol to form dimethyl ether. Small quantities of thorium, zirconium, and tantalum oxides (Dolgov and Karpinskii, 1932) and vanadium oxide (Veltistova et al., 1934; Metallgesellschaft, 1971) act as stabilizers for $ZnO-Cr_2O_3$ catalysts.

The stabilizers which have been previously discussed are intercrystalline, i.e., they are external to the lattice structure of zinc oxide. There are also intracrystalline stabilizers such as magnesium, iron, and manganese oxides which form a solid solution with zinc oxide because of the similarities of the ionic radii.

Copper Catalysts

The high activity of a methanol synthesis catalyst containing copper oxide was discovered by Patart using a mixed metal oxide of 90% CuO-10% ZnO (Fenske and Frolich, 1929). However, catalysts containing copper were not applied commercially to methanol synthesis for many years because the sensitivity of copper sites to poisons such as sulfur was high. Copper oxide by itself is a very poor methanol catalyst, but when mixed with ZnO produces a combined oxide having greater activity than either oxide alone. The addition of copper oxide, unlike chromia, to zinc oxide has a truly synergistic effect since the activation energy decreases to about 18 kcal/mol (Natta, 1955). The promoting effect is believed to be both chemical and electronic.

The ternary catalysts composed of zinc oxide, copper oxide, and a stabilizer are of major interest. Early studies established that both chromia and alumina functioned as good stabilizers for methanol catalysts

(Frolich and Lewis, 1928; Ivanov, 1934a and 1934b; Plotnikov et al., 1931). However, there was great variety in proposed optimum compositions. Natta reported high activity for catalysts with Cu/Zn/Cr ratios of 3/6/1 and 1/8/1. Although X-ray patterns of reduced catalysts showed the presence of metallic copper, the active state of the copper was believed to be a partially reduced oxide (Natta, 1955).

Recently binary and ternary methanol catalysts have been extensively characterized by physical and kinetic measurements (Herman et al., 1979; Mehta et al., 1979; Bulko et al., 1979; Herman et al., 1981) A series of binary CuO-ZnO catalysts were prepared by coprecipitation from nitrate solution using sodium carbonate. X-ray analysis identified the precipitated compounds as mixtures of $Cu_2(OH)_3NO_3$, $Zn_5(OH)_6(CO_3)_2$, and $(Cu,Zn)_2(OH)_2CO_3$. These precursors were calcined in air at 350°C to form ZnO-CuO compounds. Oxides with more than 15 wt.% CuO had some copper (up to 6%) dissolved in the ZnO phase. Transmission electron microscopy established that the morphology of ZnO changed from thin crystallites to hexagonal platelets as the CuO content rose above 30 wt.%. The composition of the precipitate was believed to determine the nature of the ZnO morphology. The reduced catalysts were composed of zinc oxide, metallic copper, and an amorphous form of copper (based on X-ray diffraction). This amorphous copper was determined to be dissolved in the ZnO phase using scanning transmission electron microscopy. Diffuse reflectance spectra showed an absorption band at 17,500 cm^{-1} which was assigned to a Cu(I) species dissolved in ZnO. Maxima for greatest catalytic activity were found at ZnO/CuO ratios of 1/2 and 7/3, corresponding to compositions with maximum amounts (12%) of copper dissolved in the

zinc oxide particles. Surface analyses with XPS and Auger epectroscopies revealed surface compositions equal to the bulk catalyst composition. Ternary catalysts containing some chromia or alumina had a zinc oxide phase with both copper and the promoter cations dissolved in the lattice, although the effect of the promoter was mostly physical. A small amount of alumina caused an increase in the surface area and an increase in the amount of dissolved copper in the ZnO phase by 33%. The addition of ceria to a binary catalyst was found to decrease the amount of dissolved copper and decrease the catalytic activity. These investigators concluded that the active component of copper-containing methanol catalysts was a solid solution of Cu(I) ions in the zinc oxide phase.

Other investigators working with ZnO-CuO and ZnO-CuO-Al_2O_3 catalysts have found that copper and aluminum ions dissolve in the zinc oxide phase without the formation of spinels (Ketchik et al., 1982). In the binary compositions, a CuO phase appeared when the amount of copper exceeded 10 atomic %. Decomposition of these solid solutions produced water and carbon dioxide, indicating that the oxides normally have hydroxyl and carbonate groups incorporated into their structures. The function of the aluminum ions was to stabilize the catalyst, while the copper ions dissolved in the zinc oxide phase were active sites in methanol synthesis (Kuznetsova et al., 1982).

An X-ray diffraction analysis of the reduction process for a ZnO-CuO-Al_2O_3 catalyst identified a stabile Cu_2O intermediate at reduction temperatures under 200°C (Ruggeri et al., 1982).

The presence of gaseous CO_2 was found to retard the reduction of Cu_2O to metallic copper. Binary ZnO-CuO catalysts also formed an inter-

mediate Cu_2O phase during reduction (Himelfarb et al., 1983). The reduction rate was dependent on CuO crystallite size and CuO dispersion in these mixed metal oxides.

The valence states of copper in precursor, calcined, and reduced ZnO-CuO catalysts have been determined using X-ray photoelectron and Auger spectroscopies (Okamoto et al., 1982; Okamoto et al., 1983a and 1983b). The coprecipitated precursors had two types of Cu^{2+} species which were attributed to the copper ions in $Cu_2(OH)_2CO_3$ and $(Zn,Cu)_2(OH)_2CO_3$. The calcined oxides had three types of cupric ions: crystalline cupric oxide, an amorphous surface layer of copper oxide, and cupric oxide dissolved in the zinc oxide phase. The reduced catalysts contained copper metal particles and a two-dimensional monolayer of Cu^{o}-Cu^{+} species over zinc oxide. The two-dimensional layer, which had been formed from the cupric ions dissolved in zinc oxide, was believed to be the active site for methanol synthesis. The cuprous ions in these binary catalysts were very stable under reducing and mild oxidizing conditions.

Catalyst Preparation

Investigations to develop improved methanol catalysts have continued through the years as evident by the large number of patents issued. These developments have occurred because the method of catalyst preparation has a great effect on the catalytic activity. The metal oxides can be directly mixed and fused together to form a methanol catalyst (Larson, 1936), but the activity of this type of catalyst was low compared to

other types. Both catalytic activity and stability depended on the homogeneity of the phases in the catalyst. X-ray studies of several low-pressure catalysts have established that the most active catalysts have the greatest homogeneity of components (Shishkov et al., 1979). A ternary $ZnO-CuO-Al_2O_3$ catalyst prepared by kneading was less active than the same catalyst prepared by coprecipitation; the latter was found to have its components in a finely divided state (Kotera et al., 1976; Shimomura et al., 1978).

Preparation techniques can be critical in establishing the ultimate properties of the catalyst. The types of salts used, the precipitating agent, the precipitation temperature, the calcination conditions, and other factors have an impact on the eventual catalytic behavior. The general practice is to coprecipitate a solution of metal nitrates with a carbonate solution; the precipitate is then filtered and washed. The precipitated metal "carbonates" are then dried and calcined to form metal oxides. Salts of metal halides or sulfates produce catalysts with lower activities, presumably due to contamination of active sites (Natta, 1955). Sulfur will poison low-pressure catalysts by selectively adsorbing on copper sites (Wood et al., 1980). An alkali metal carbonate has been found to yield a more active catalyst than those precipitated with an alkali metal hydroxide or ammonium hydroxide (Dodge, 1933). It is important to thoroughly wash the precipitate because the presence of alkali metals in the catalyst will enhance the formation of higher alcohols. Ammonium carbonate or ammonium bicarbonate may be used as the precipitating agent to avoid this problem (Stiles, 1978). After the precipitate is dried, calcination should occur at a temperature

high enough to decompose the nitrate and carbonate components to the oxides, yet at a temperature low enough to minimize the growth of crystallites. Natta has shown that there was an inverse relationship between catalytic activity and crystallite size for zinc oxide (Natta, 1955). Calcination temperatures generally fall within the 300-500°C range. The final step in catalyst preparation is the reduction of the oxides, usually performed in the reactor just prior to actual use (catalyst activation). A hydrogen/inert gas mixture with a hydrogen content of 2-5% is passed over the catalyst at the reduction temperature until the reduction is complete. It is important that local temperatures during reduction remain low to avoid crystallite growth and also to prevent the complete reduction of copper to the zero valent oxidation state.

A novel methanol catalyst has been prepared by leaching an alumina-zinc-copper alloy with aqueous NaOH to produce a Raney catalyst (Friedrich et al., 1983a and 1983b). These catalysts were highly selective to methanol formation (99%) and quite resistant to copper sintering. The greatest activity was related to both surface area and the concentration of zinc oxide on the catalyst surface (these catalysts were mostly copper). Although metallic copper was ascribed to the most active component of the Raney catalysts, these investigators also suggested that the catalytic activity depended on a complex interaction between the copper and zinc oxide.

EXPERIMENTAL APPARATUS AND METHODS

Catalyst Preparation

A series of binary copper-zinc oxide catalysts with relatively low copper content was prepared by coprecipitating the metal nitrates with ammonium bicarbonate according to the method developed by Stiles (1978). A 1 liter solution of the mixed metal nitrates (1 N) and 1/2 liter of distilled water were poured into a 4 liter glass kettle and gradually heated to 60°C. The initial pH of the solution was typically between 3 and 4. When the precipitation temperature was reached, a slow flow of CO_2 was bubbled through the nitrate solution and mild stirring was begun. A 1 liter solution of 1 N ammonium bicarbonate was added dropwise to the nitrate solution in the region near the CO_2 sparger. The temperature of the solution was measured continuously via a thermocouple well and the pH was monitored periodically by inserting a probe into the solution manually. The pH probe could not be kept in the solution continuously without forming a film on the glass membrane which resulted in erroneous readings. After the bicarbonate solution was completely added, some solid ammonium bicarbonate was gradually added to the solution until a pH of approximately 7 was reached. The total amount of ammonium bicarbonate added to the solution was approximately 2.5 moles per mole of metal nitrates in the initial solution. The solution was stirred for an additional half hour before removing the kettle and filtering its contents through a 50 micron fritted glass filter. The precipitate was washed with 1 liter of distilled water. The binary precipitates were light blue and the filtrates were navy blue. Pure

precipitated zinc oxide had a white precipitate and a clear filtrate. Precipitates were dried in air overnight at 110°C and then were calcined in flowing oxygen at 400°C for 8 hours.

Some ternary oxides containing chromia or alumina were prepared in the same manner, starting with a mixture of three metal nitrates. These precipitates were composed of smaller crystallites that did not settle as readily as binary particles, and were more difficult to filter and wash. The ternary precipitates were also light blue with navy blue filtrates. Pure precipitated alumina had a white gel-like precipitate and clear filtrate, while pure precipitated chromia had a fine grey precipitate and clear filtrate. The precipitated alumina was calcined at the slightly higher temperature of 450°C.

An impregnated 95/5 ZnO/CuO catalyst was prepared by mixing a copper nitrate solution with Kadox 25. This slurry was dried at 110°C to yield a light blue solid which was subsequently calcined in oxygen at 400°C for 8 hours.

Catalyst Characterization

X-Ray diffraction

A Picker powder diffractometer was used to identify the solid-state crystalline phases in the precipitates, oxides, and reduced oxides. Thin powder films were placed on glass slides and exposed to Mo Kα X-rays, using a step size of 0.05° during scanning. The detector signals were collected and processed by computer facilities which used a plotting routine to present the data as intensity versus 2θ value.

Compounds were identified by comparing the patterns with standards for pure crystalline phases.

The Guinier X-ray patterns were taken with an Enraf Nonius Delft camera. Approximately 0.05 g of each sample was mixed with 0.02 g silica powder (an internal standard) and this mixture was spread lightly over a piece of adhesive tape. Three samples were mounted adjacent to each other in the sample compartment of the Guinier instrument and the film was exposed to radiation for five hours.

X-Ray photoelectron and Auger electron spectroscopies

The techniques of X-ray photoelectron spectroscopy (XPS), also known as electron spectroscopy for chemical analysis (ESCA), and Auger electron spectroscopy (AES) can provide information about the elemental composition, oxidation state, bonding, and electronic structure of the surface of a solid. These spectroscopies have been used very successfully to increase the knowledge of surface phenomena in heterogeneous catalysis.

XPS uses X-rays to excite core electrons with enough energy to cause ionization. The kinetic energies of the emitted electrons are measured with a magnetic or electrostatic analyzer. Binding energies are calculated from the Einstein relation:

$$E_B = h\nu - E_k - \phi$$

The binding energy equals the incident energy minus the kinetic energy minus a correction term taking into account the spectrometer work function and sample charging effects. This process is depicted in Figure 1;

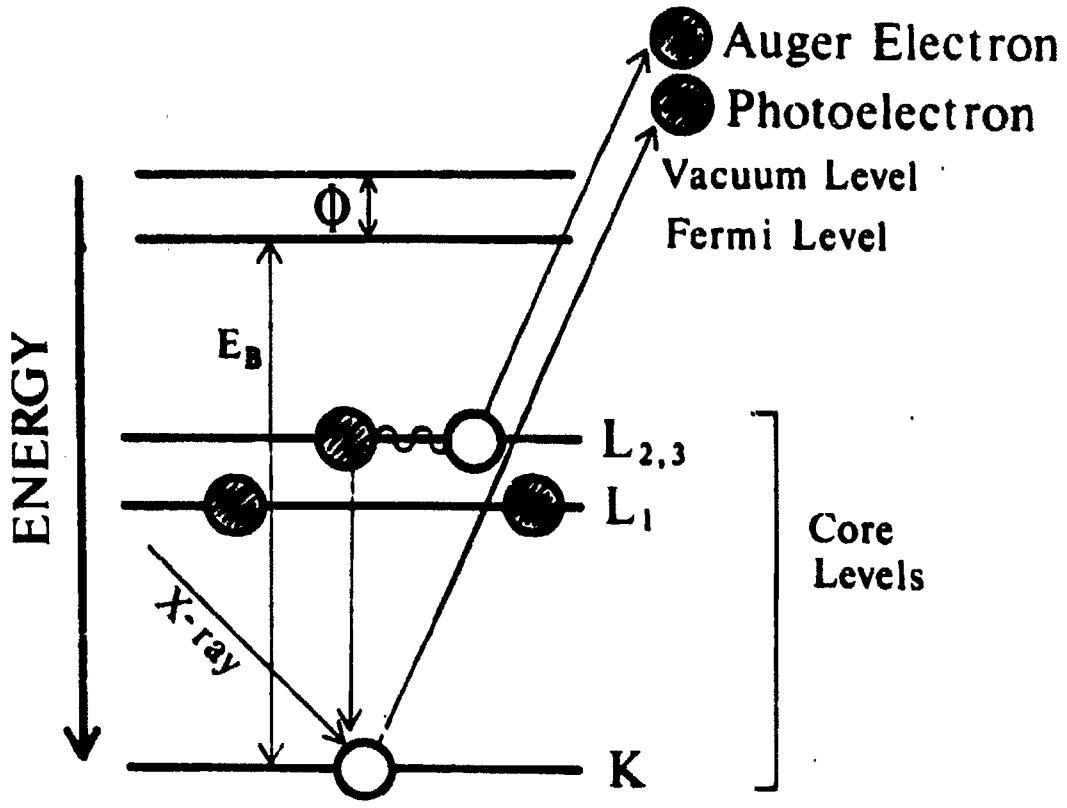

Figure 1. Energy level diagram of photoelectron and Auger electron generation

incident X-rays excite a core electron resulting in the ejection of that electron.

Subsequent relaxation of electrons in the sample can cause the emission of Auger electrons. As an electron from a more energetic level replaces a core electron ejected by the X-ray source, some energy is transferred to other electrons in the same principle electron level. If this energy is sufficient, an electron in this higher level is ejected. Figure 1 shows how a $KL_{2,3}L_{2,3}$ Auger electron is generated. Since Auger electrons result from a secondary process, their kinetic energies are independent of the incident excitation source. Auger transitions are unique for the various elements, thus making this technique popular for elemental analysis; information on oxidation states can also be obtained.

Both X-ray photoelectron and Auger spectra were obtained from an AEI 200B spectrometer coupled with a Nicolet 1180 computer for data manipulation. The X-ray source was Al $K\alpha_{1,2}$ radiation which has an energy of 1486.6 eV. After pretreatment, samples were tightly sealed and transferred via a dry box to avoid atmospheric contamination or oxidation. Sample were prepared for analysis by lightly dusting some powder on adhesive tape.

Surface area and micropore distribution

A Micromeritics AccuSorb 2100E analyzer was used to determine BET surface areas and micropore distributions. All samples were heated at 200°C under vacuum ($< 10^{-4}$ torr) overnight to remove adsorbed gases on the surfaces. Measurements were taken using nitrogen gas at liquid

nitrogen temperature (-195°C). A value of 16.2 $\mathring{A}^2$ was used for the area of a nitrogen molecule in BET determinations. The micropore distribution was determined from the desorption isotherm of each sample, using a cylindrical pore model to estimate pore radii.

RESULTS OF CATALYST CHARACTERIZATION

Cation Composition of the Binary Oxides

The relative amount of zinc and copper in the precipitated oxides does not necessarily equal the relative amount in the initial nitrate solution because the precipitation kinetics and/or thermodynamics might allow one of the cations to preferentially remain in solution. The analytical technique of atomic absorption was used to determine the relative amount of zinc and copper in the binary oxides.

Standard solutions of zinc and copper were prepared by dissolving the oxide in hydrochloric acid and diluting the sample with distilled, deionized water. The zinc standard had 0.95 ppm Zn and the copper standard had 4.8 ppm Cu. The usual method for preparing the precipitated oxides involved dissolving approximately 0.5 g of the oxide in hydrochloric acid and diluting the sample in a 1000 ml volumetric flask. The solution for copper analysis was made by taking 10 ml of the diluted solution and further diluting this aliquot in a 250 ml volumetric flask. The solution for zinc analysis was made by taking 10 ml of the copper solution and diluting it in a 250 ml volumetric flask. These solutions made from the binary oxides must have cation concentrations less than those in the standard solutions to ensure the accuracy of the results because the zinc and copper standards have cation concentrations near the upper limit of a linear range (concentration vs signal intensity). Distilled water is used to establish the lower limit (0 ppm) and the standards establish the upper limits for the particular conditions used in this analysis. A linear relationship between these limits is then

used to determine the cation concentrations in the precipitated oxides. In some cases, the filtrate from the precipitation reaction was analyzed to check for consistency in the results by making a material balance; generally the filtrate was diluted by a factor of 100 for both zinc and copper analyses. Instrumentation parameters and cation ratios are given in Table 2. Both zinc and copper concentrations are based on the average of ten readings.

Using the preparation of 86/14 Zn/Cu oxide as an example, the cation ratio in the precipitate can be calculated by determining the amounts of zinc and copper lost in the filtrate and subtracting these amounts from the original nitrate composition. The filtrate had a much higher proportion of copper to zinc than the initial solution in all the cases examined. Because the amount of filtrate was approximately 2.5 liters, the amount of copper lost can be calculated as:

$$(1.41 \text{ ppm})(100)(2500 \text{ ml}) = 0.35 \text{ g Cu}$$

and the amount of zinc lost was:

$$(0.55 \text{ ppm})(100)(2500 \text{ ml}) = 0.14 \text{ g Zn}$$

The amounts of copper and zinc in the original nitrate solution were:

$$(0.14 \text{ mole Cu})(63.5 \text{ g/mol}) = 8.89 \text{ g Cu}$$
$$(0.86 \text{ mole Zn})(65.4 \text{ g/mol}) = 56.2 \text{ g Zn}$$

Thus, the amounts of copper and zinc in the precipitate should be:

Table 2. Atomic absorption parameters and binary oxide compositions

	Zn lamp	Cu lamp
Wavelength	213.9 nm	324.8 nm
Current	15 mA	15 mA
Time constant	0.5 s	0.5 s
Slit height	0.7 nm	0.7 nm
Fuel flowrate	2.5 l/min	2.5 l/min
Air flowrate	17.5 l/min	17.5 l/min

Binary oxide	Zn, ppm (dilution)	Cu, ppm	Zn/Cu
95/5 Zn/Cu	0.631 ± .005 (25)	0.72 ± 0.02	96/4
filtrate	0.821 ± .006 (2)	0.98 ± 0.01	63/37
90/10 Zn/Cu	0.91 ± .02 (20)	1.5 ± 0.00	92/8
85/15 Zn/Cu	0.63 ± .01 (25)	2.68 ± 0.04	85/15
86/14 Zn/Cu	0.64 ± .01 (25)	2.61 ± 0.04	86/14
filtrate	0.55 ± .01	1.41 ± 0.05	28/72
80/20 Zn/Cu	0.81 ± .02 (20)	4.1 ± 0.05	80/20
2/1 Zn/Cu	0.681 ± .004	0.31 ± 0.02	69/31
filtrate	0.580 ± .004	3.64 ± 0.03	14/86

$$8.89 - 0.35 = 8.54 \text{ g Cu}$$

$$56.2 - 0.14 = 56.1 \text{ g Zn}$$

The Zn/Cu ratio corresponds to 87/13 which is consistent with the result of 86/14 for the precipitate. The material balances for the other oxides were also consistent. Even though an enrichment of copper in the filtrate occurred, the amount was not enough to significantly alter the precipitate composition. However, if less concentrated nitrate solutions had been used, the cation ratio in the precipitates could have been changed considerably.

X-Ray Powder Diffraction

Identification of the precursors for methanol catalysts proved to be most difficult because samples were partially amorphous and comparisons with pure crystalline phases did not match exactly. The precursor of precipitated zinc oxide (Figure 2) was composed of smithsonite, $ZnCO_3$, and hydrozincite, $Zn_5(CO_3)_2(OH)_6$. The precursor of precipitated copper oxide (Figure 3) was malachite, $CuCO_3 \cdot Cu(OH)_2$. The precursor of 80/20 Zn/Cu oxide was typical of the binary oxides with relatively high zinc contents; although an exact identification of crystalline phases could not be determined with certainty, it appeared that hydrozincite was the major phase with some smithsonite and some rosalite, $(Cu,Zn)_2(OH)_2CO_3$, present (Figure 4). Because these precipitates were prepared with CO_2 bubbling through the solution, carbonates rather than nitrates were favored in the formation of the precursors.

After calcining the precursors in oxygen at 400°C for 8 hours, the oxidized materials showed only zinc oxide and cupric oxide. The presence of CuO ($2\theta = 17.56°$) did not become apparent until the copper content exceeded that of the 90/10 Zn/Cu oxide (Figure 5). Reduction of these oxides in carbon monoxide at 200°C did not affect the ZnO phase but some copper metal ($2\theta = 19.56°$) was formed (Figure 6). There was no evidence of a cuprous oxide phase.

The powder patterns of ternary oxides were very similar to the binary oxide patterns. As indicated in Figure 7, ZnO was the only distinct phase observed in $ZnO/CuO/Cr_2O_3$ precipitated oxides with copper and chromium contents up to 10% (metal atom %). Pure metal oxides of

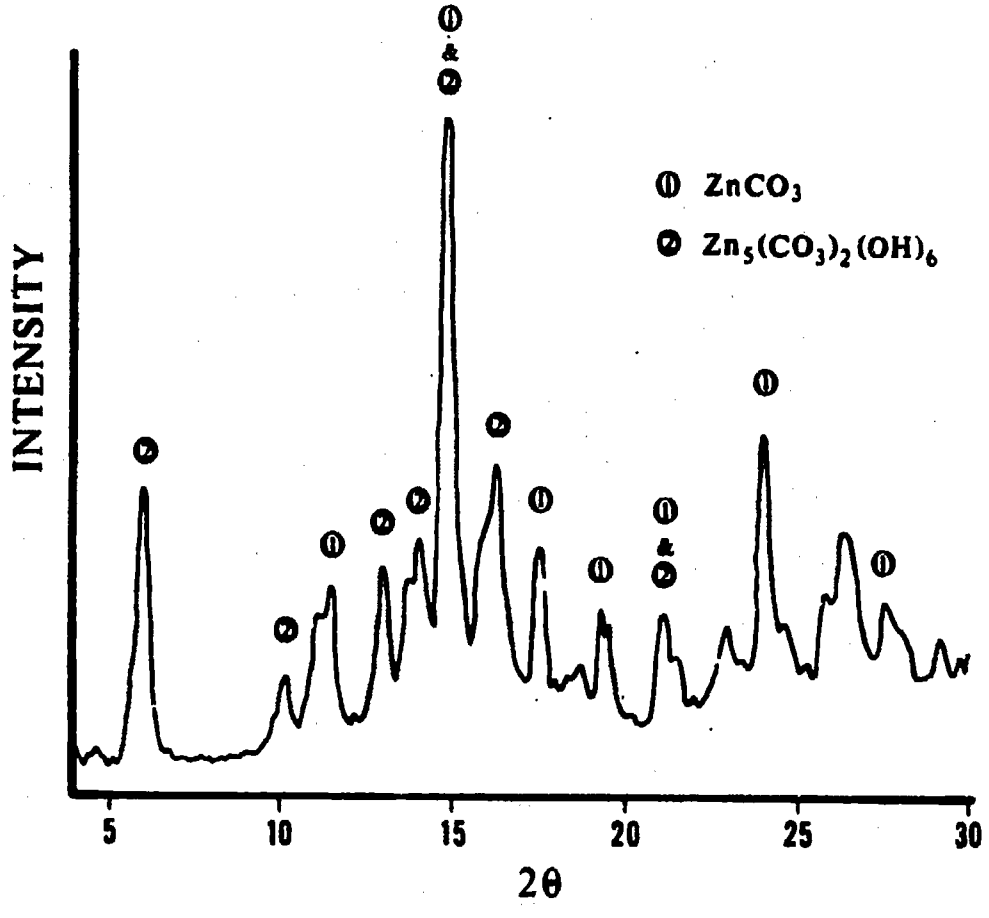

Figure 2. Powder diffraction pattern of zinc oxide precursor

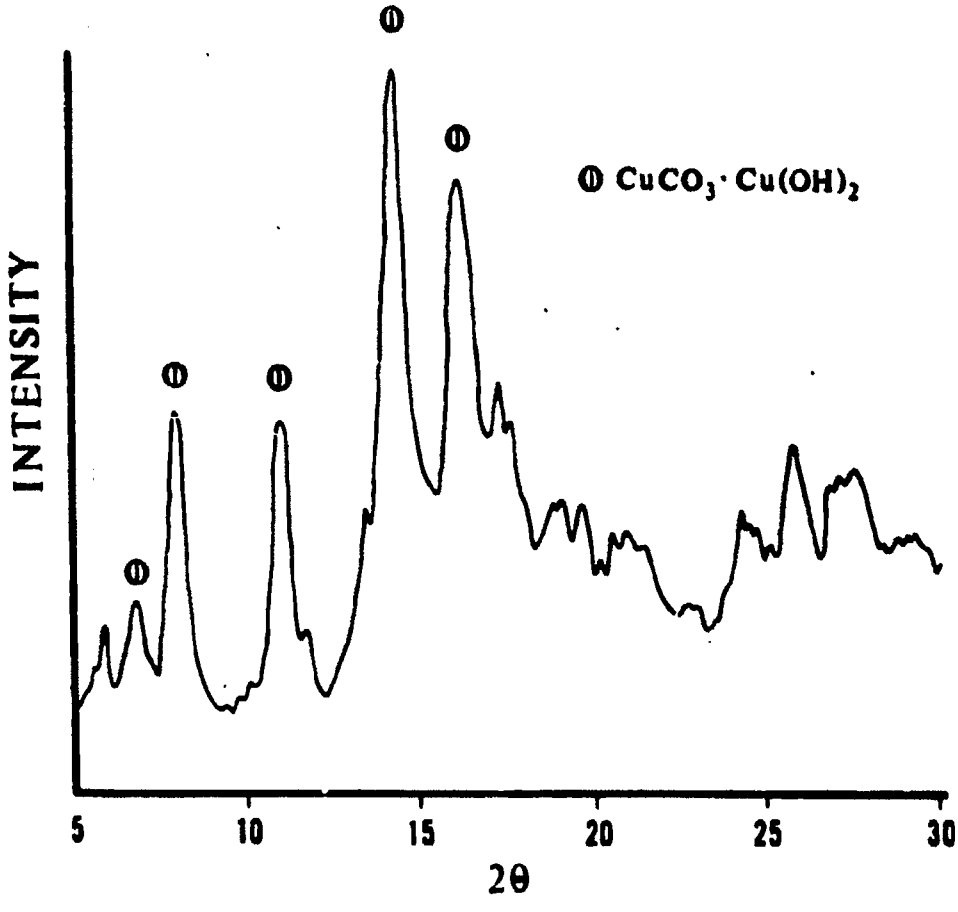

Figure 3. Powder diffraction pattern of copper oxide precursor

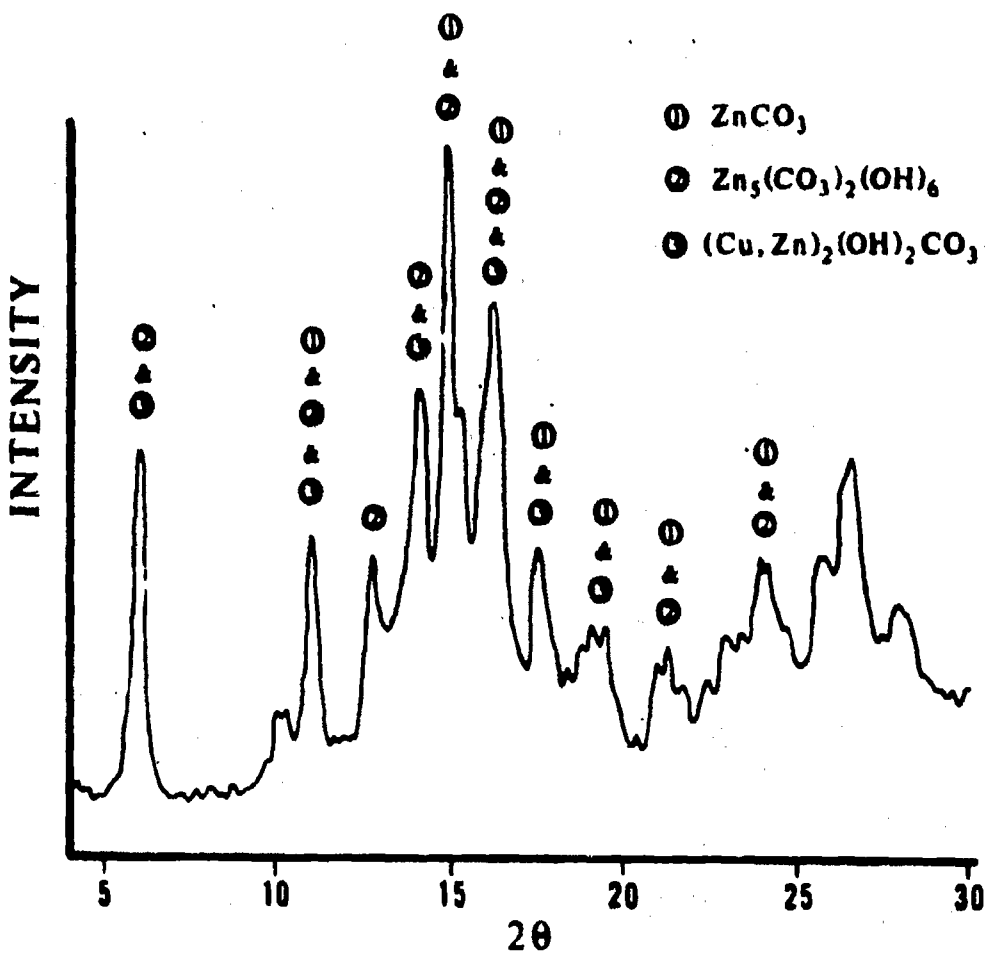

Figure 4. Powder diffraction pattern of a binary precursor

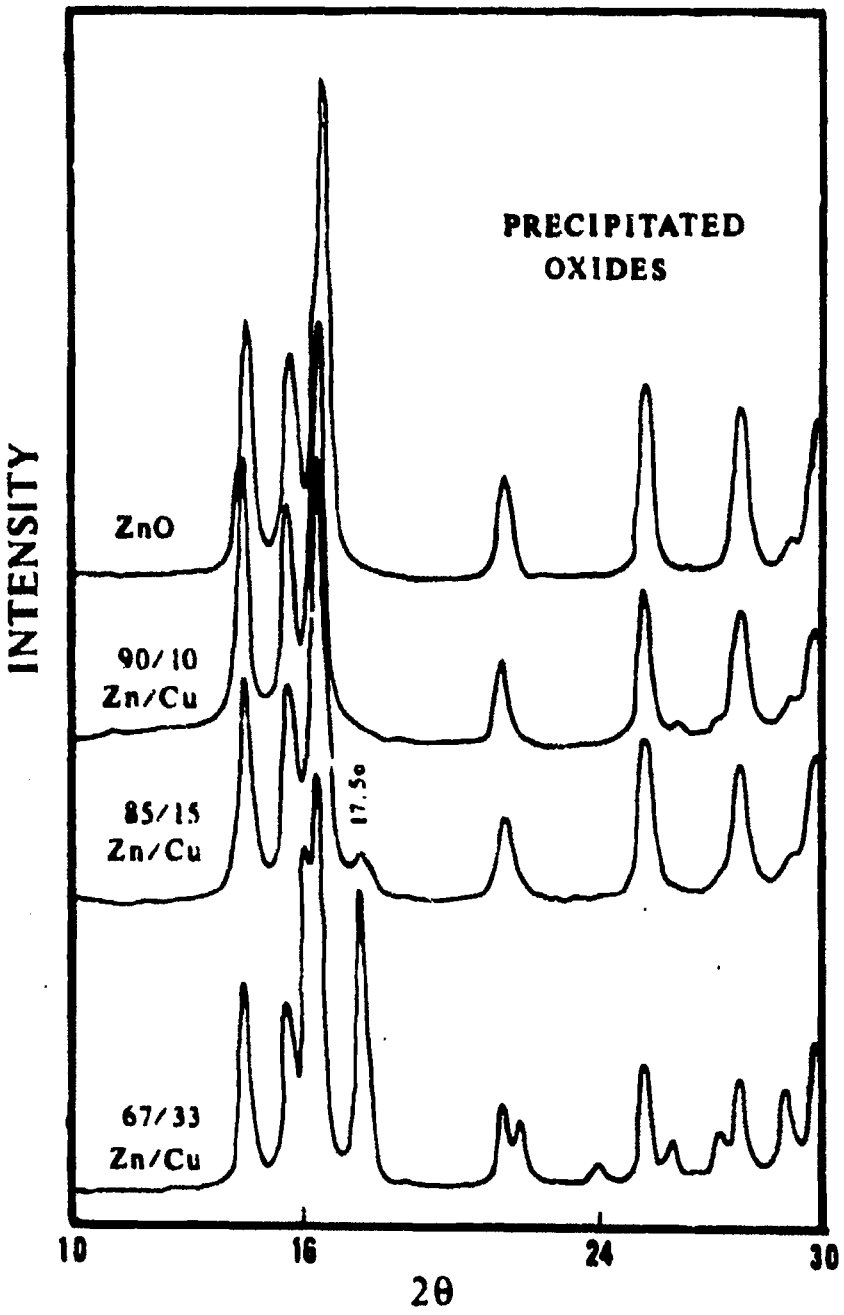

Figure 5. Powder diffraction patterns of precipitated oxides

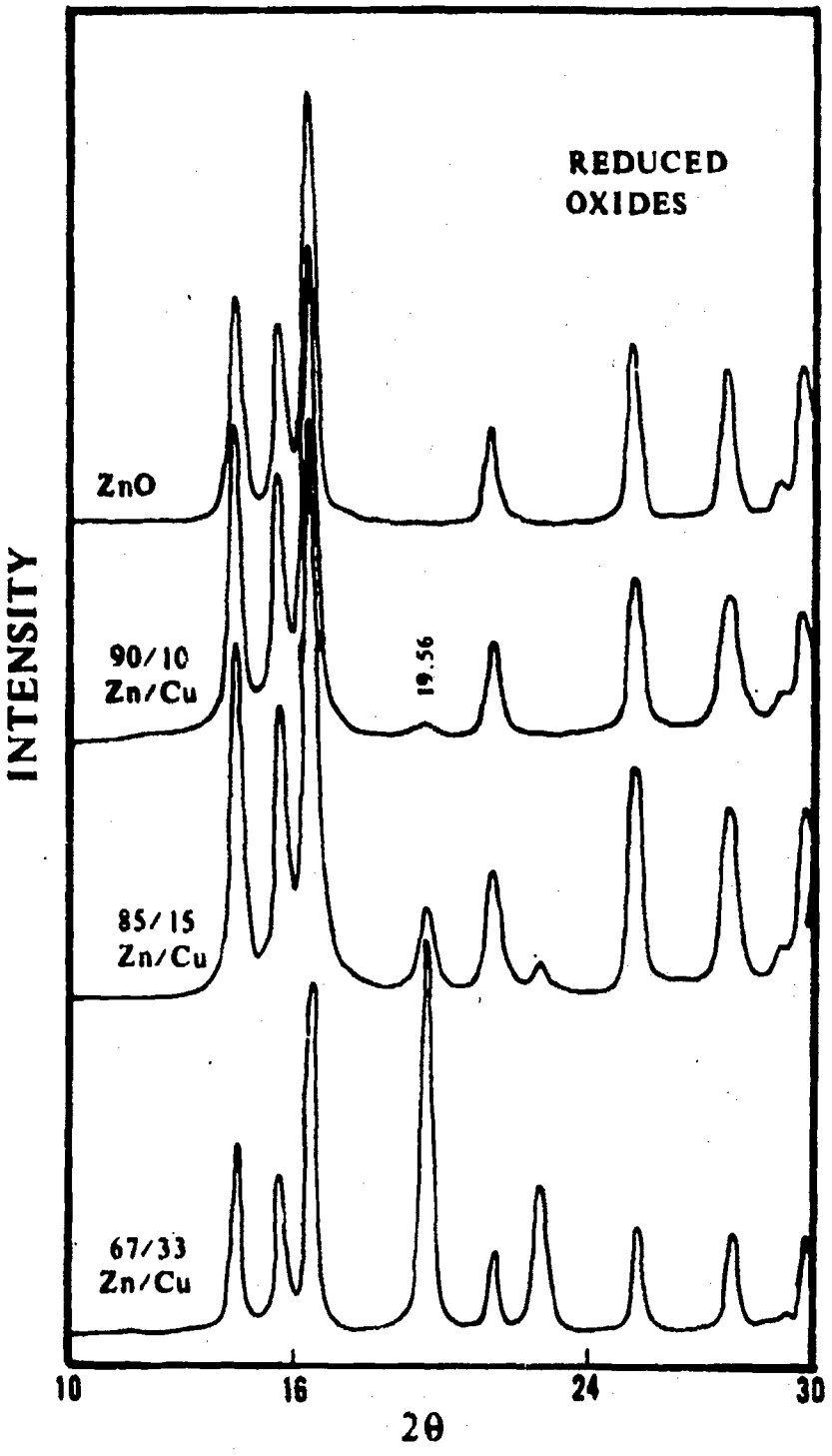

Figure 6. Powder diffraction patterns of reduced oxides

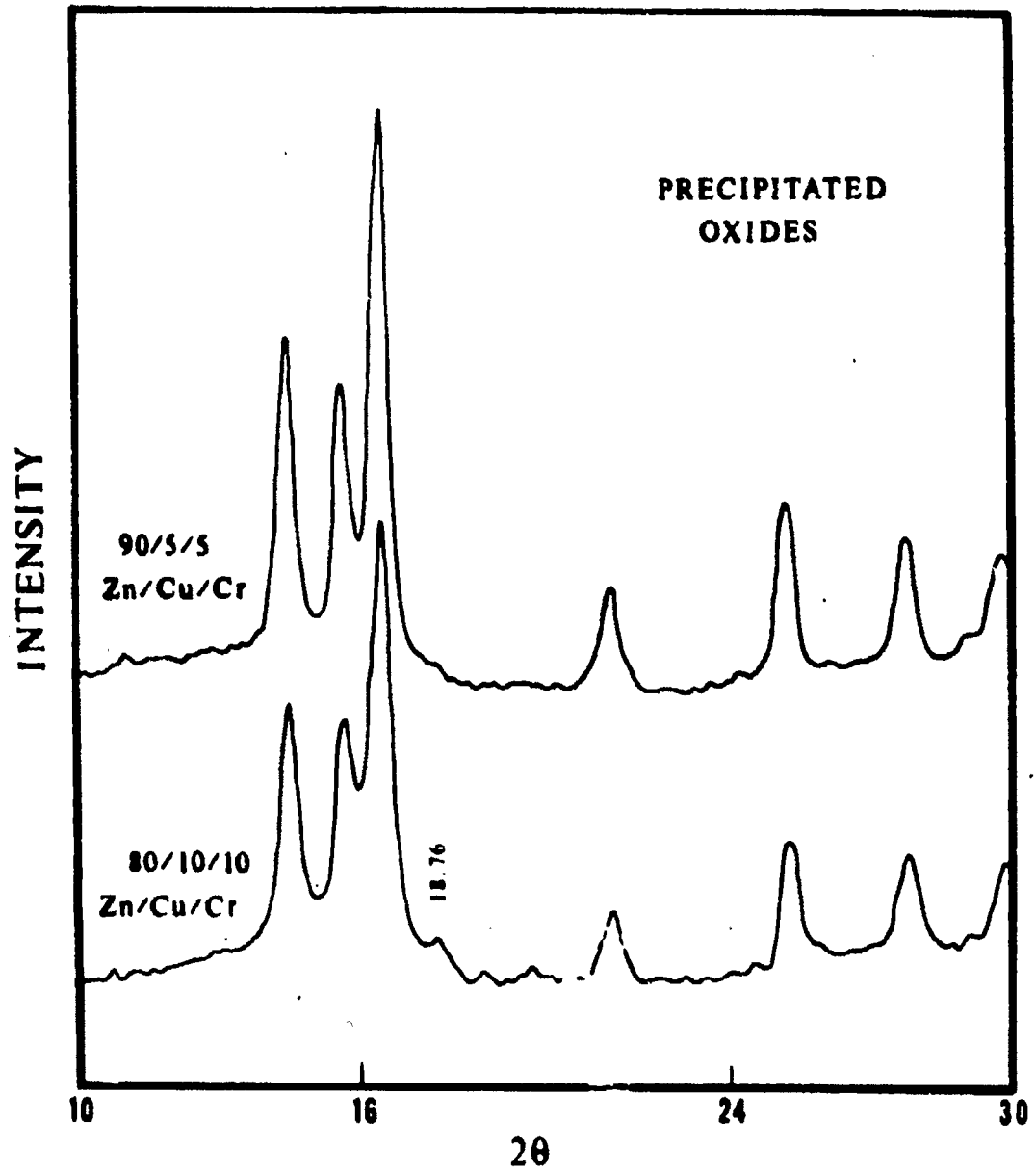

Figure 7. Powder diffraction patterns of ternary oxides

chromium and aluminum were prepared under the precipitation conditions used in the preparation of ternary catalysts to identify the crystal phases formed. After precipitating chromium nitrate with ammonium bicarbonate in the standard manner, the calcined precipitat was identified as Cr_2O_3 (Figure 8). There was some indication in Figure 7 that a Cr_2O_3 phase ($2\theta = 18.76^{o}$) had begun to appear for the 80/10/10 Zn/Cu/Cr oxide composition. A preparation using aluminum nitrate precipitated with ammonium bicarbonate and calcined to the oxide yielded the pattern shown in Figure 9. Although the oxide can be seen to be quite amorphous, the two distinct peaks identify the oxide as γ-Al_2O_3.

Guinier X-Ray

Copper and zinc can form a solid solution known as brass, but little is known about the solubility of the oxides. The results of the atomic absorption analysis showed that copper contents in the precipitated oxides were very close to the original composition of the nitrate solutions. However, the powder diffraction patterns have indicated that some of the copper may be incorporated in the ZnO phase before a cupric oxide phase develops. The patterns of mixtures of ZnO and CuO were not conclusive in establishing whether or not the amounts of cupric oxide in the precipitated oxides were less than would be expected if all the copper were in the CuO phase. Another approach to address this question was Guinier X-ray analysis, which was utilized to determine the lattice dimensions of the ZnO crystallites as the copper content of the precipitated oxides was increased.

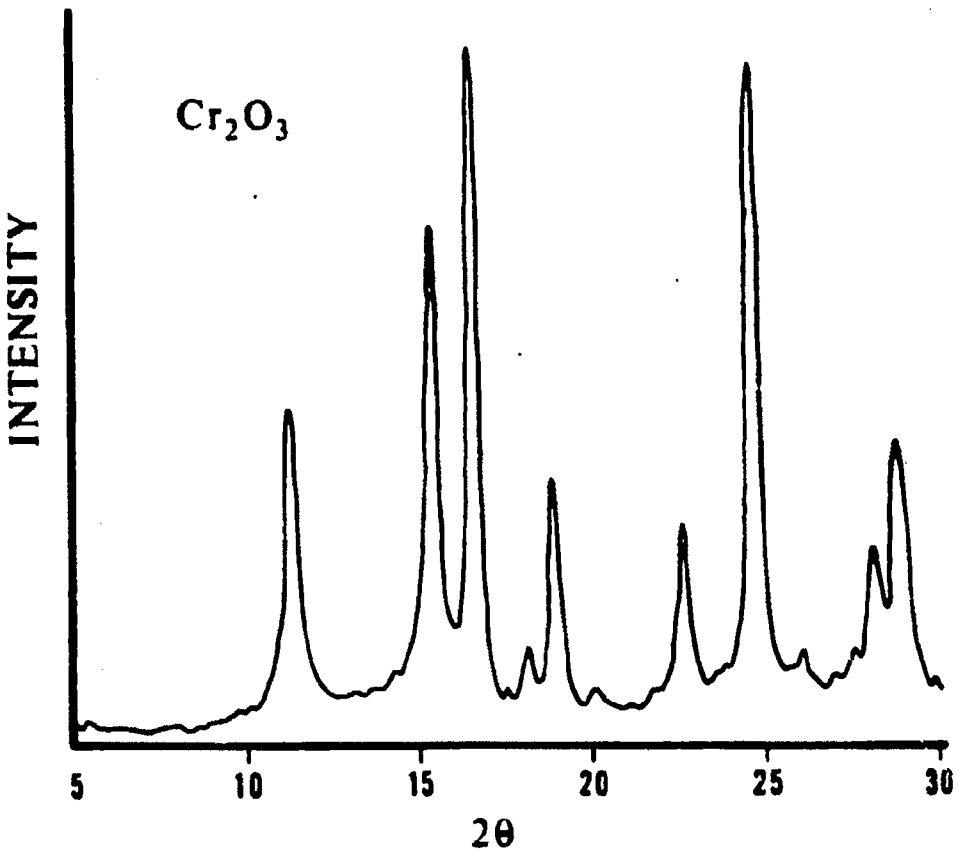

Figure 8. Powder diffraction pattern of chromium oxide

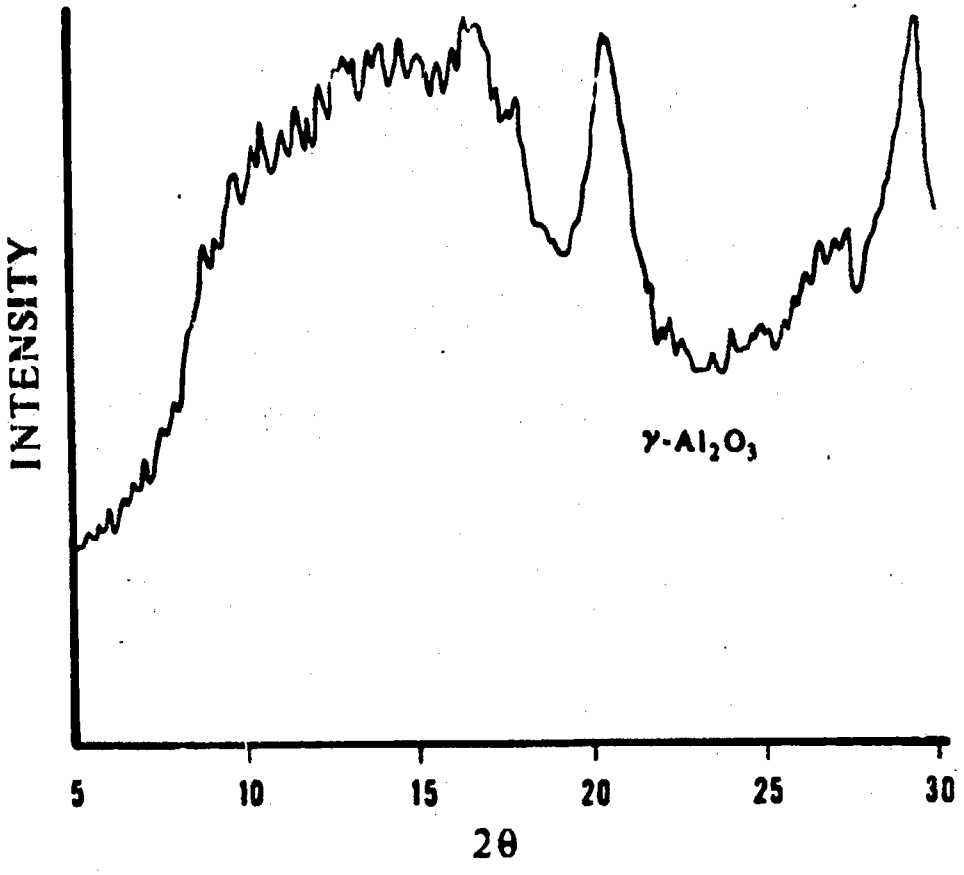

Figure 9. Powder diffraction pattern of aluminum oxide

Precipitated oxides of pure ZnO, 95/5 Zn/Cu oxide, and 90/10 Zn/Cu oxide were analyzed with the Guinier X-ray technique. The positions of the diffraction lines on the developed film were measured, using the Si lines as an internal standard to correspond line positions with 2θ values. The interplanar distances were calculated from Bragg's law:

$$d_{hkl} = \lambda/2 \sin\theta$$

where λ is 1.54051 Å for the X-rays used in these experiments. Because ZnO has a hexagonal lattice structure, the lattice parameters are $a = b \neq c$ and $\alpha = \beta = 90^{o}$ with $\gamma = 120^{o}$. This information combined with the Miller indices and interplanar spacings, given in Table 3, led to the determination of lattice parameters a and c from the computer program LATT (Ames Laboratory). The values of a and c did not change as the copper content of the precipitated oxides was increased (Table 4). These three oxides were also reduced in CO at 200°C and analyzed in the same manner as the oxides except that these samples were prepared in a dry box to avoid any oxidation after the reduction step. These results, given in Tables 3 and 4, also showed no change in the lattice paramters as the copper content increased; the values for a and c were the same as those for the oxides. The diffraction patterns for the reduced oxides did not show any lines for copper metal.

Surface Oxidation States

XPS and AES were utilized to identify the oxidation states of Cu and Zn in binary oxides subjected to various treatments, with the

Table 3. Data from Guinier X-ray analysis

Oxides			ZnO		95/5 Zn/Cu		90/10 Zn/Cu	
h	k	l	2θ	d_{hkl}	2θ	d_{hkl}	2θ	d_{hkl}
1	0	0	31.786	2.8130	31.768	2.8145	31.790	2.8126
0	0	2	34.454	2.6010	34.438	2.6021	34.455	2.6009
1	0	1	36.280	2.4742	36.275	2.4745	36.289	2.4736
1	1	0	56.613	1.6245	56.604	1.6247	56.610	1.6245
1	0	3	62.882	1.4767	62.848	1.4775	62.852	1.4774
1	1	2	67.898	1.3793	67.958	1.3783	67.962	1.3782
Reduced oxides			**ZnO**		**95/5 Zn/Cu**		**90/10 Zn/Cu**	
h	k	l	2θ	d_{hkl}	2θ	d_{hkl}	2θ	d_{hkl}
1	0	0	31.730	2.8178	31.726	2.8181	31.750	2.8161
0	0	2	34.378	2.6065	34.423	2.6032	34.416	2.6037
1	0	1	36.225	2.4778	36.238	2.4769	36.211	2.4787
1	1	0	56.593	1.6250	56.584	1.6252	56.580	1.6253
1	0	3	62.844	1.4775	62.842	1.4776	62.835	1.4777
1	1	2	67.981	1.3778	67.946	1.3785	67.948	1.3785

Table 4. Lattice parameters

Oxides	a	c
ZnO	3.250 ± .001	5.205 ± .003
95/5 Zn/Cu	3.2491 ± .0004	5.207 ± .001
90/10 Zn/Cu	3.250 ± .001	5.205 ± .002
Reduced oxides	**a**	**c**
ZnO	3.249 ± .001	5.208 ± .003
95/5 Zn/Cu	3.250 ± .001	5.207 ± .001
90/10 Zn/Cu	3.250 ± .001	5.208 ± .001

intention to establish what oxidation states likely exist on an active catalyst. Because methanol synthesis is a high-pressure process and these techniques involve high-vacuum conditions, no direct determination of actual surface oxidation states during methanol synthesis conditions was possible.

Two samples of 90/10 Zn/Cu oxide were heated overnight at 200°C under vacuum to remove residual surface impurities. One sample was cooled and removed in a fully oxidized state, while the other sample was reduced in carbon monoxide at 200°C for 8 hours, cooled, and removed for analysis. The kinetic energies of the photoelectrons from the oxidized and reduced samples were recorded. The kinetic energies of the C 1s, Zn $2p_{3/2}$, and Cu $2p_{3/2}$ photoelectrons are given in Table 5. The most obvious difference between these two samples was the absence of the broad, short peak (the copper shake-up satellite) in the reduced sample as shown in Figure 10. The shake-up peak results from the promotion of a valence electron to an unfilled higher energy level when the photoelectron leaves the atom. Because Cu(II) has an intense shake-up satellite and reduced states of copper do not, the reduced sample has only reduced states of copper. This conclusion was supported by the calculated binding energies of the Cu $2p_{3/2}$ electrons. The binding energies reported in Table 5 were calculated using the Einstein relation. The correction term for each sample was determined from the kinetic energy of the C 1s electron and a value of 285.0 eV for the binding energy of this electron (the carbon in the adhesive tape was used as an internal standard). Correction terms of 9.2 and 9.7 eV were calculated for the oxidized and reduced samples, respectively. Some reported binding energies for various states

Table 5. Results from X-ray photoelectron and Auger electron spectroscopies

Photoelectron kinetic energy (eV)	C 1s	Zn $2p_{3/2}$	Cu $2p_{3/2}$
oxidized 90/10 Zn/Cu	1192.4	454.8	543.4
partially reduced 90/10 Zn/Cu	1191.9	454.4	543.6
oxidized 67/33 Zn/Cu	1191.2	454.4	542.8
partially reduced 67/33 Zn/Cu	1192.9	455.4	545.0
fully reduced 67/33 Zn/Cu	1193.5	456.0	545.7

Photoelectron binding energy (eV)	Zn $2p_{3/2}$	Cu $2p_{3/2}$
oxidized 90/10 Zn/Cu	1022.6	934.0
partially reduced 90/10 Zn/Cu	1022.5	933.3
oxidized 67/33 Zn/Cu	1021.8	933.4
partially reduced 67/33 Zn/Cu	1022.5	932.9
fully reduced 67/33 Zn/Cu	1022.5	932.8

Auger kinetic energy (eV)	Cu $L_3M_{4,5}M_{4,5}$
oxidized 67/33 Zn/Cu	918.6
partially reduced 67/33 Zn/Cu	916.5
fully reduced 67/33 Zn/Cu	915.7, 917.7

of zinc and copper are given in Table 6. Comparing experimental binding energies from Table 5 with the literature values from Table 6, it was determined that the oxidized samples had both zinc and copper in the 2+ oxidation state, whereas the reduced sample had zinc in the 2+ oxidation state and copper in either the 1+ or metallic state. The binding energies of Cu_2O and Cu metal are too close to be able to distinguish between them. However, the measurement of the kinetic energies of the X-ray induced Auger electrons can readily differentiate between Cu_2O and Cu metal. Unfortunately the Zn Auger electrons were so much more intense

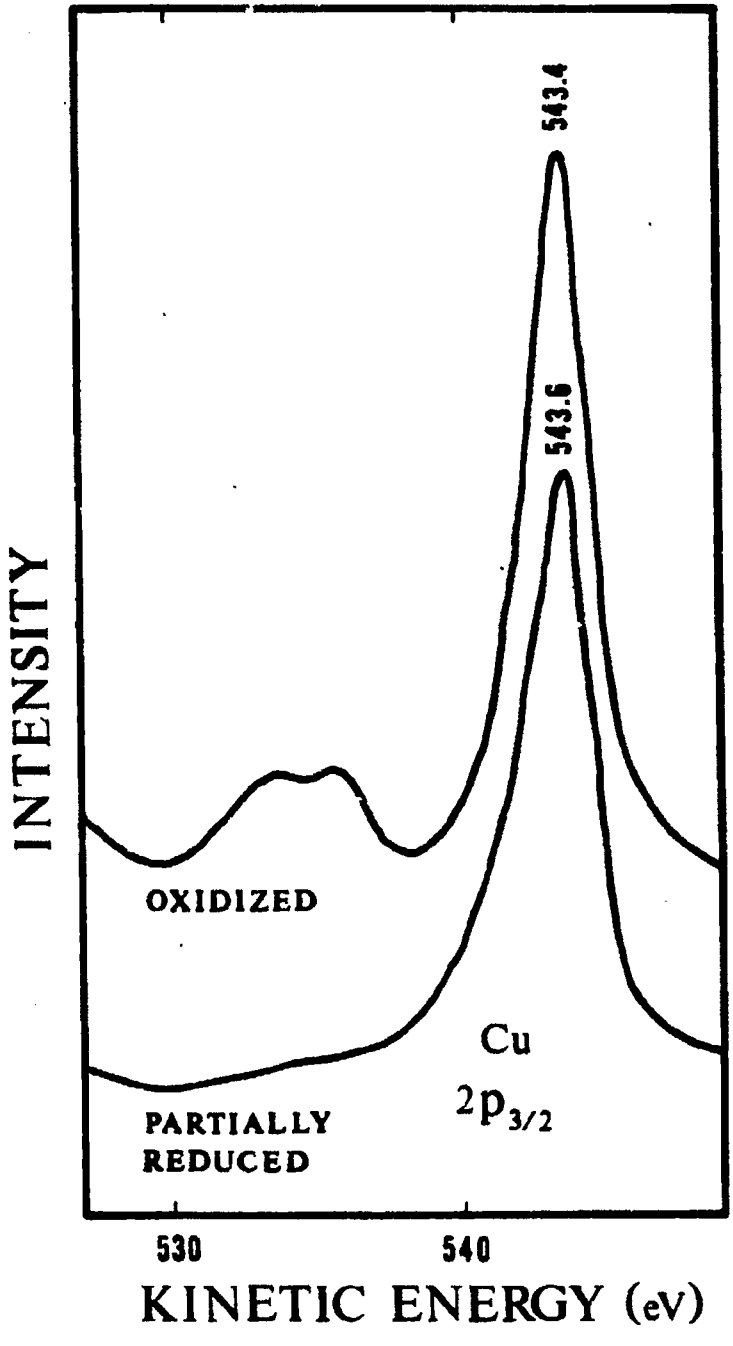

Figure 10. XPS spectra for 90/10 Zn/Cu oxide

Table 6. Literature XPS and AES energies for various states of copper and zinc

	Photoelectron binding energy (eV)[a]
	$2p_{3/2}$
ZnO	1022.5
Zn metal	1021.7
CuO	933.5
Cu_2O	932.2
Cu metal	932.4

	Auger electron energy (eV)[b]
	$L_3M_{4,5}M_{4,5}$
CuO	918.2
Cu_2O	916.7
Cu metal	919.0

[a]Wagner et al., 1979.

[b]McIntyre, 1982.

than the Cu Auger electrons from this reduced sample that the Cu Auger electrons were not observed.

The intensity of the Cu Auger electrons was increased by using a catalyst with a higher copper content. Three samples of 67/33 Zn/Cu oxide were heated overnight at 200°C under vacuum to remove surface impurities. One sample was cooled and removed. Another sample was reduced in hydrogen for 2 hours; since this system was static, the gas phase contained water at its saturation point of 200°C and 1 atmosphere. The remaining sample was subjected to several cycles of reduction in hydrogen followed by evacuation of the gas phase, until reduction of the sample was complete (no water was present in the gas phase). Figure 11

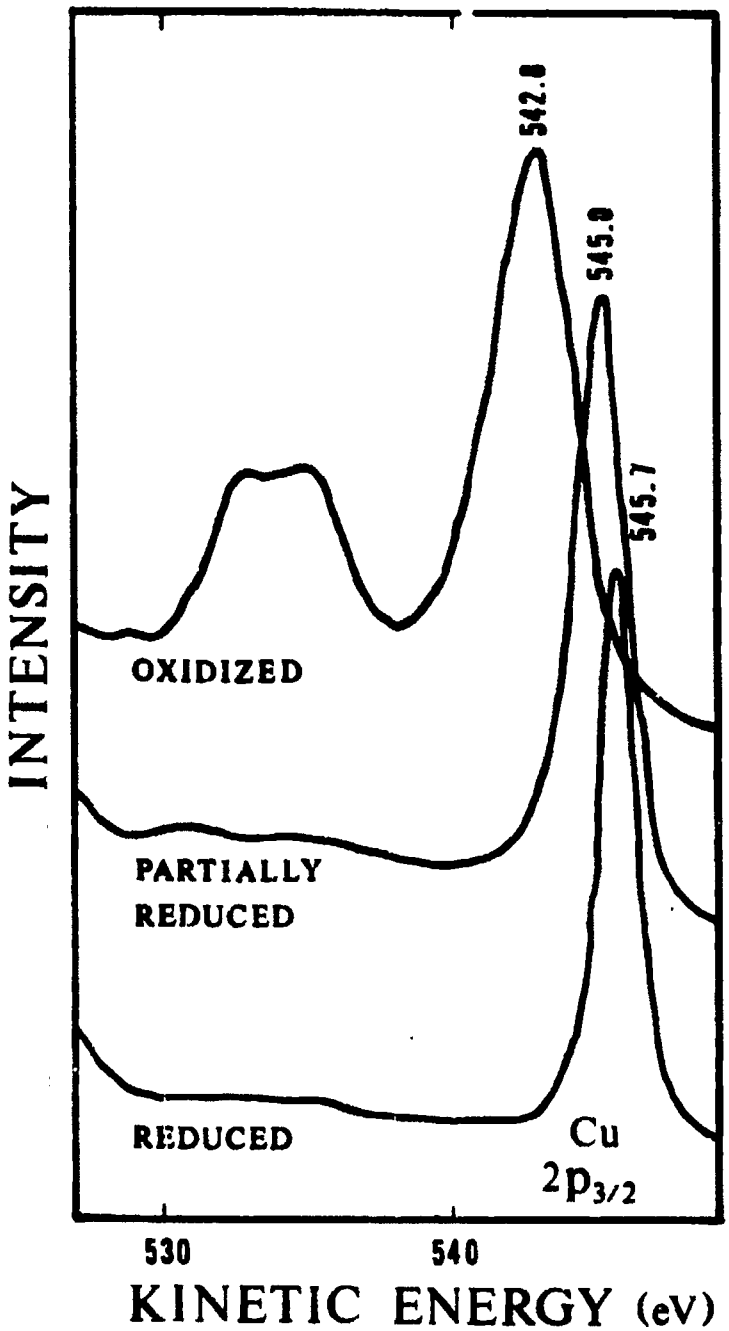

Figure 11. XPS spectra for 67/33 Zn/Cu oxide

shows the kinetic energies of the Cu $2p_{3/2}$ electrons in the oxidized, partially reduced, and fully reduced samples. Neither the partially reduced nor fully reduced samples have the Cu shake-up satellite, indicating that these samples contain no CuO. Correction terms of 10.4, 8.7, and 8.1 eV were calculated for the oxidized, partially reduced, and fully reduced samples, respectively, using the Einstein relation and the kinetic energies in Table 5. These kinetic energies and correction terms were used to determine the binding energies reported in Table 5. Comparing experimental and literature values, the oxidized sample had both zinc and copper in the 2+ oxidation state, while both reduced samples had zinc in the 2+ oxidation state and copper in either the first oxidation or metallic state. This time the Cu Auger electrons were sufficiently intense to permit identification of the reduced oxidation states. Figure 12 shows the kinetic energies of the $L_3M_{4,5}M_{4,5}$ Auger electrons for Cu in these three samples. Because the kinetic energies of Auger electrons reported in the literature were relative to the Fermi level, whereas the experimental kinetic energies were relative to the vacuum level, the correction term of the Einstein relation was added to the experimental values to yield the Auger kinetic energies given in Table 5. When these values were compared to literature values given in Table 6, the following conclusions were reached. In agreement with the XPS results, the oxidized sample had Cu in the 2+ oxidation state. The partially reduced sample had all the Cu in the 1+ oxidation state. The fully reduced sample had two types of Cu present, corresponding to copper in the 1+ oxidation state and metallic copper. The energy difference of 2 eV between these two peaks as well as the absence of a

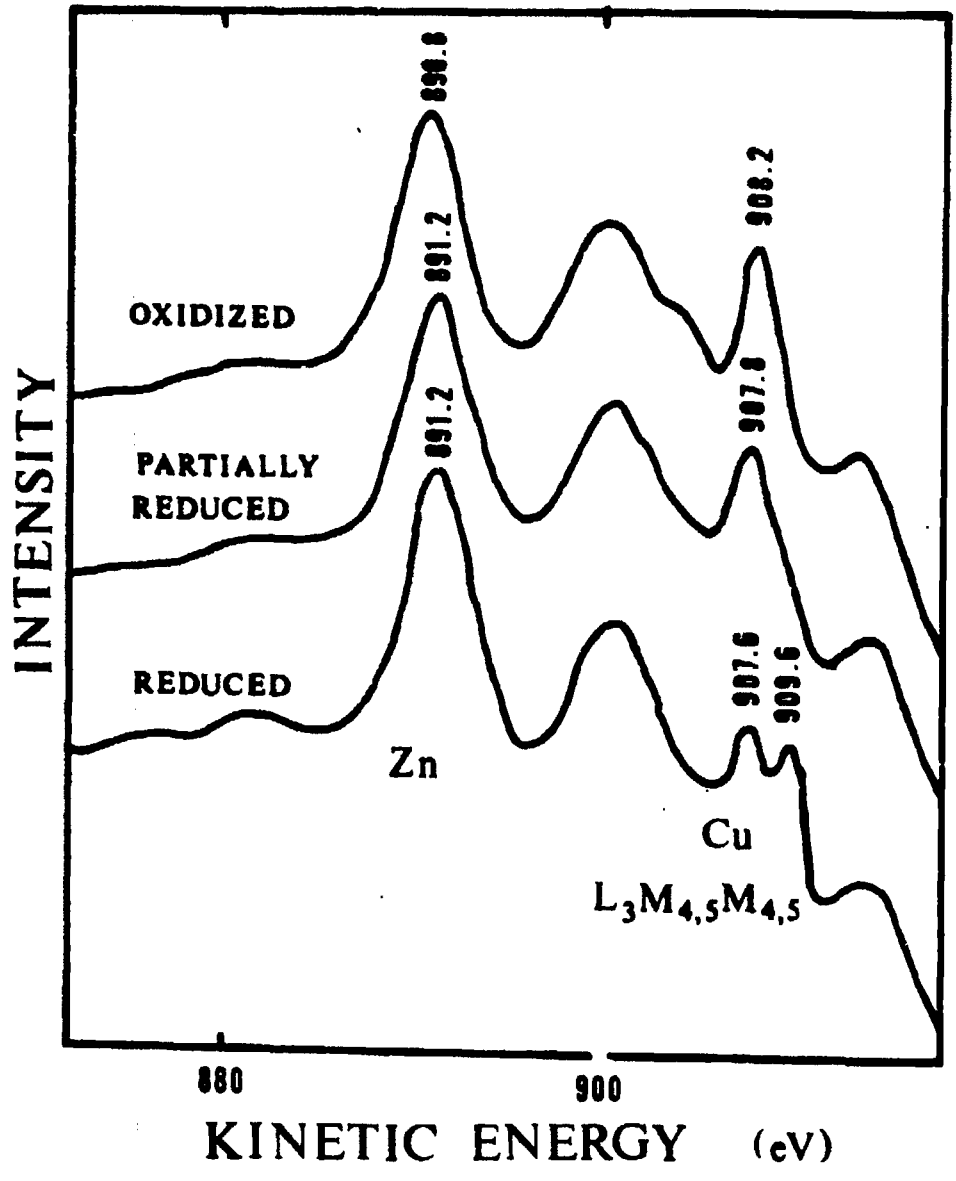

Figure 12. Auger spectra for 67/33 Zn/Cu oxide

shake-up satellite in the XPS plot supported this conclusion.

A sample calculation for determining binding energies and Auger kinetic energies can be found in Appendix A.

Surface Area and Micropore Distribution

The BET surface areas reported in Table 7 were measured on powdered oxides prepared by precipitation at 60°C and calcination at 400°C. The precipitated oxides of copper and zinc had surface areas of 15 and 20 m^2/g, respectively. Coprecipitated binary oxides of zinc and copper had surface areas in the range of 20-30 m^2/g, the value increasing as the zinc content increased. The coprecipitated ternary oxides containing small amounts of chromia or alumina had surface areas twice the magnitude of binary oxides. Because infrared and reactivity measurements were conducted with compressed powders, the surface areas of some oxides pressed into wafers were determined. The surface areas of 90/10 ZnO/CuO and 80/20 ZnO/CuO were 28 and 22 m^2/g, respectively, showing that compression of the powders at the load used in this work (1200 kg/cm^2) had no observable effect on the surface area. The calcination process was found to significantly affect the surface area of the oxide. The surface area of the precipitate of 67/33 ZnO/CuO was reduced from 29 to 20 m^2/g when calcined at 400°C and was reduced to 1.5 m^2/g when calcined at 600°C, indicating that severe sintering had occurred at the higher temperature. The surface area of Kadox 25 was measured as 9.1 m^2/g, in agreement with values determined by other investigators (Amberg and Seanor, 1965; Ueno et al., 1971; Boccuzzi et al., 1978a). The impregnated 95/5 ZnO/CuO

Table 7. BET surface areas of metal oxides

Catalyst (molar ratio)	Surface area (m^2/g)
ZnO/CuO	
100/0	20
95/5	27
90/10	27
85/15	26
80/20	23
67/33	20
0/100	15
$ZnO/CuO/Cr_2O_3$	
90/5/2.5	49
80/10/5	58
$ZnO/CuO/Al_2O_3$	
80/10/5	65

prepared from Kadox 25 had a surface area of 4.7 m^2/g.

By continuing adsorption isotherms to the saturation pressure of nitrogen at liquid nitrogen temperature, pore distribution analyses of the micropores could be obtained from the desorption isotherms. The results for two binary and two ternary oxides are given in Figure 13. The distribution of micropore radii was quite narrow for binary oxides and slightly broader for ternary oxides. All of these oxides had a most probable micropore radius in the range of 100-120 Å. Micropore volumes and surface areas calculated from the desorption isotherms are given in Table 8. All of these oxides had very similar micropore volumes. The surface areas of the binary oxides were larger than the BET values, suggesting that the cylindrical pore model used in these calculations needs to be modified to better represent these catalysts. A sample calculation

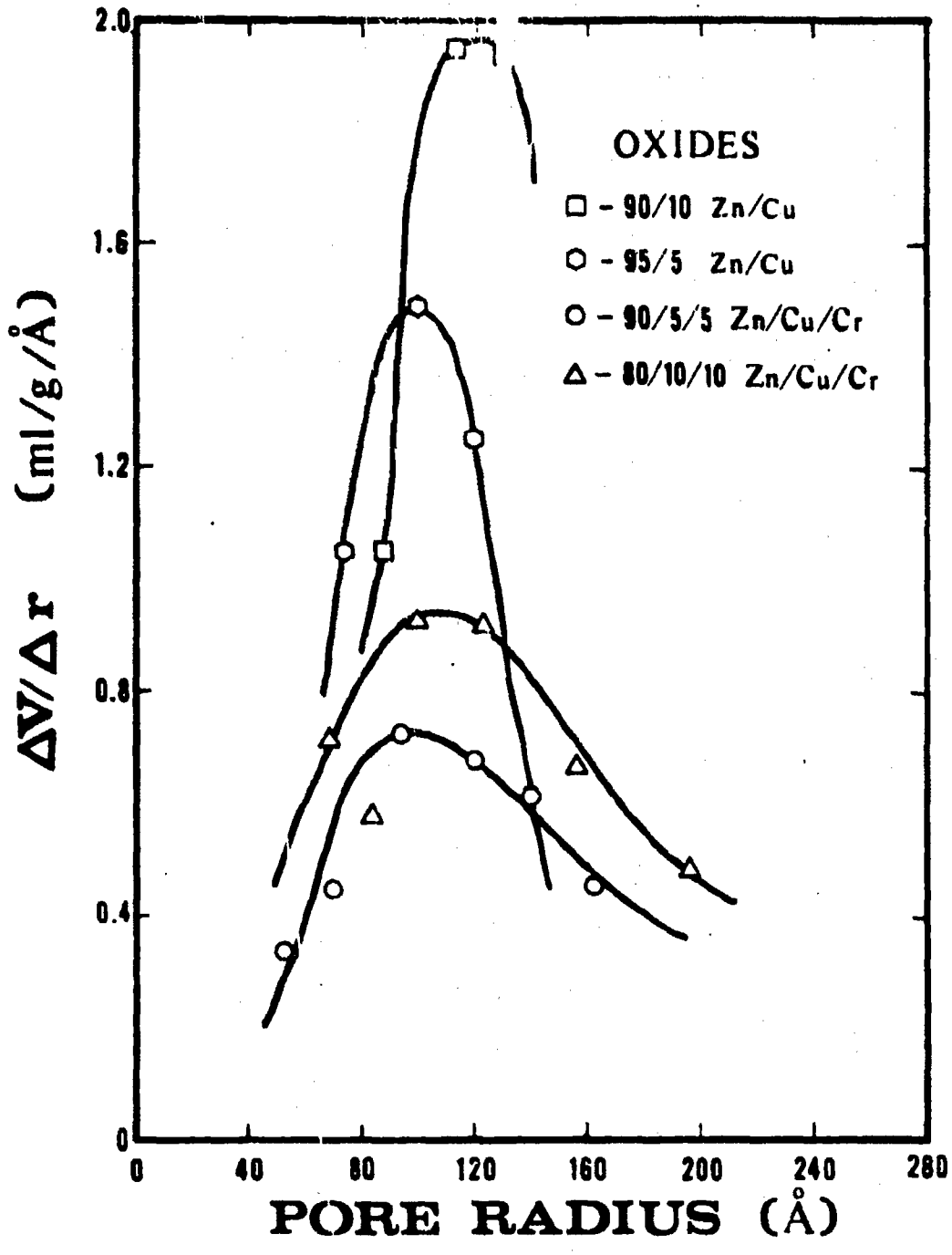

Figure 13. Micropore size distribution

Table 8. Micropore volume and surface area

Catalyst (mole %)	Pore volume (ml/g)	Surface area (m^2/g)
ZnO/CuO		
95/5	0.22	45
90/10	0.21	42
$ZnO/CuO/Cr_2O_3$		
90/5/2.5	0.23	36
80/10/5	0.27	44

of a BET surface area and pore distribution analysis can be found in Appendix B.

DISCUSSION OF RESULTS

The primary objective in catalyst preparation was to develop suitable mixed metal oxide catalysts for methanol synthesis which were also amenable to transmission infrared studies. The color of the oxide was a good indicator of whether or not the oxide could satisfactorily transmit infrared radiation. Precipitated zinc oxide was white whereas precipitated copper oxide was black; the former oxide was very good while the latter was very poor in transmitting infrared radiation when the sample was a thin wafer. Binary and ternary oxides with less than 14 atomic % copper oxide were brown and transmitted infrared radiation as well as pure zinc oxide. Oxides with greater amounts of copper oxide appeared dark brown or black and were nearly opaque to infrared radiation. Apparently, the black coloration developed as a cupric oxide phase was formed. The brown color arose from an intimate mixture of copper oxide and zinc oxide, possibly a solid solution of copper oxide in the zinc oxide phase. Mechanical mixtures of copper oxide and zinc oxide, as well as the impregnated 95/5 ZnO/CuO, were grey rather than brown. The Guinier X-ray patterns showed that the zinc oxide lattice was unaffected by copper contents up to 10 metal atom %. This result was consistent with values given for the ionic radii of Zn^{2+} and Cu^{2+}, which are 0.60 Å and 0.62 Å, respectively (Shannon and Prewitt, 1969). Since these radii are nearly equal, the lattice dimensions of zinc oxide would not be expected to change if some copper ions were incorporated in the ZnO crystallites.

The existence of some copper in an X-ray amorphous state has been

proposed to explain the observation that less cupric oxide was detected in coprecipitated oxides than would be expected if all the copper were in this phase (Semenova et al., 1977; Herman et al., 1979). One possible explanation for this deficiency of cupric oxide not previously considered would be a loss of copper during precipitation via the filtrate. The coprecipitation method used in this investigation yielded a dark blue filtrate, suggesting that part of the copper had complexed with ammonia to form soluble complexes of the type $Cu(NH_3)_x(H_2O)_{6-x}$, where x has values from 1 to 4. Precipitates and filtrates were analyzed for zinc and copper contents by atomic absorption. Although the amount of copper lost in the filtrate exceeded the amount of zinc, the total amount in the filtrate was sufficiently small to have negligible effect on the composition of the precipitates. Therefore, the copper composition in the oxides was very close to the copper composition in the original nitrate solutions.

The catalyst precursors were identified as hydrozincite, smithsonite, rosalite, and malachite. With the exception of smithsonite, these precipitated compounds have been observed in previous studies which attributed the formation of the precursors to the reactions (Herman et al., 1979):

$$Zn^{2+} + 2OH^- \rightarrow Zn(OH)_2$$

$$2Zn^{2+} + 4HCO_3^- + 3Zn(OH)_2 \rightarrow Zn_5(OH)_6(CO_3)_2 + 2H_2O + 2CO_2$$

$$Zn^{2+} + 2HCO_3^- + Cu(OH)_2 \rightarrow CuZn(OH)_2CO_3 + H_2O + CO_2$$

Unlike the previous studies, the precipitation reactions were conducted with carbon dioxide bubbling through the solution. The presence of carbon dioxide inhibited the formation of hydrozincite and rosalite, while promoting the formation of smithsonite:

$$Zn^{2+} + HCO_3^- + OH^- \rightarrow ZnCO_3 + H_2O$$

The effect of smithsonite on the morphology of the zinc oxide crystallites has not been determined.

The X-ray patterns of the precipitated oxides showed only zinc oxide and cupric oxide; the amount of alumina or chromia in the ternary compositions was too low to observe these phases. The surface areas of the binary oxides were in the 20-30 m^2/g range, while ternary oxides had approximately double the surface area of binary oxides. The addition of small amounts of alumina or chromia to a binary composition brought about a large change in surface area without changing the crystal phase. Compression of the powdered oxides into thin wafers, which reduced the bulk volume by approximately an order of magnitude, did not change the BET surface area. It seems that most of the surface area was in the micropores ($r < 200$ Å). Both binary and ternary oxides had a most probable micropore radius near 100 Å, indicating that the increase in surface area of ternary oxides arose from an increase in the number of pores rather than a decrease in pore radius relative to pore volume.

Reduction of the catalysts did not change surface areas. X-ray spectra showed some formation of metallic copper but no cuprous oxide phase. The XPS-Auger spectra revealed a very different result. Reduction of a 67/33 Zn/Cu binary oxide reduced all the cupric ions. When reduction

took place without removal of reaction products from the gas phase, the copper was found exclusively in the +1 oxidation state. When reduction took place with the removal of reaction products, a comparable amount of copper was detected in both the +1 oxidation and metallic states. Therefore, a small amount of oxidant in the gas phase during reducing conditions favored the formation of the cuprous ion. Even during severely reducing conditions (at 200°C), the cuprous ion was stable.

The location of the copper in reduced coprecipitated oxides might be shown by determining the effect of copper content on the lattice dimensions of zinc oxide. An increase in the lattice dimensions would occur if copper existing as a solid solution in zinc oxide was reduced. Copper in the +1 oxidation state (coordination number 4) would have an ionic radius of 0.90 Å and copper in the zero valent oxidation state (metallic copper) would have a radius of 1.28 Å (Lange's Handbook of Chemistry, 1973). The Guinier X-ray results have indicated, however, that the lattice dimensions of the zinc oxide crystallites for reduced binary oxides did not change for oxides with copper contents up to 10%. The metallic copper must be a separate phase or on the surface of the zinc oxide crystallites to explain the observed result. The cuprous ion could be within the zinc oxide crystallite if the coordination number was 2; the ionic radius would be about 0.60 Å (Shannon and Prewitt, 1969). Further experimentation will be necessary to clarify the precise location of copper ions.

PART II.

CHEMISORPTION ON METHANOL SYNTHESIS CATALYSTS

LITERATURE REVIEW

In heterogeneous catalysis, the interactions between reactants and the catalyst which lead to the formation of products can be very complex. Often the catalyst surface contains many different adsorbed species. The first objective in studies of reaction intermediates is the identification of adsorbed species. In this study, the emphasis has been placed on the use of infrared spectroscopy for the characterization of surface species on methanol synthesis catalysts. Various gaseous compounds have been adsorbed on zinc oxide and mixed metal oxides during spectroscopic measurements.

Adsorption on Zinc Oxide

Zinc oxide has been one of the most extensively studied oxides over the past two decades. The strong interest in zinc oxide has been mainly due to its high transparency to infrared radiation which, combined with a controlled-atmosphere cell, has provided a very successful technique for identifying adsorbed species under reaction conditions. The catalytic behavior and nature of adsorbed compounds on zinc oxide, recently reviewed by John (1980), will be addressed in the next several sections.

Zinc oxide is an n-type semiconductor with both zinc and oxygen ions tetrahedrally coordinated. Contrary to an earlier assumption that the surface of ZnO powders were mostly composed of equal areas of polar (0001) and nonpolar ($10\bar{1}0$) planes (Morimoto and Morishige, 1975), the ratio of polar to nonpolar planes was determined to be 1:6, respectively,

by transmission electron microscopy (Bowker et al., 1981).

The (0001) plane consists of surface zinc ions coordinated to three lattice oxygens, whereas the $(10\bar{1}0)$ plane contains rows of zinc and oxygen ions arranged in pairs.

In normal practice, the ZnO surfaces are crystallographically imperfect and contain impurities. Atmospheric water and carbon dioxide form an amorphous layer of $Zn_5(OH)_6(CO_3)_2$ on zinc oxide which can be decomposed by heating the sample above 200°C in vacuo (Nagao et al., 1974). Residual surface carbonates can be removed by successive oxidation and evacuation steps, producing a "clean" surface containing hydroxyl groups observed in an infrared spectrum as bands at 3670, 3640, 3620, 3555, and 3440 cm^{-1} (Atherton et al., 1971). The first three bands were assigned to isolated hydroxyls on polar planes, while the latter two bands were assigned to hydrogen-bonded hydroxyls on nonpolar planes. The surface could be gradually dehydroxylated by increasing the outgassing temperature above 200°C, causing a decrease in the intensity of the hydrogen-bonded hydroxyls. The chemisorption of water on several types of ZnO which had received various surface pretreatments was found to be associated mostly with the nonpolar $(10\bar{1}0)$ plane (Morimoto and Nagao, 1974; Nagao et al., 1978), supporting the infrared results. The water adsorption isotherms and heats of immersion for the different oxides were correlated with the area of various planes estimated with scanning electron microscopy. Photoelectron studies have determined that the interaction of water with the polar (0001) plane of ZnO near ambient temperatures was insignificant, although at lower temperatures (80-200°K), an oxygenated surface will undergo additional hydroxylation (Abbati

et al., 1978; Au et al., 1982).

A summary of infrared bands assigned to residual hydroxyl bands on ZnO is presented in Table 9.

Table 9. Residual hydroxyl groups on zinc oxide

Hydroxyl infrared bands, cm^{-1}	Reference
3670, 3640, 3620, 3555, 3440	Atherton et al., 1971
3670, 3642, 3620, 3595, 3450	Nguyen and Sheppard, 1981
3640, 3575, 3530, 3440	Morimoto et al., 1976
3660, 3610, 3550, 3439	Scholten and van Montfoort, 1973

The adsorption of hydrogen on zinc oxide produces several types of surface complexes that are infrared active. Eischens, Pliskin, and Low (1962) established that a reversible type of adsorption occurring at 30°C (Type I) formed two infrared bands. Hydrogen adsorbs dissociatively at ambient temperature on zinc oxide pair sites to produce bands at 1710 and 3500 cm^{-1}, due to ZnH and OH species, respectively. This type of adsorption was found to be reversible, covering between 5 and 10% of the surface (Dent and Kokes, 1969a). Also at ambient temperature an irreversible adsorption (Type II) occurred that was infrared inactive and unreactive in ethylene hydrogenation. A reversible type of adsorption occurring at -195°C (Type III) is believed to be molecularly adsorbed hydrogen which produces a band at 4019 cm^{-1} (Chang et al., 1973). A recent infrared study of hydrogen adsorption on zinc oxide at ambient temperature identified two additional bands associated with Type I

adsorption; bands at 817 and 845-850 cm^{-1} were assigned to bending frequencies for ZnH and OH species, respectively (Boccuzzi et al., 1978a). More significant was the assignment of broad bands near 3400 and 1475 cm^{-1} to dissociated hydrogen atoms bridged between neighboring oxygen and zinc ions, respectively (Type II).

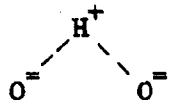

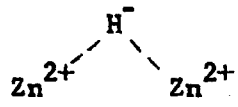

Deuteration of Type I species shifted the bands to 1232 and 2584 cm^{-1} for ZnD and OD, respectively (Kokes et al., 1972). The electrical conductivity of ZnO can increase when hydrogen is adsorbed in an infrared inactive form (Cimino et al., 1962). This adsorption has been proposed to occur on interstitital zinc atoms (Scholten and van Montfoort, 1973), but other studies have found that the amount of adsorbed hydrogen did not relate to the interstitial zinc concentration (Gerasimova et al., 1973).

Carbon monoxide adsorption on zinc oxide at ambient temperature occurs as two types: a reversible, weakly adsorbed species which produces a band in the 2174-2212 cm^{-1} region depending on the degree of oxidation of zinc oxide, and a strongly adsorbed species producing bands in the 1300-1600 cm^{-1} region which desorbs as carbon dioxide (Taylor and Amberg, 1961; Amberg and Seanor, 1965). The band near 2200 cm^{-1} was believed to be a weakly adsorbed carbon monoxide molecule that, due to polarization, had a CO stretching frequency well-above that for gaseous carbon monoxide. Bands near 1530, 1470, and 1330 cm^{-1} were assigned to surface carbonate species, and other bands at 1575, 1342, and 1287 cm^{-1} were

assigned to a carboxylate species (see Figure 14). A similar study of CO_2 adsorption on ZnO dispersed in Aerosil found bidentate and unidentate carbonate bands at 1640 and 1430 cm^{-1}, respectively; at 200°C, bands at 1570 and 1380 cm^{-1} were assigned to a carboxylate species (Matsushita and Nakata, 1962). Carbon dioxide was strongly adsorbed on sites formed by partial dehydroxylation of the surface, and was displaced by gaseous H_2O (Atherton et al., 1971; Morimoto and Morishige, 1974; Morimoto and Morishige, 1975).

The interaction of CO and CO_2 with specific planes of ZnO has been examined with a variety of techniques. Low temperature (90°K) chemisorption of CO occurred on both polar and nonpolar planes by σ interaction of the carbon end of the molecule to zinc ions (Gay et al., 1980; Sayers et al., 1980; McClellan et al., 1981). At higher temperatures (25-200°C), CO adsorbed irreversibly on nonpolar surfaces, yielding CO_2 when desorbed (Hotan et al., 1979). Two types of adsorbed CO_2 were identified by temperature programmed desorption on nonpolar and stepped planes: the weaker species was assumed to occur on zinc-oxygen pairs, while the stronger species occurred on anion vacancies or steps (Cheng and Kung, 1982). The CO_2 desorbed as a result of CO adsorption was the stronger species. Reversible CO adsorption took place on polar and stepped planes. At higher temperatures, CO adsorption on polar, stepped, and nonpolar planes resulted in CO_2 desorption.

When carbon monoxide was adsorbed on ZnO in the presence of hydrogen significant shifts were observed in Type I hydrogen adsorption bands (Dent and Kokes, 1969b; Boccuzzi et al., 1978b). The stretch frequency of the OH band shifted continuously to higher wavenumbers with increasing

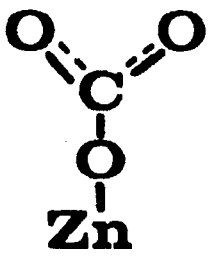

UNIDENTATE
CARBONATE

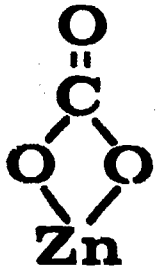

BIDENTATE
CARBONATE

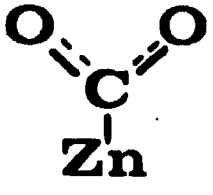

CARBOXYLATE

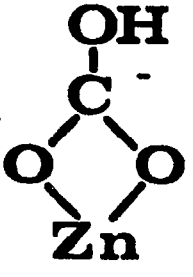

BICARBONATE

Figure 14. Adsorbed carbonates on ZnO

carbon monoxide pressure; the maximum value observed by Boccuzzi was 3523 cm^{-1}. The ZnH band transformed into a triplet structure which gradually shifted to lower wavenumbers with increasing carbon monoxide pressure. The triplet arose from interactions caused by carbon monoxide adsorption on zinc ions adjacent to the ZnH species. Additional weak bands have been observed at 2770 and 2661 cm^{-1} which were assigned to a formyl species (see Figure 15) (Saussey et al., 1982). An interaction occurred between CO and a weakly adsorbed species of hydrogen at room temperature, although the exact nature of this surface product was unknown (Giamello and Fubini, 1981).

The reaction of carbon dioxide and hydrogen on ZnO at 230°C was studied using simultaneous infrared and kinetic measurements (Ueno et al., 1970). An intermediate adsorbed species identified as a formate ion produced infrared bands at 2870, 1572, 1369, and 1379 cm^{-1}; these bands were assigned to the C-H stretching frequency, the asymmetric and symmetric O-C-O stretching frequencies, and the in-plane C-H bending frequency, respectively. Formic acid adsorption on ZnO formed formate ions which decomposed to yield ZnH and gaseous CO_2 (Noto et al., 1967). Formic acid decomposition on a nonpolar ($1\bar{1}00$) plane produced adsorbed CO and atomic oxygen; the carbon end of the CO molecule was proposed to be bonded to an oxygen ion rather than zinc (Lüth et al., 1976).

The adsorption and decomposition of methanol on ZnO have been investigated. At room temperature, dissociative adsorption produced hydroxyl and methoxy groups (Nagao and Morimoto, 1980). At 200°C, methoxy groups decomposed to formate ions and hydrogen; formate ions decomposed to yield CO (Ueno et al., 1971). Formate ions also reacted

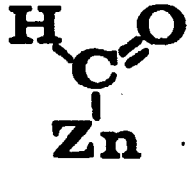

FORMYL

FORMALDEHYDE

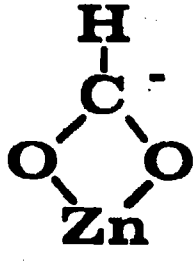

FORMATE

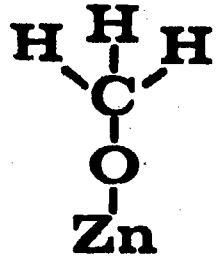

METHOXY

Figure 15. Adsorbed hydrocarbons on ZnO

with gaseous methanol to produce CO_2 and H_2. Methoxy groups can be displaced by gaseous water to form hydroxyl groups. The adsorption of methanol on a nonpolar ($1\bar{1}00$) surface produced a methoxy species bonded to the surface through the oxygen atom (Rubloff et al., 1976). Methanol decomposition on polar, stepped, and nonpolar planes of ZnO was investigated using temperature programmed desorption (Cheng et al., 1983). The product composition from the various surfaces indicated that the decomposition reaction was structure-sensitive. Nonpolar planes with anion vacancies and stepped planes produced methane, hydrogen, carbon monoxide, and carbon dioxide. The polar plane produced formaldehyde, water, hydrogen, carbon monoxide, and carbon dioxide.

Summaries of formate and methoxy infrared band assignments are presented in Tables 10 and 11, respectively.

Adsorption on Copper and Copper Oxide

The huge success of utilizing transmission infrared spectroscopy for characterizing surface species on ZnO has not been enjoyed in the characterization of copper and copper oxide because of strong infrared absorption. To overcome this problem, some studies have used infrared-transmitting supports such as silica or alumina to obtain a spectrum. Carbon monoxide adsorption on copper oxide (CuO) supported by silica produced bands near 2170 and 2140 cm^{-1} which were assigned to chemisorbed and physically adsorbed CO, respectively (London and Bell, 1973). Reflection-absorption spectroscopy has been utilized successfully in studies of adsorbed CO on copper. Initial investigations on copper

Table 10. Infrared bands of surface formates on zinc oxide

Fundamental frequencies, cm^{-1}	HCOOH adsorption[a]	CH_3OH decomposition[b]
$\nu_1(A_1)$ C-H stretching	2870	2870
$\nu_2(A_1)$ symmetric C-O stretching	1369	1367
$\nu_3(A_1)$ symmetric C-O bending	–	–
$\nu_4(B_1)$ asymmetric C-O stretching	1572	1571
$\nu_5(B_1)$ in-plane C-H bending	1379	1382
$\nu_6(B_2)$ out-of-plane C-H bending	–	–

[a]Ueno et al., 1970.

[b]Ueno et al., 1971.

[c]Miyata et al., 1981.

[d]Hota et al., 1977.

Butanol oxidation[c]	Methylpropene oxidation[c]	Propene oxidation[d]	DCOOD adsorption[a]
2870	2872	2870	2190
1364	1364	1365	1342
–	–	–	–
1578	1574	1572	1572
–	–	–	–
–	–	–	–

Table 11. Infrared bands of surface methoxides on zinc oxide

Fundamental frequencies, cm^{-1}	CH_3OH adsorption[a]	CH_3OH adsorption[b]	CD_3OD adsorption[a]
Asymmetric CH_3 stretching	2930	2930	2200
Symmetric CH_3 stretching	2830	2813	2050
Asymmetric CH_3 bending	–	–	–
Symmetric CH_3 bending	1470	–	–
CH_3 rocking	–	–	–
C-O stretching	–	–	–

[a]Ueno et al., 1971.

[b]Nagao and Morimoto, 1980.

films revealed a band in the 2100-2110 cm^{-1} region (Pritchard and Sims, 1970). The frequency of adsorbed CO has been found to depend on the crystal face (Pritchard et al., 1975) and on the surface coverage of CO (Horn and Pritchard, 1975; Hollins and Pritchard, 1979; Ryberg, 1982). The effects of dipole-dipole interactions and the extent of π bonding tend to offset each other. The bonding geometry of CO can range from perpendicular on the (100) face to parallel on the (311) face (Sayers et al., 1981).

Formic acid adsorption on copper at room temperature formed both monodentate (1640 cm^{-1}) and bidentate (1350 cm^{-1}) formates characterized with a polarization modulation infrared technique (Wadayama et al., 1983). Methanol adsorbed on oxidized copper surfaces to yield a methoxy species; formaldehyde and hydrogen were formed by the decomposition of

methoxy groups (Wachs and Madix, 1978; Sexton, 1979; Bowker and Madix, 1980). Formaldehyde reacted with adsorbed oxygen on a copper surface to form a very stable formate species which ultimately decomposed to H_2 and CO_2 (Wachs and Madix, 1979).

Adsorption on Alumina and Chromia

Although alumina and chromia were minor components in the mixed metal oxides investigated in this work, some infrared studies have been reviewed to demonstrate that the types of adsorption on these oxides have much in common with adsorption on zinc oxide. Alumina has been one of the most extensively studied oxides because of its importance in catalytic applications. Residual hydroxyl groups have been observed on γ-alumina with bands at 3800, 3780, 3744, 3733, and 3700 cm^{-1} (Peri, 1965). Band positions were affected by temperature and the extent of surface hydration. Carbon monoxide adsorbed weakly to produce a band at 2200 cm^{-1} and was also oxidized to yield surface carbonates (Parkyns, 1967). These same carbonates were produced by CO_2 adsorption (Parkyns, 1969). Bicarbonate species formed bands at 3605, 1640, 1480, and 1233 cm^{-1} while a bidentate carbonate species was assigned to bands at 1850 and 1180 cm^{-1}. Physically adsorbed CO_2 produced a band in the 2346-2367 cm^{-1} region. Other investigators have also observed these surface compounds during CO_2 adsorption (Fink, 1967; Gregg and Ramsay, 1969; Morterra et al., 1977; King, 1980).

Formic acid adsorption on alumina produced a formate ion and a surface proton (Noto et al., 1967). Only the C-H stretching frequency

at 2915 cm^{-1} was identified. Methanol adsorption produced methoxy groups and physically adsorbed methanol at room temperature, while at higher temperatures (above 150°C), a formate species was also formed (Greenler, 1962; Kagel, 1967; Hertl and Cuenca, 1973). It was proposed that a methoxy group reacted with an adjacent hydroxyl group to produce hydrogen and a bidentate formate species.

The adsorption of water, carbon monoxide, and carbon dioxide on chromia has been investigated using transmission infrared spectroscopy (Zecchina et al., 1971a and 1971b). Light scattering was a major problem at higher wavenumbers, obscuring detail in the hydroxyl region. Five OD bands were observed at 2700, 2675, 2600, 2535, and 2430 cm^{-1} which arose from the dissociative chemisorption of D_2O; the coordinative chemisorption and physical adsorption of water also occurred on the surface. Carbon monoxide adsorption at room temperature produced two types of species: a σ-bonded species with a band frequency of 2170-2184 cm^{-1}, depending on the surface coverage, and an adsorbed CO species with partial π bonding having a stretching frequency near 2130 cm^{-1}. Water and carbon monoxide were adsorbed on the same sites. Carbon dioxide adsorption formed bicarbonate and carbonate species as well as a physically adsorbed CO_2 species.

The decomposition of olefins over chromia has been found to produce an adsorbed formate species with bands in the regions of 2800-3000 cm^{-1}, 1560-1565 cm^{-1}, and 1360 cm^{-1} which correspond to the C-H stretching frequency, the O-C-O asymmetric stretching frequency, and O-C-O symmetric stretching frequency of the formate, respectively (Budneva et al., 1975; Kuznetsov et al., 1977). Methanol adsorption produced physically ad-

sorbed methanol, methoxy groups, and formate groups on chromia (Davydov et al., 1971). Methanol decomposition on an oxygenated surface yielded a band at 1620 cm^{-1} which was assigned to the C=O stretching frequency of a formaldehyde species on the surface.

Adsorption on Mixed Metal Oxides

Infrared spectroscopy has not been utilized in adsorption studies on mixed metal oxides for methanol synthesis. The formation of surface species generally has been based on the amount of a gaseous compound adsorbed on the surface and the nature of desorbed species. A study of CO adsorption on a Cu-Zn-Al oxide catalyst as a function of the oxygen content of the oxide indicated that CO formed a surface carbonate at temperatures above 40°C (Ostrovskii et al., 1978). Carbon monoxide adsorption on a strongly reduced surface was very slow. Hydrogen adsorption on a Cu-Zn-Cr oxide catalyst was found to increase with increasing copper content (Rudnitskii et al., 1973). This hydrogen was not associated with reduction of the catalyst and could be directly related to the activity for methanol synthesis. The simultaneous adsorption of carbon monoxide and hydrogen on a Cu-Zn-Cr oxide catalyst at atmospheric pressure showed that each reactant enhanced the adsorption of the other (Tsuchiya and Shiba, 1965). An intermediate surface species having the formula $-OCH_3$ was proposed based on the amounts of each reactant adsorbed. A critical assumption in this approach was that the methoxy species dominated the surface.

Fourier Transform Infrared Spectroscopy

The use of infrared spectroscopy for the observation and identification of adsorbed species on solid surfaces, especially heterogeneous catalysts, has been very popular in experimental research (Little, 1966; Hair, 1967; Kiselev and Lygin, 1975). Advances in optics and computer technologies have made Fourier transform infrared (FT-IR) spectroscopy a practical alternative to dispersive infrared methods. The basic components of an FT-IR spectrometer consist of an interferometer with the associated optical components and a dedicated computer for performing a Fourier transformation of the data and for executing spectral manipulations of the data. FT-IR spectroscopy offers several advantages compared to dispersive methods (Bell, 1972; Griffiths, 1975; Green and Reedy, 1978). Faster scanning times are possible since all wavelengths are measured simultaneously (Felgett's advantage). The utilization of an internal helium-neon reference laser permits a more accurate wavelength calibration (Connes' advantage). Other advantages include greater energy throughput (Jacquinot's advantage), no interference by stray light or sample emission, and better mechanical reliability (the interferometer mirror is the only moving part during the measurement scans). Infrared spectra of adsorbed species under in situ conditions frequently require that spectral contributions due to gaseous species and the catalyst itself be removed. The computer capabilities of the FT-IR spectrometer can be utilized to remove these background effects. FT-IR spectroscopy is advantageous in transmission infrared spectroscopy for

samples having low transmittance of radiation and for studying transients involving limited data acquisition time (Bell, 1980).

EXPERIMENTAL APPARATUS AND METHODS

Fourier Transform Infrared Spectrometer

A Bruker-Physik AG Model IFS 113 spectrometer was used to obtain infrared spectra. Both the spectrometer and the data system were supplied by USA Bruker Instruments and serviced by IBM. The spectrometer, shown in Figure 16, is divided into four compartments; the detector, sample, interferometer, and source sections. During use, the sample compartment can be isolated from the other sections. The source chamber has both a Globar and a mercury arc lamp source. The radiation from the source is directed through an aperature into the interferometer chamber to a filter assembly, and through to the beamsplitter. Because the infrared beam comes to a focus at this point, the beamsplitters for both mid- and far-IR are sufficiently small to be placed on a single rotatable wheel controlled by the computer. The two beams leaving the beamsplitter are reflected on opposite sides of a movable double-sided plane mirror. The modulated beam combines at the beamsplitter and is directed to the sample chamber; rotatable mirrors permit beam switching. The radiation passes through the sample chamber to the detector chamber. Two DTS detectors, optimized for either far-IR or mid-IR radiation, measure the intensity of the infrared beam.

The resolution can be varied from 0.05 to 8.0 cm^{-1}, with a minimum scanning time at 8.0 cm^{-1} of 0.2 sec. The data system utilizes a special 24-bit word. Data are stored either on a removable disc or on a floppy disc. Preprogrammed experiments can be executed. The control board permits scope display of inferograms and spectra, which may be

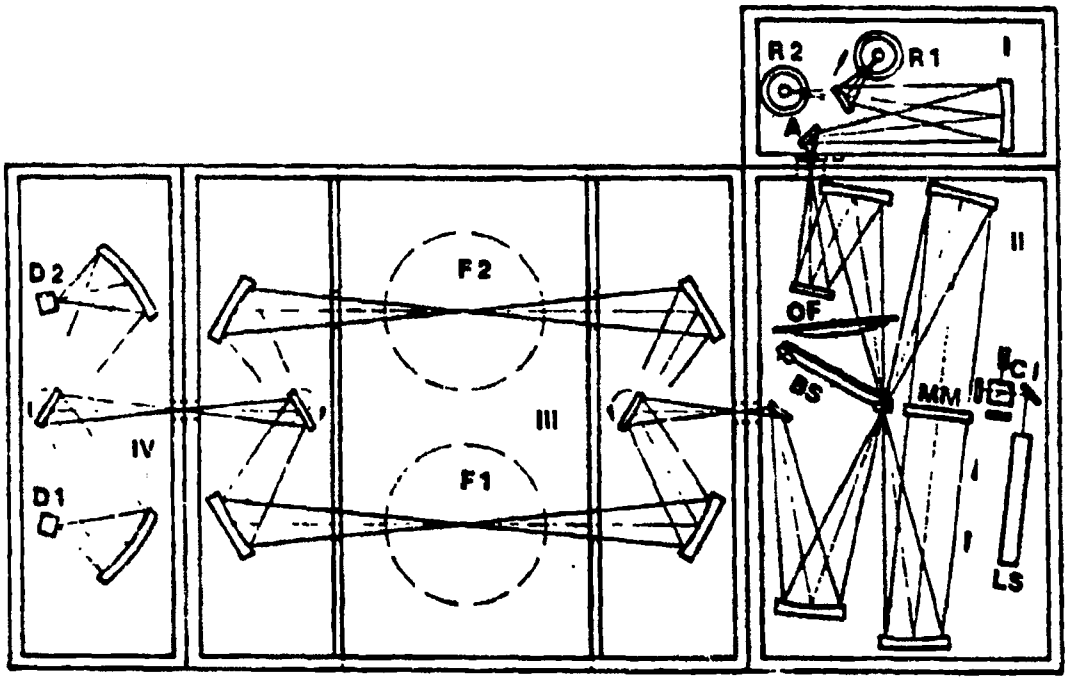

R1	Globar source	MM	Moving mirror
R2	Mercury arc lamp	LS	Laser source
A	Variable aperature	F1	Sample
OF	Optical filter	F2	Reference
BS	Beam splitter	D1, D2	Detectors

Figure 16. Bruker IFS 113 FT-IR spectrometer

manipulated using role and zoom controls. The computer can operate in three task regions simultaneously; data acquisition, data manipulation, and data output (plots) can be undertaken at the same time.

Infrared Photoacoustic Spectroscopy

Although methanol synthesis catalysis typically have a copper content above 30% (metal atom %), these catalysts cannot be studied in their pure state by transmission infrared techniques due to very poor transmittance. Infrared radiation striking a solid that does not transmit photons may either reflect or be absorbed. Recent advancements in the practical application of photoacoustic spectroscopy (PAS) to the characterization of solids provide a method for detecting the radiation absorbed by a sample. This technique is under development in this laboratory, and offers a possible means to characterize those methanol catalysts with high copper contents.

When PAS is combined with FT-IR spectroscopy, a sensitive and relatively quick analytical system is formed. The modulated infrared beam passes through a window into the sample chamber and is absorbed by the sample (Figure 17). The radiation is converted to heat by nonradiative de-excitation of the sample. Because the infrared energy is modulated, the surface heats and cools as the incident energy rises and falls. This thermal cycle causes the gaseous boundary layer next to the surface to expand and contract, producing sound waves detected by a sensitive microphone. The signal is then processed by the FT-IR data system into an infrared spectrum.

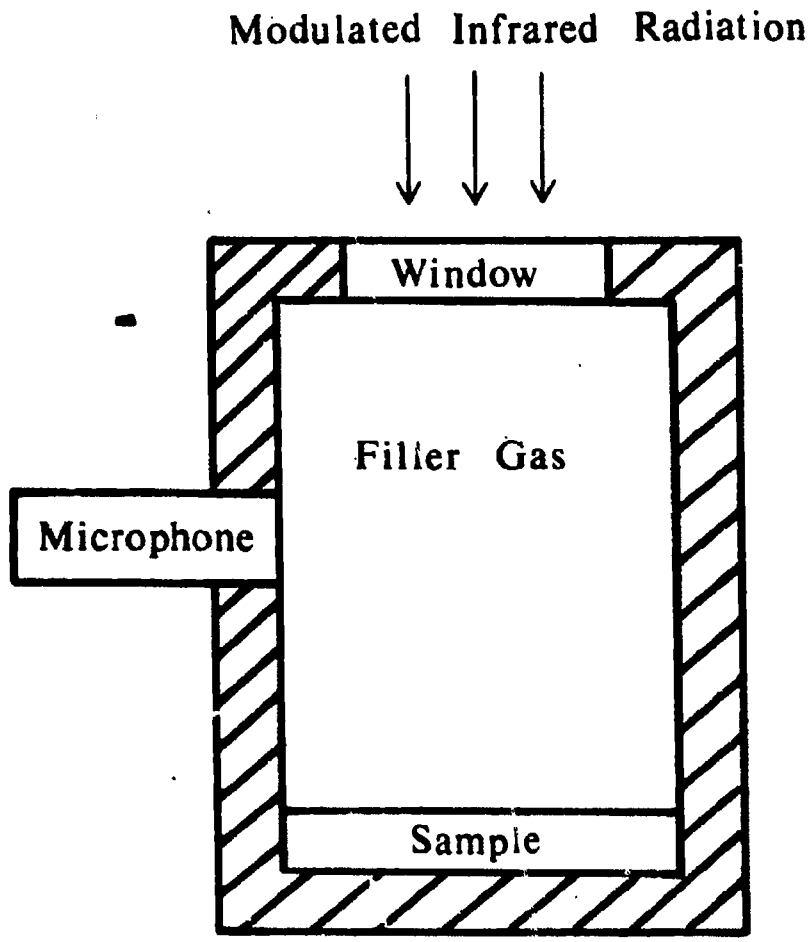

Figure 17. Photoacoustic cell

Sample Preparation for Transmission Infrared Studies

All oxides used in transmission infrared studies were heated at 350°C overnight under a vacuum of 10^{-4} torr to remove adsorbed carbonates and water. After cooling the oxide to room temperature in helium, this powder was transferred in air to a vial and capped to prevent contamination by atmospheric CO_2. Samples could be taken from a vial over a period of several months before this treatment needed to be repeated. Zinc oxide wafers were prepared by pressing some powder under a load of 3200 kg into a wafer 20.6 mm in diameter and 0.2-0.3 mm thick. Binary and ternary oxides were pressed under a load of 4500 kg into wafers 0.06-0.12 mm thick. Zinc oxide wafers were relatively thick because thinner wafers were too brittle to handle; binary and ternary wafers were made as thin as possible to achieve sufficient transmittance for in situ studies. All these oxides tended to adhere to the metal faces of the die; thin sheets of Mylar were placed on the die faces when ZnO and binary oxides were compressed, whereas thin sheets of glassine paper were used with ternary oxides. Wafers were carefully transferred into the infrared cell and placed in the spectrometer. Details of the infrared cell design will be presented in Part III. Adsorbed water on the catalyst wafer was removed by flowing nitrogen gas through the cell overnight (about 12 hours) at atmospheric pressure and 200°C (pretreatment #1). In some cases, the nitrogen gas was passed through water before entering the cell during an overnight treatment at atmospheric pressure and 200°C (pretreatment #2). In some experiments, the catalyst was reduced by flowing a 5% hydrogen stream (the balance was nitrogen) through

the cell for 1 hour at atmospheric pressure and 200°C (pretreatment #3).

All adsorption experiments were conducted in a continuous flow mode. Gaseous adsorbates were passed through the cell at 60 cc/min STP. Liquids such as water, methanol, or formic acid solution were introduced to the cell in low concentrations by passing a carrier gas (normally nitrogen) through the liquid when the liquid was enclosed in a glass container (saturator). Formaldehyde was introduced to the cell at its vapor pressure (1.4 torr at 25°C) by heating solid paraformaldehyde in the saturator while carrier gas flowed through. The outlet line from the saturator developed some paraformaldehyde on the inner walls, indicating that the formaldehyde was at saturation. Flow conditions in the line to the cell were 60 cc/min, 25°C, and 1 atmosphere. High purity gases were used and the adsorbates are listed in Table 12.

Table 12. Adsorbate specifications

1.	Eastman Formic Acid (88%), Reagent ACS
2.	Kodak Paraformaldehyde, 90% min.
3.	Fisher Scientific Methanol, Reagent ACS
4.	Aldrich Chemical Methanol-d, 99.5% + D
5.	Aldrich Chemical Methanol-d_4, 99.5% + D

RESULTS O. · · PHER· ADSORPTION

Adsorpti · . on · ·xide

The method of preparation of zinc · . has a very strong effect on its infrared transmission property. Zinc oxide made by the oxidation of metallic zinc (dry process) transmits infrared radiation well, whereas precipitated zinc oxide (wet process) rapidly loses transmittance when the oxide is reduced. Reduction involves the removal of some oxygen creating excess zinc (possibly interstitial zinc) and releasing electrons to the conduction band of the oxide. A commercially available ZnO compound (Kadox 25) prepared by the dry process was used in these adsorption studies to avoid excessive transmission losses.

An oxidized (pretreatment #1) zinc oxide wafer was reduced in a 5% hydrogen-95% nitrogen stream at 200°C for an hour (pretreatment #3). Figure 18 shows that some of the residual surface carbonate species (bands at 1512, 1466, 1383, and 1326 cm^{-1}) were reduced to surface formate groups (bands at 2976, 2879, 2738, 1582, and 1370 cm^{-1}). The residual surface hydroxyl groups (bands at 3665, 3620, 3565, and 3450 cm^{-1}) were unaffected by the exposure to hydrogen.

The adsorption of carbon monoxide on zinc oxide (pretreatment #1) at 200°C and 1 atmosphere is shown in Figure 19. The transmission was strongly reduced by carbon monoxide (band at 2143 cm^{-1}) making it very difficult to observe infrared bands under 2000 cm^{-1} (Figure 19b). After 8 hours of exposure to carbon monoxide, the cell was flushed with nitrogen to reveal a significant increase in formate groups (bands at 2970, 2875, 2738, 1572, 1381, and 1366 cm^{-1}). The bidentate carbonate

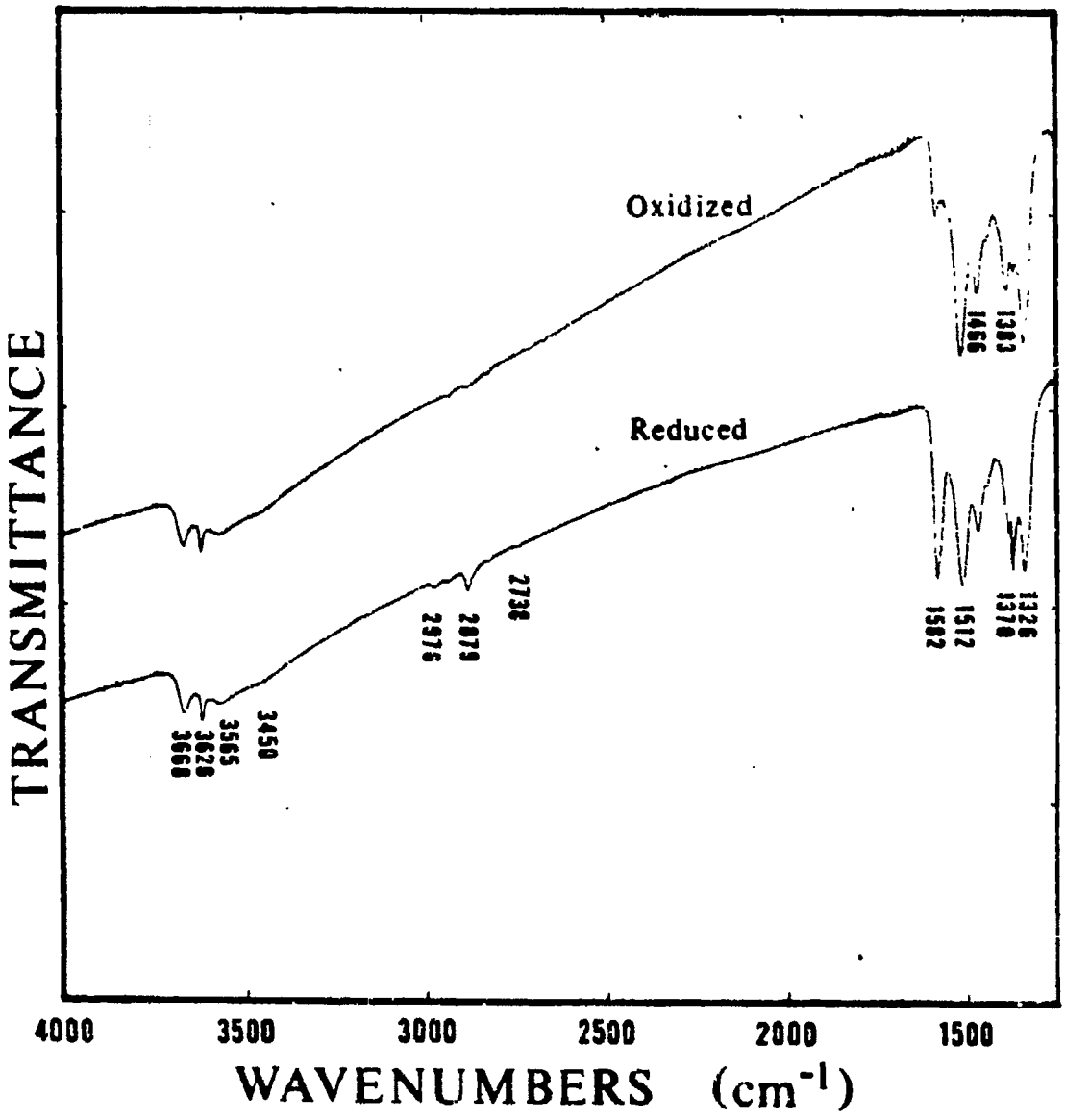

Figure 18. Reduction of Kadox 25 in hydrogen at 200°C

Figure 19. Carbon monoxide adsorption on Kadox 25 at 200°C

a) oxidized surface

b) exposure to CO for 5 minutes

c) purged sample after 8 hours of CO exposure

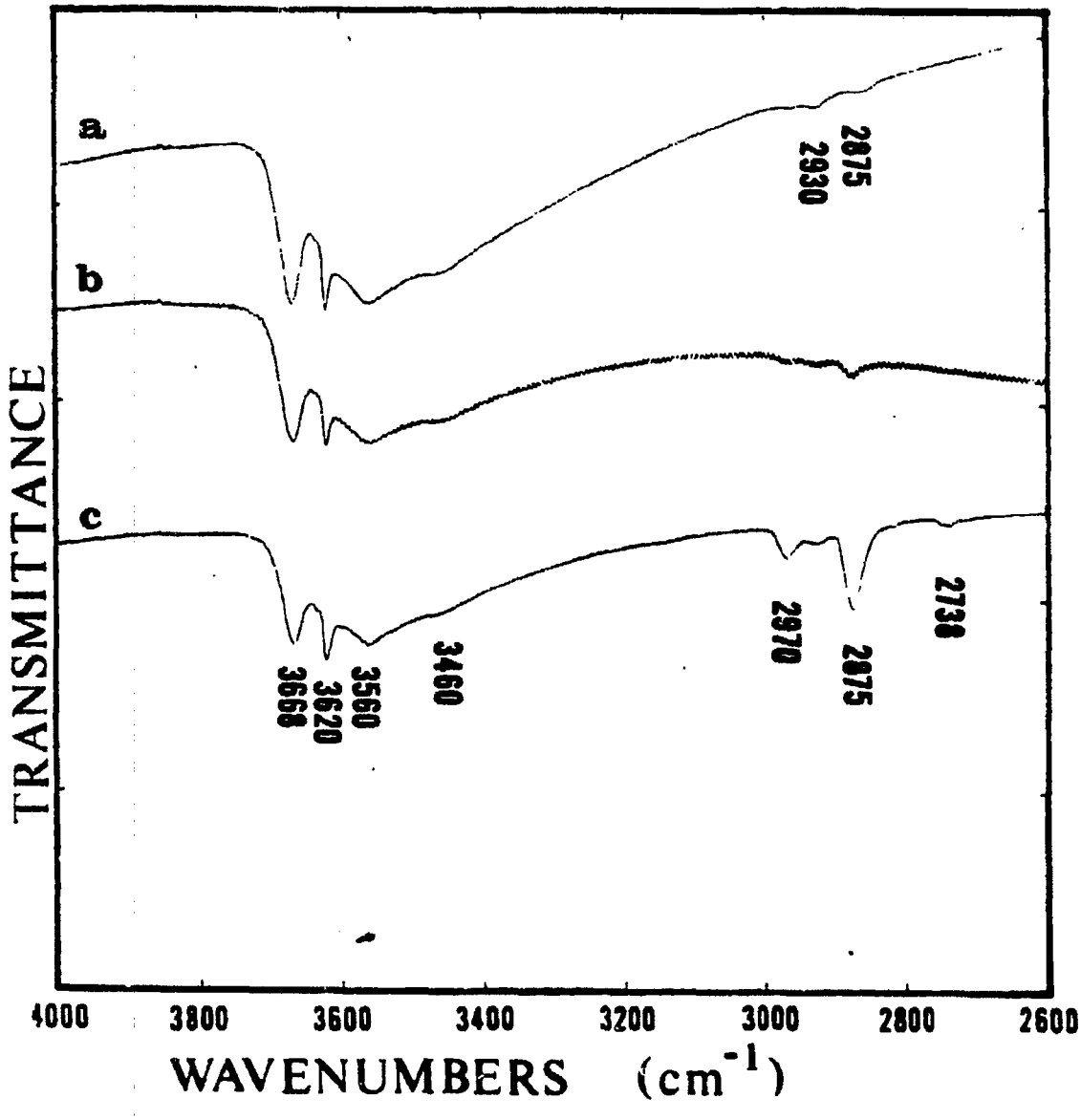
a
b
c
2875
2930
2970
2875
2730
3660
3620
3698
3460
TRANSMITTANCE
4000
3800
3600
3400
3200
3000
2800
2600
WAVENUMBERS (cm-1)

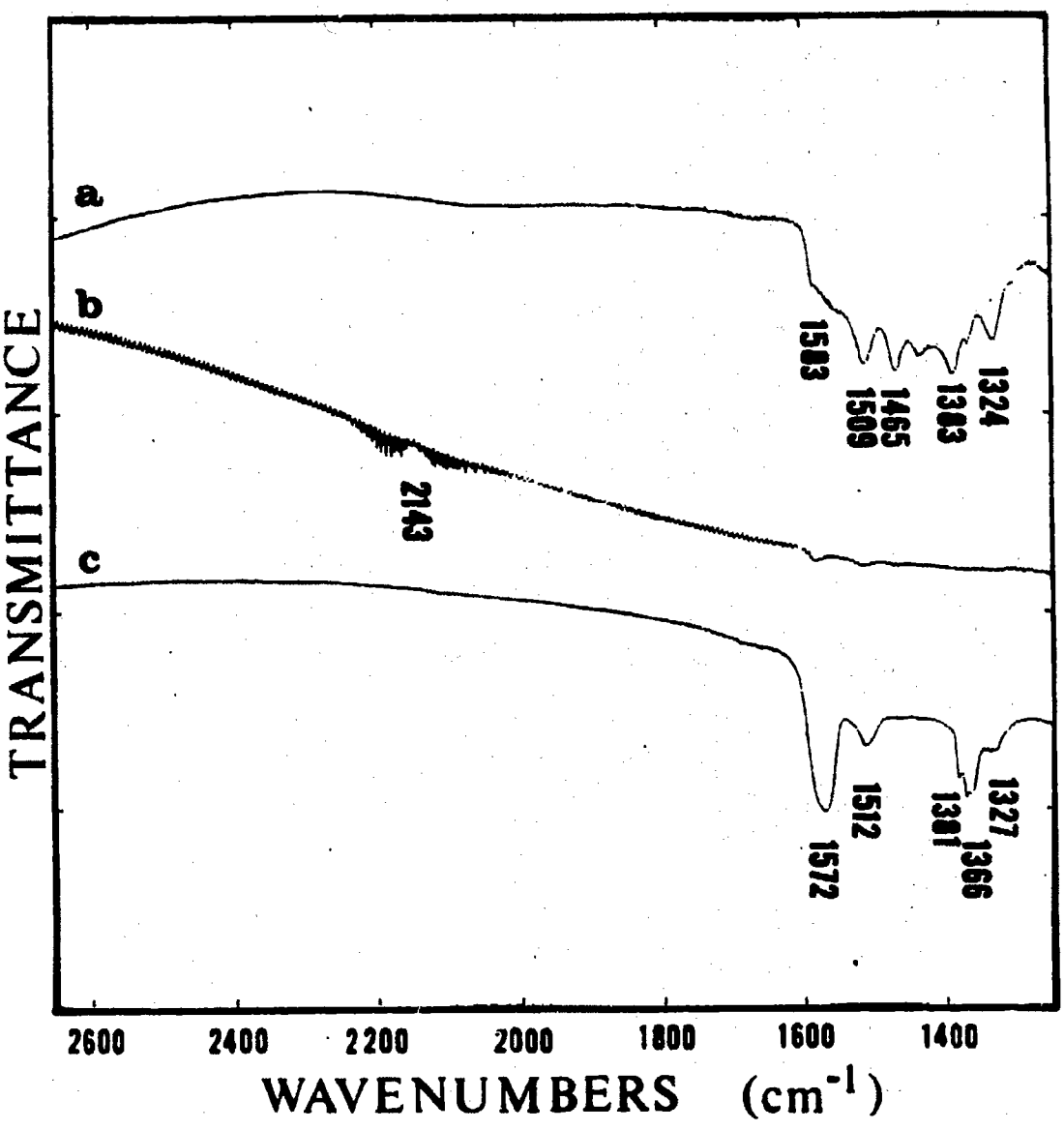

Figure 19. Continued

species (bands at 1512 and 1327 cm^{-1}) have diminished and the unidentate carbonate (bands at 1465 and 1383 cm^{-1}) has disappeared. The hydroxyl region (4000-3000 cm^{-1}) was unaffected by the exposure to carbon monoxide.

The adsorption of carbon monoxide and hydrogen (H_2/CO = 2/1) on zinc oxide (pretreatment #1) at 200°C and 1 atmosphere is shown in Figure 20. The infrared spectra were quite similar to those for carbon monoxide adsorption; the transmission was very low causing a loss of information at lower frequencies. The development of formate groups was indicated by the growth of bands at 2970 and 2875 cm^{-1}.

The presence of stable formate species on Kadox 25 was verified by exposing the oxide to formic acid. The adsorption of formic acid solution (88% HCOOH, 12% H_2O) on zinc oxide (pretreatment #3) at 165°C and 1 atmosphere is shown in Figure 21. The lower adsorption temperature was used to slow the decomposition rate of surface species. Exposure to formic acid solution caused a formate species (bands at 2970, 2882, 2737, 1576, and 1382 cm^{-1}) to form which lacks the sharp detail of the initial formate groups on the reduced surface, possibly because of interactions among species at relatively high concentrations. The hydroxyl groups have been displaced by formate and adsorbed water (bands at 3430 and 1660 cm^{-1}). The formation of gaseous carbon dioxide (vibrational-rotational bands at 2350 cm^{-1}) occurred when the cell was isolated (no flow through the cell), indicating that carbon dioxide rather than carbon monoxide was the primary product of surface formate decomposition.

Figure 20. Adsorption of a CO-H_2 mixture on Kadox 25 at 200°C

a) oxidized surface

b) exposure for 5 minutes

c) exposure for 1 hour

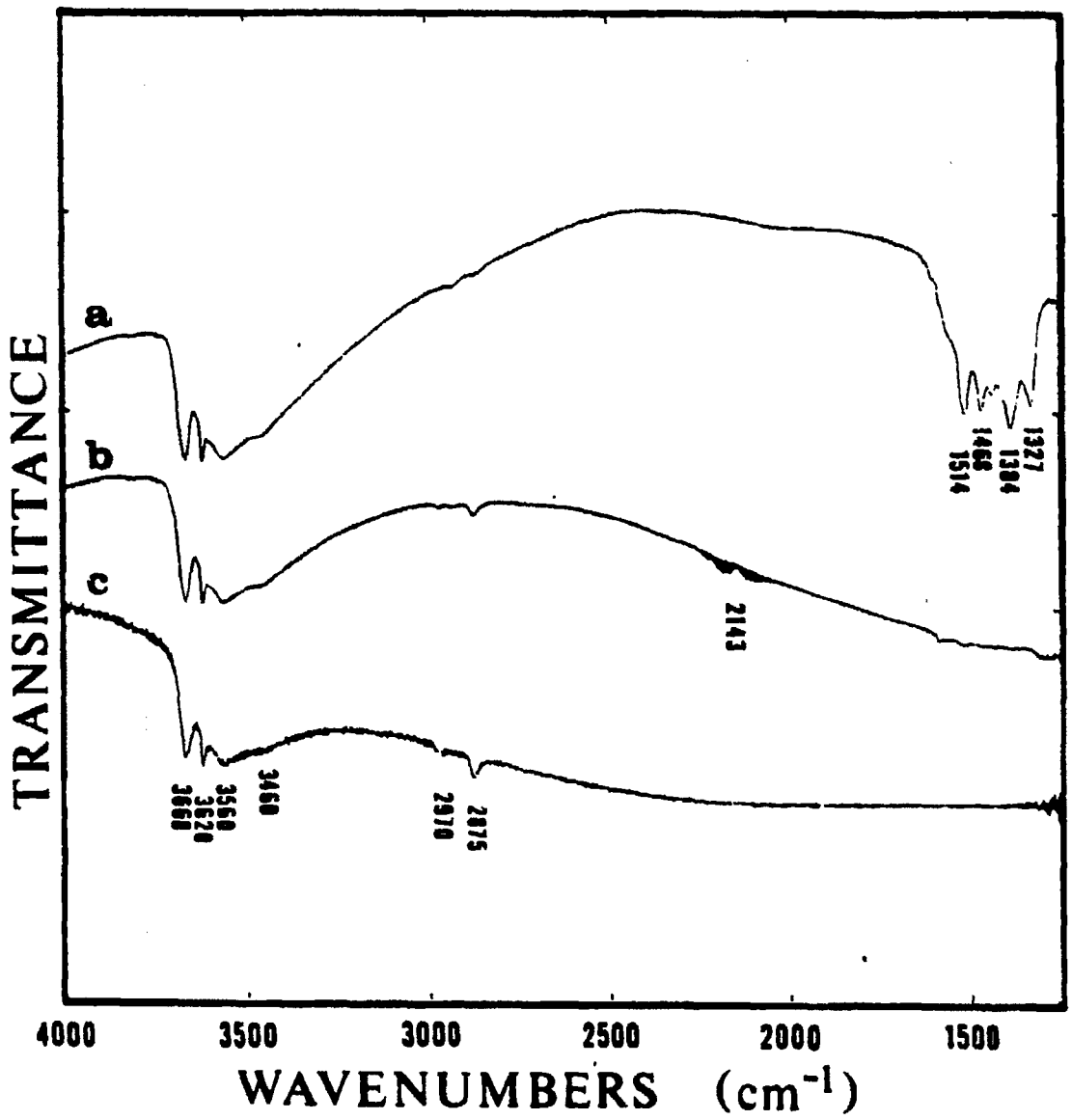
TRANSMITTANCE
a
b
c
1514
1469
1384
1327
2143
3460
2910
2875
4000
3500
3000
2500
2000
1500
WAVENUMBERS (cm-1)

Figure 21. Formic acid adsorption on Kadox 25 at 165°C

a) reduced surface

b) exposure to formic acid solution

c) decomposition of surface formate species in an isolated cell

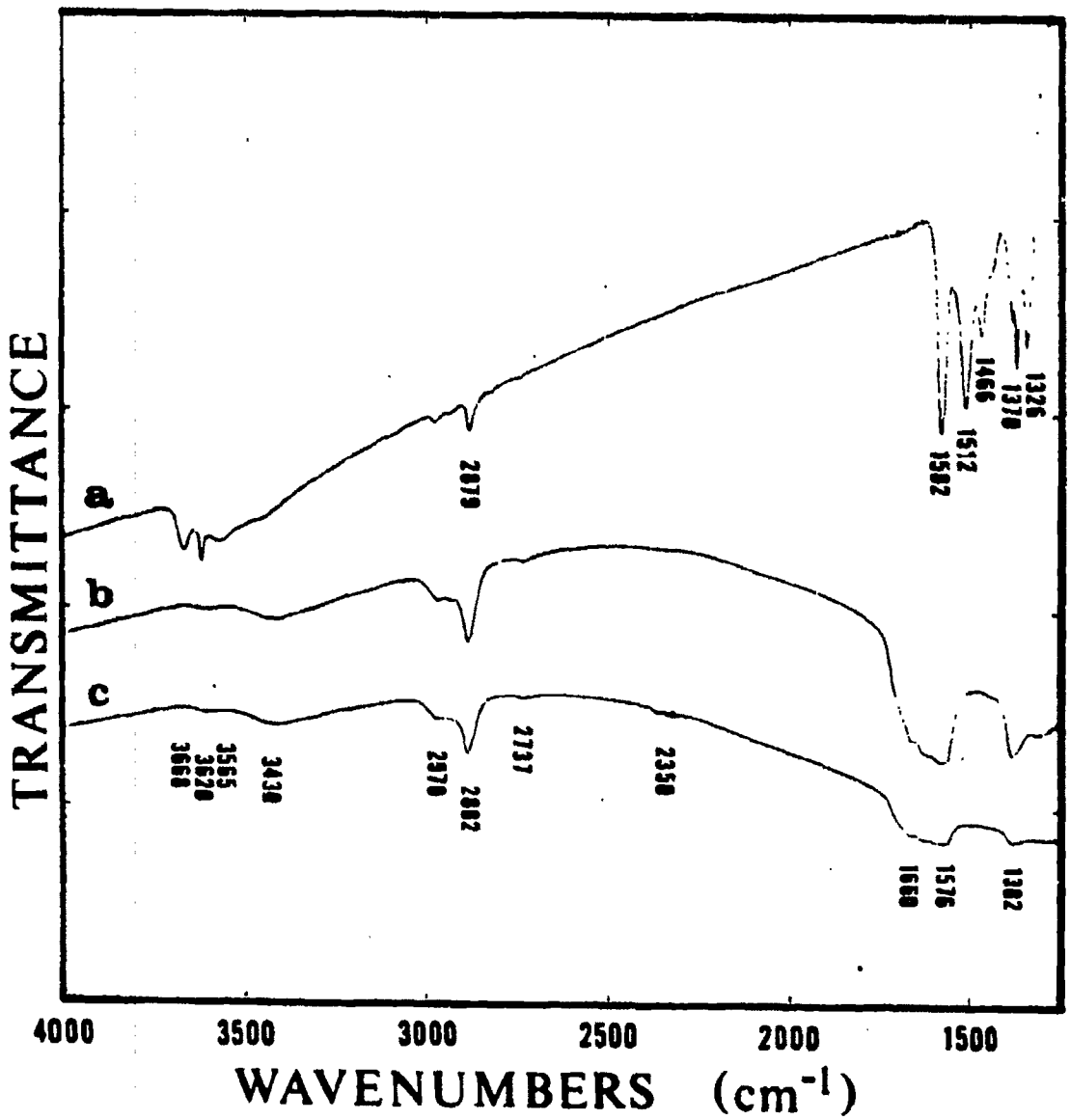
TRANSMITTANCE
a
b
c
2879
1582
1512
1469
1378
1326
3668
3555
3520
3438
2870
2802
2717
2358
1660
1576
1382
4000
3500
3000
2500
2000
1500
WAVENUMBERS (cm-1)

Adsorption on Binary Oxides

Two precipitated binary oxides, 95/5 Zn/Cu and 90/10 Zn/Cu oxides, transmitted sufficient radiation for infrared studies. These binary oxides had the same residual hydroxyl groups as those found on pure zinc oxide and had some residual surface carbonate groups. The reduction of a 95/5 Zn/Cu oxide in a 5% H_2-95% N_2 stream at 200°C (pretreatment #3) is shown in Figure 22. Surface carbonate groups (bands at 1516, 1469, 1380, and 1322 cm^{-1}) were partially reduced to formate species (bands at 2970, 2878, 1576, 1381, and 1366 cm^{-1}). A new hydroxyl band developed at 3252 cm^{-1}. Reduction with deuterium shifted the residual hydroxyl groups to OD groups (bands at 2706, 2667, 2630, and 2560 cm^{-1}) and created a new OD group at 2420 cm^{-1}. If a binary oxide was reduced with hydrogen and subsequently exposed to deuterium, all the hydroxyl groups except the species at 3252 cm^{-1} were rapidly shifted to OD groups.

The adsorption of carbon monoxide on the binary oxides was affected by the condition of the catalyst surface. Figures 23 and 24 show the adsorption of carbon monoxide at 200°C and 1 atmosphere on an oxidized 95/5 and 90/10 Zn/Cu catalyst, respectively. Carbon monoxide adsorbed as a carbonyl species (band at 2093 cm^{-1}) and caused gradual reduction of the oxide. The unidentate carbonate groups quickly disappeared and formate species slowly developed. The vibrational-rotational bands for gaseous carbon monoxide occurred at 2143 cm^{-1}.

The adsorption of a carbon monoxide and hydrogen mixture (CO/H_2 = 1/2) on oxidized 95/5 and 90/10 Zn/Cu catalysts at 200°C and 1 atmosphere is shown in Figures 25 and 26, respectively. Reduction of the oxide

Figure 22. Reduction of 95/5 Zn/Cu oxide at 200°C

a) oxidized surface

b) exposure to 5% H_2 for 30 minutes

c) exposure to 5% H_2 for 2 hours

d) exposure of an oxidized surface to deuterium for 30 minutes

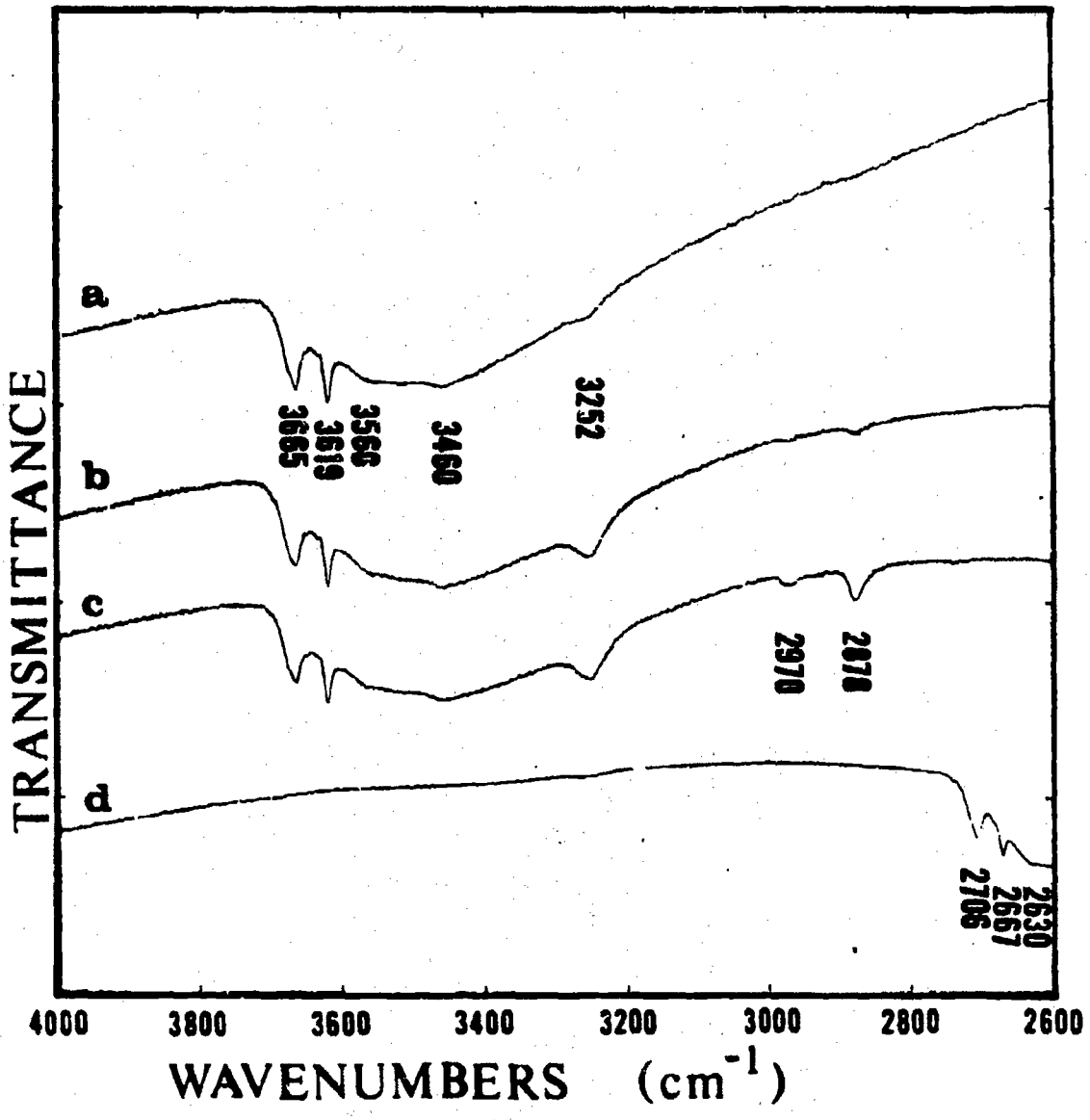
a
b
c
d
3665
3619
3566
3460
3252
2970
2878
2706
2667
2630
TRANSMITTANCE
4000
3800
3600
3400
3200
3000
2800
2600
WAVENUMBERS (cm-1)

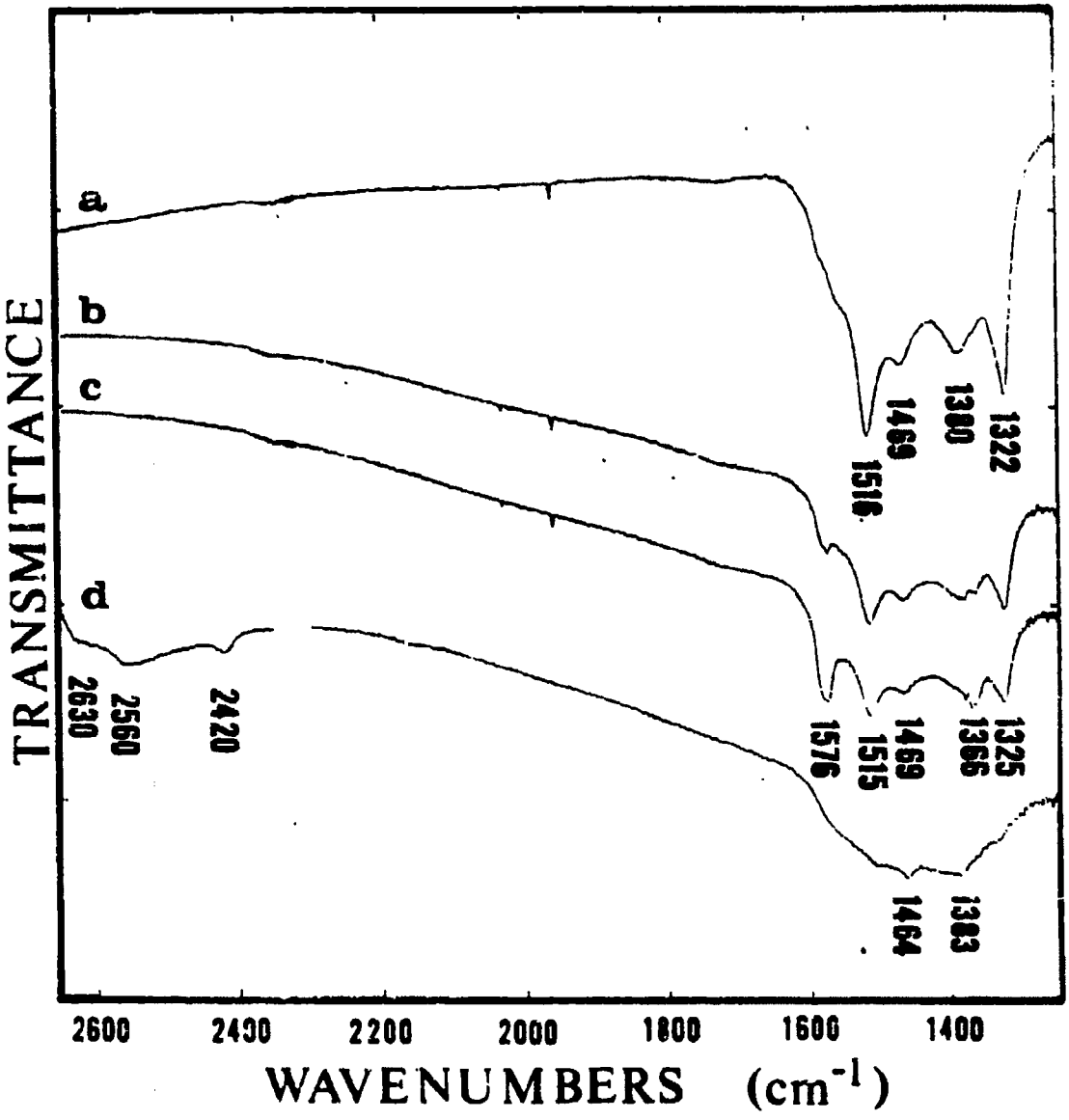

Figure 22. Continued

Figure 23. Carbon monoxide adsorption on 95/5 Zn/Cu oxide at 200°C

a) oxidized surface

b) exposure for 5 minutes

c) exposure for 1 hour

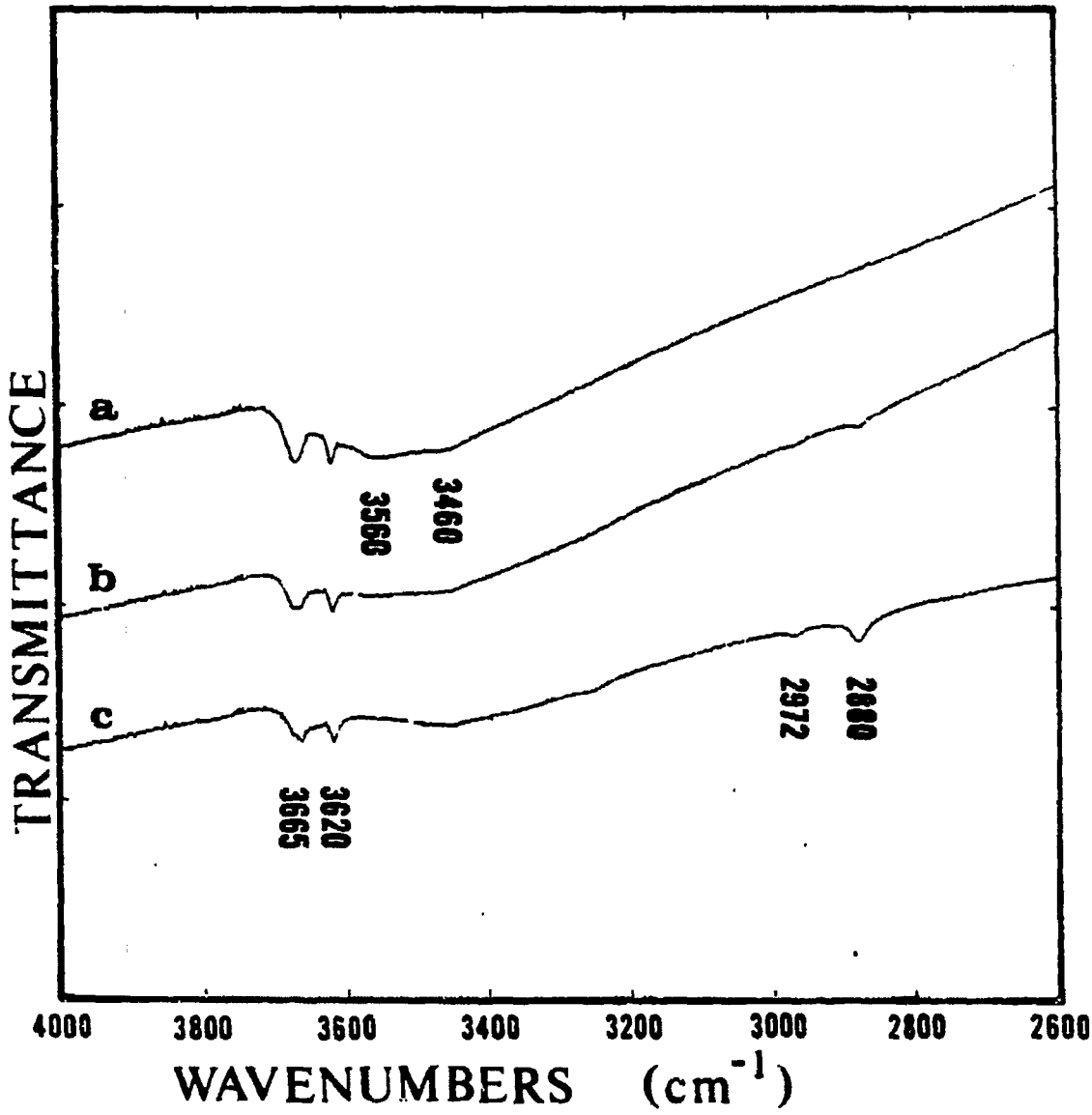
TRANSMITTANCE
a
b
c
3590
3460
3695
3620
2972
2880
4000
3800
3600
3400
3200
3000
2800
2600
WAVENUMBERS (cm-1)

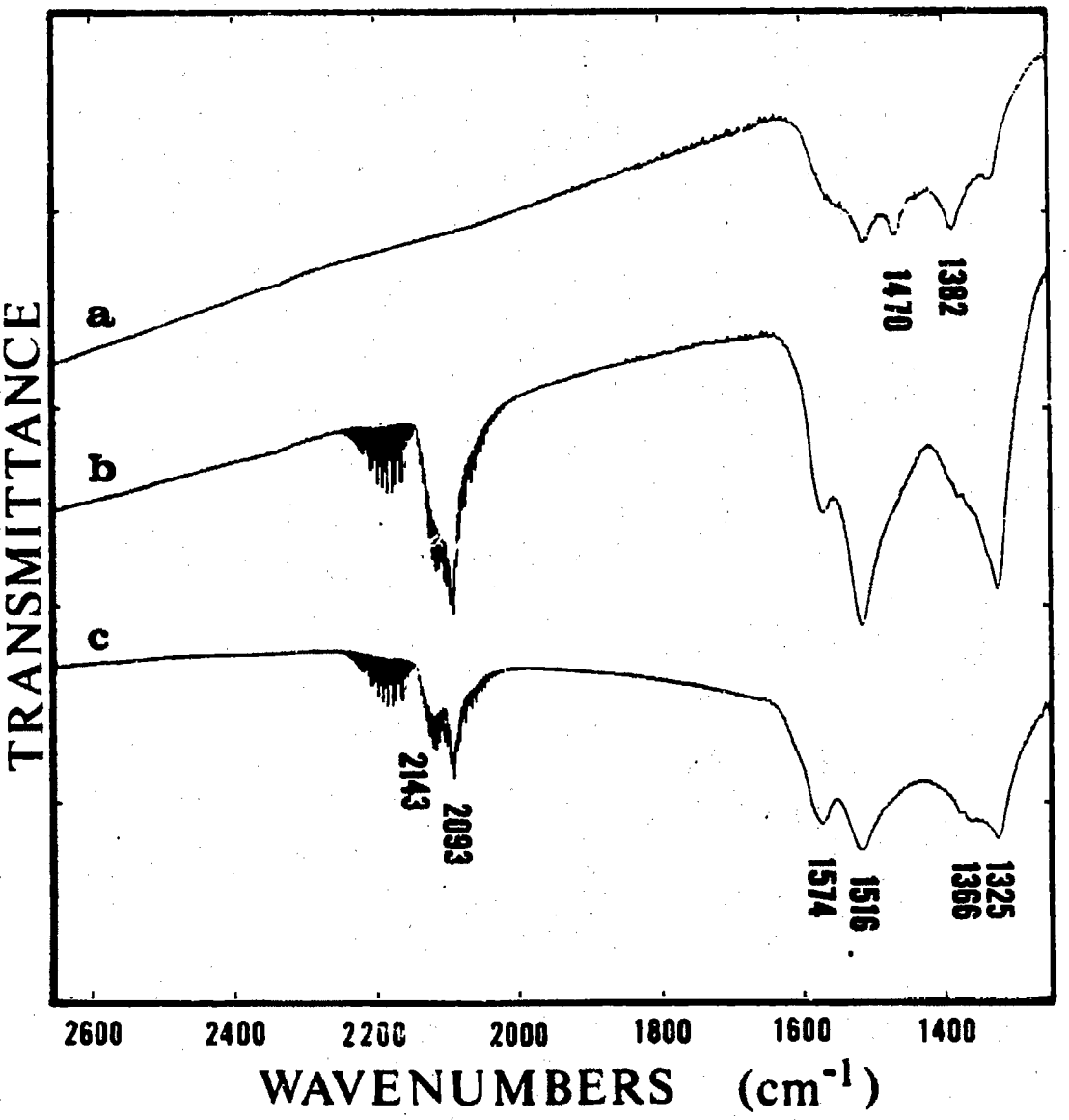

Figure 23. Continued

Figure 24. Carbon monoxide adsorption on 90/10 Zn/Cu oxide at 200°C

a) oxidized surface

b) exposure for 5 minutes

c) exposure for 1 hour

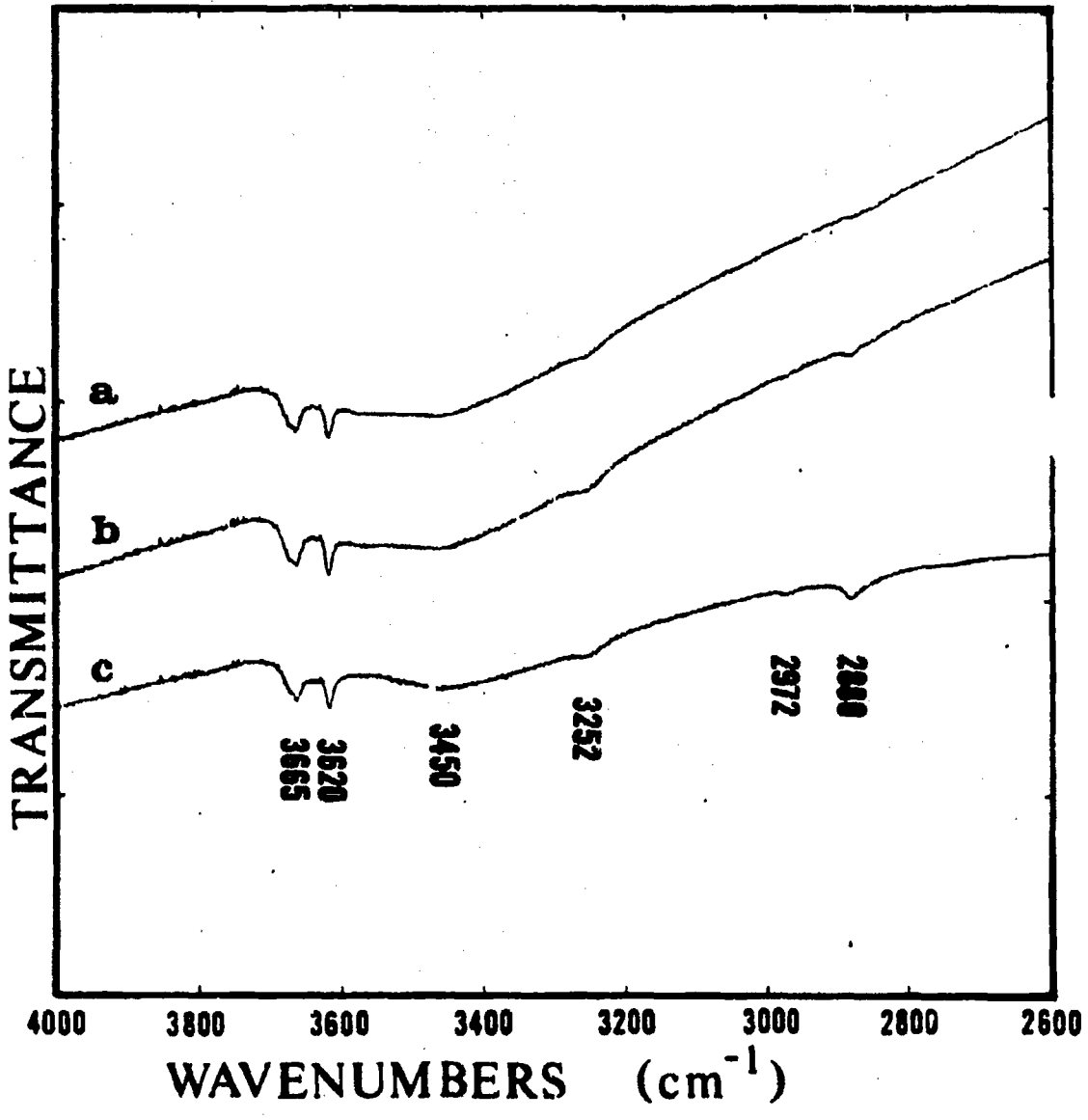
TRANSMITTANCE
a
b
c
3665
3620
3450
3252
2972
2880
4000
3800
3600
3400
3200
3000
2800
2600
WAVENUMBERS (cm-1)

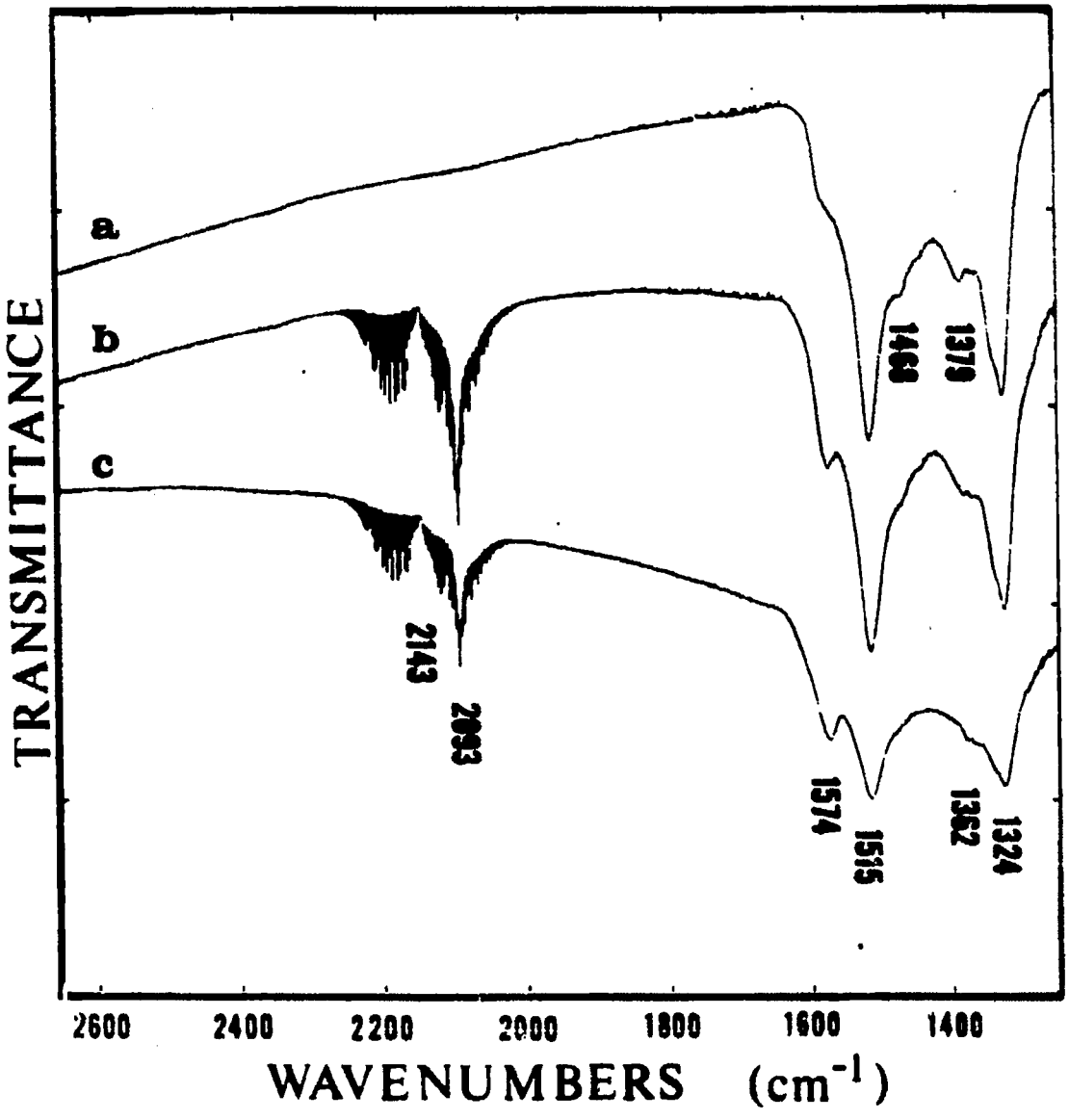

Figure 24. Continued

Figure 25. Adsorption of CO-H_2 mixture on 95/5 Zn/Cu oxide at 200°C

a) oxidised surface

b) exposure for 5 minutes

c) exposure for 1 hour

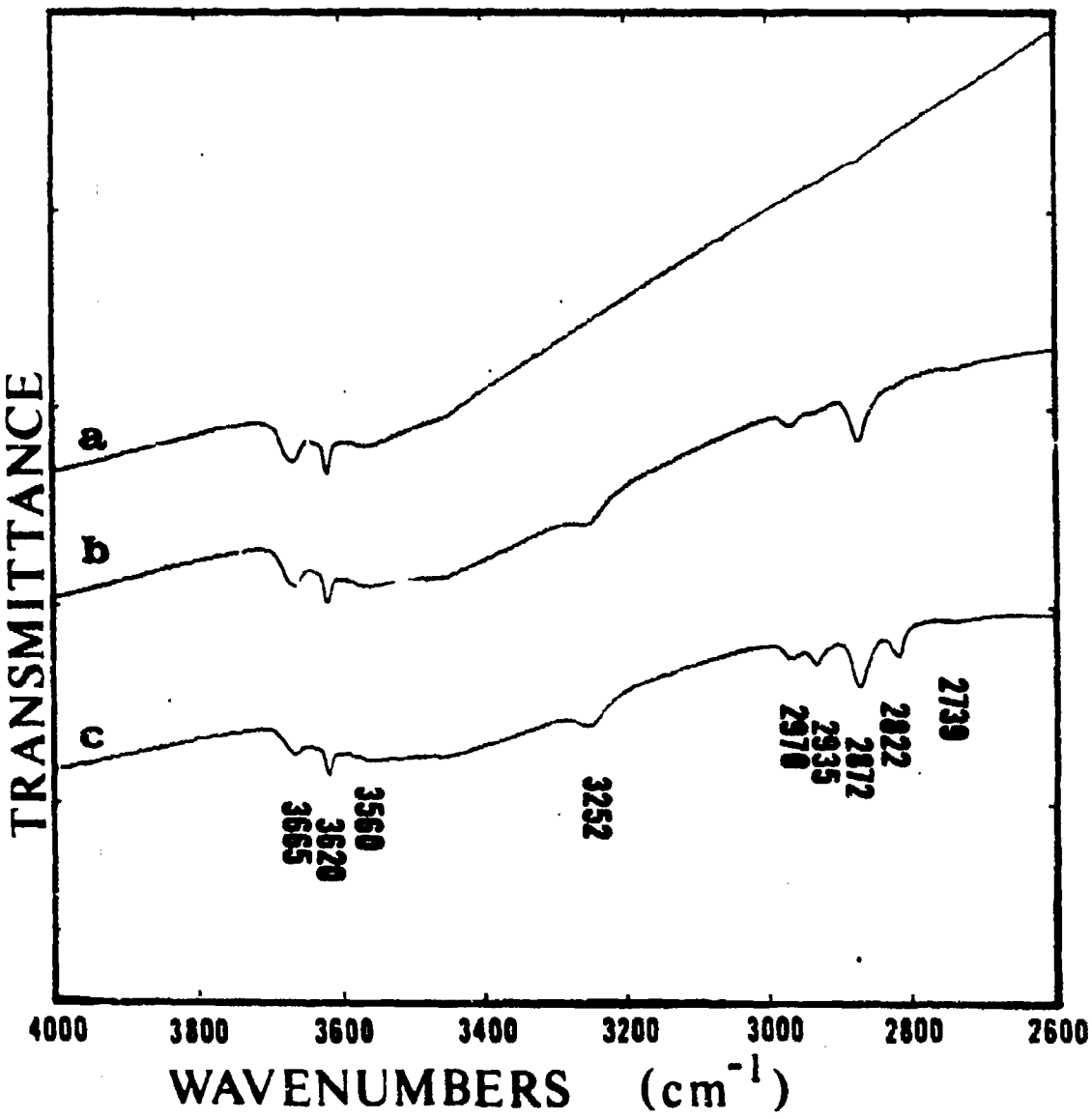
TRANSMITTANCE
a
b
c
3665
3620
3560
3252
2970
2935
2872
2822
2739
4000
3800
3600
3400
3200
3000
2800
2600
WAVENUMBERS (cm-1)

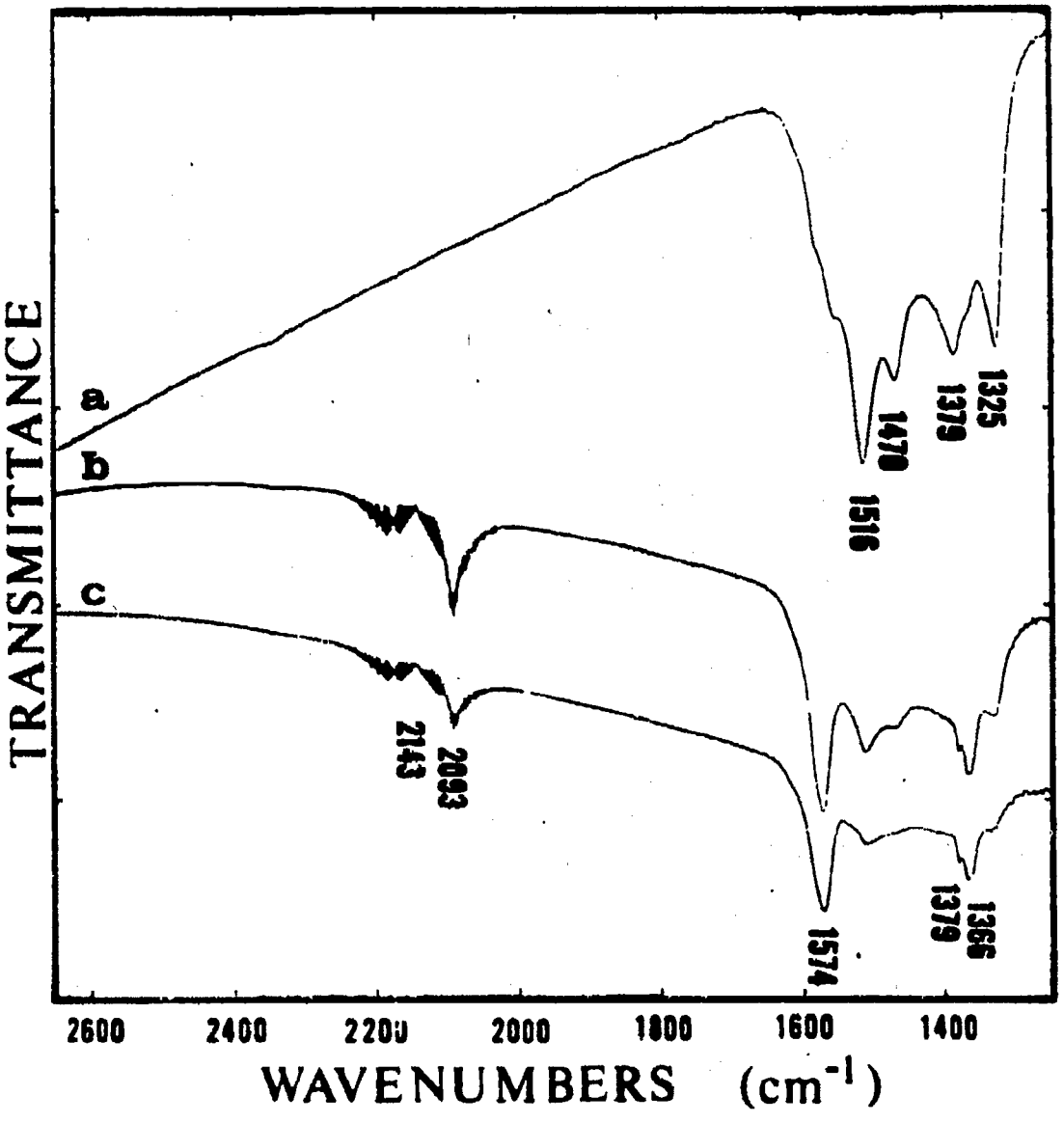

Figure 25. Continued

Figure 26. Adsorption of CO-H_2 mixture on 90/10 Zn/Cu oxide at 200°C

a) oxidized surface

b) exposure for 5 minutes

c) exposure for 1 hour

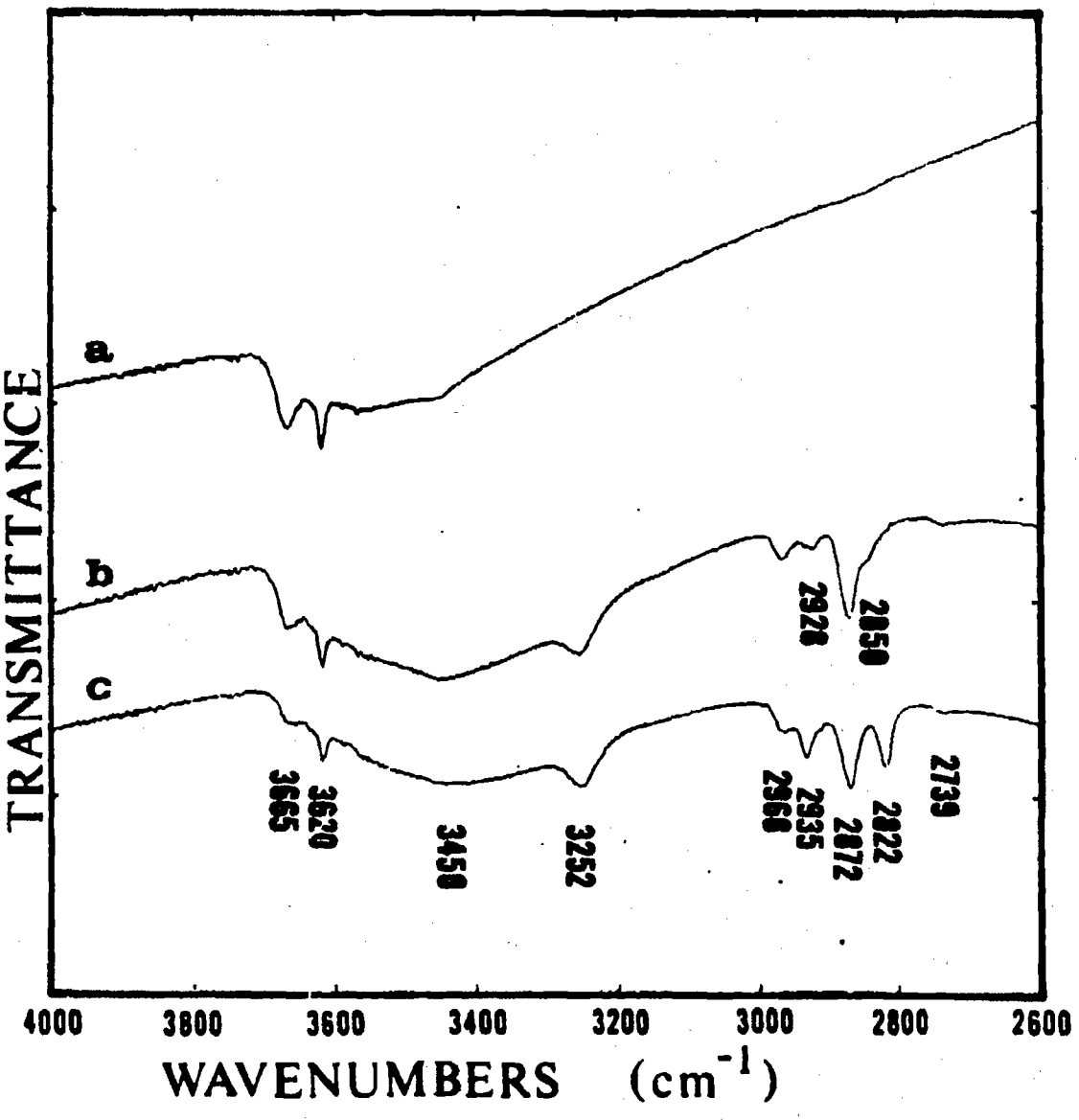
TRANSMITTANCE
a
b
c
2928
2850
3695
3620
3450
3252
2958
2935
2872
2822
2736
4000
3800
3600
3400
3200
3000
2800
2600
WAVENUMBERS (cm-1)

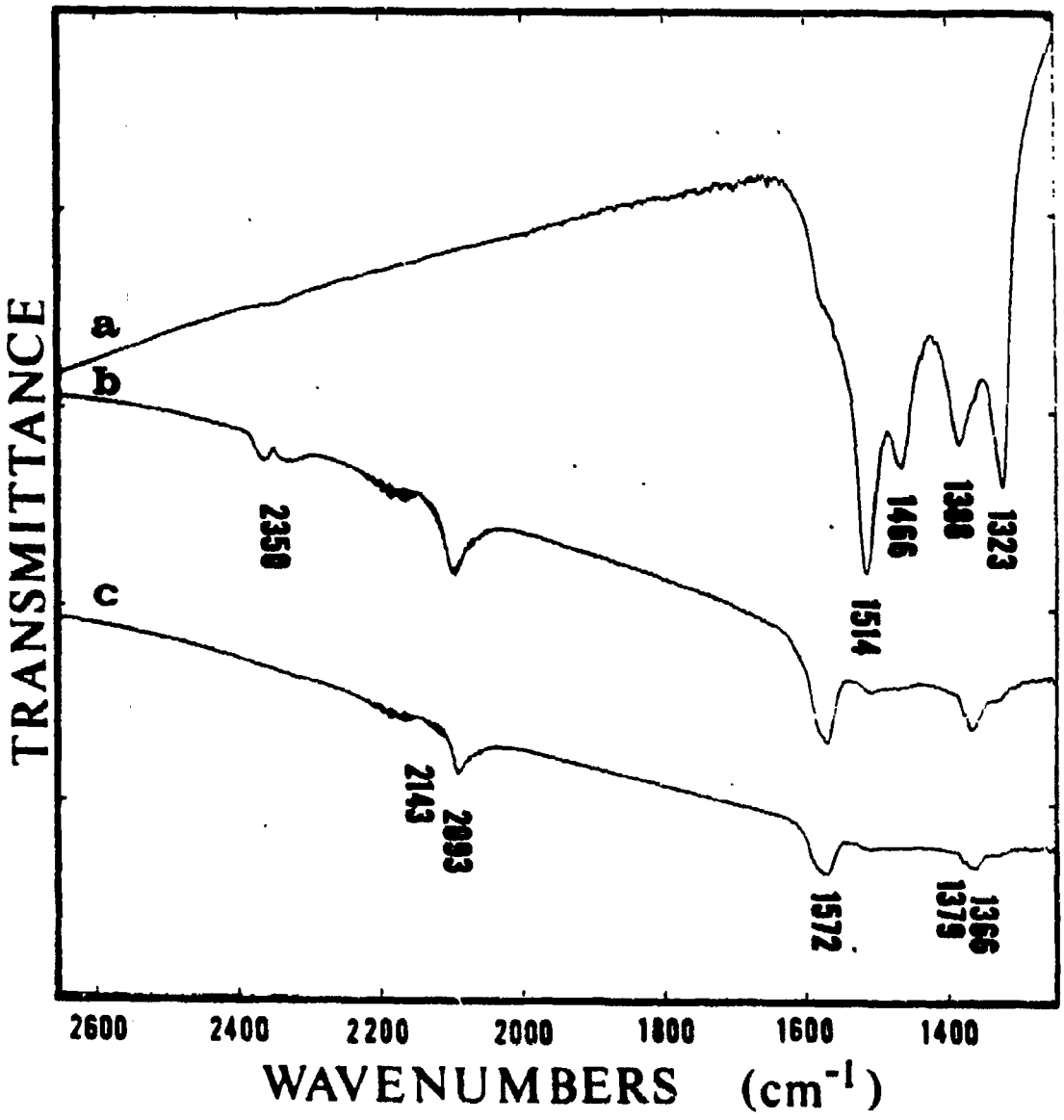

Figure 26. Continued

was rapid in each experiment, indicated by the loss of transmittance and the quick development of the hydroxyl band at 3252 cm^{-1}. The carbonyl species and formate groups were rapidly formed. Methoxy groups (bands at 2935 and 2822 cm^{-1}) gradually developed accompanied by the gradual disappearance of the hydroxyl at 3665 cm^{-1}, suggesting that these species occupied the same sites. The rate of hydrogenation of surface species on the 90/10 Zn/Cu oxide was faster than the rate on 95/5 Zn/Cu oxide. The presence of gaseous CO_2 (band at 2350 cm^{-1}) in the spectrum of 90/10 Zn/Cu oxide immediately after reduction indicated that the water-gas shift reaction was possible. Catalyst reduction by hydrogen was more rapid than reduction by carbon monoxide, forming water which quickly reacted with carbon monoxide to yield carbon dioxide and hydrogen. The carbon dioxide did dissipate within an hour, but the lack of vibrational-rotational bands suggested that the carbon dioxide interacted with the catalyst surface. The presence of CO_2 could also be responsible for the observation of a transient, unstable surface species (bands at 2928 and 2850 cm^{-1}) which was assigned to an adsorbed formaldehyde species.

Carbon monoxide and deuterium (CO/D_2 = 1/2) were adsorbed concurrently on an oxidized 95/5 Zn/Cu catalyst (pretreatment #1) at 200°C to check the band assignments for deuterated surface species. The formation of the OD group at 2418 cm^{-1} showed reduction of the oxide. A carbonyl species (band at 2091 cm^{-1}) was formed and surface carbonate groups were deuterated to yield a formate species (bands at 2166, 1570, and 1336 cm^{-1}). The deuterated methoxy species (one band at 2055 cm^{-1}

Figure 27. Adsorption of CO-D_2 mixture on 95/5 Zn/Cu oxide

a) oxidized surface

b) exposure for 10 minutes

c) exposure for 1 hour

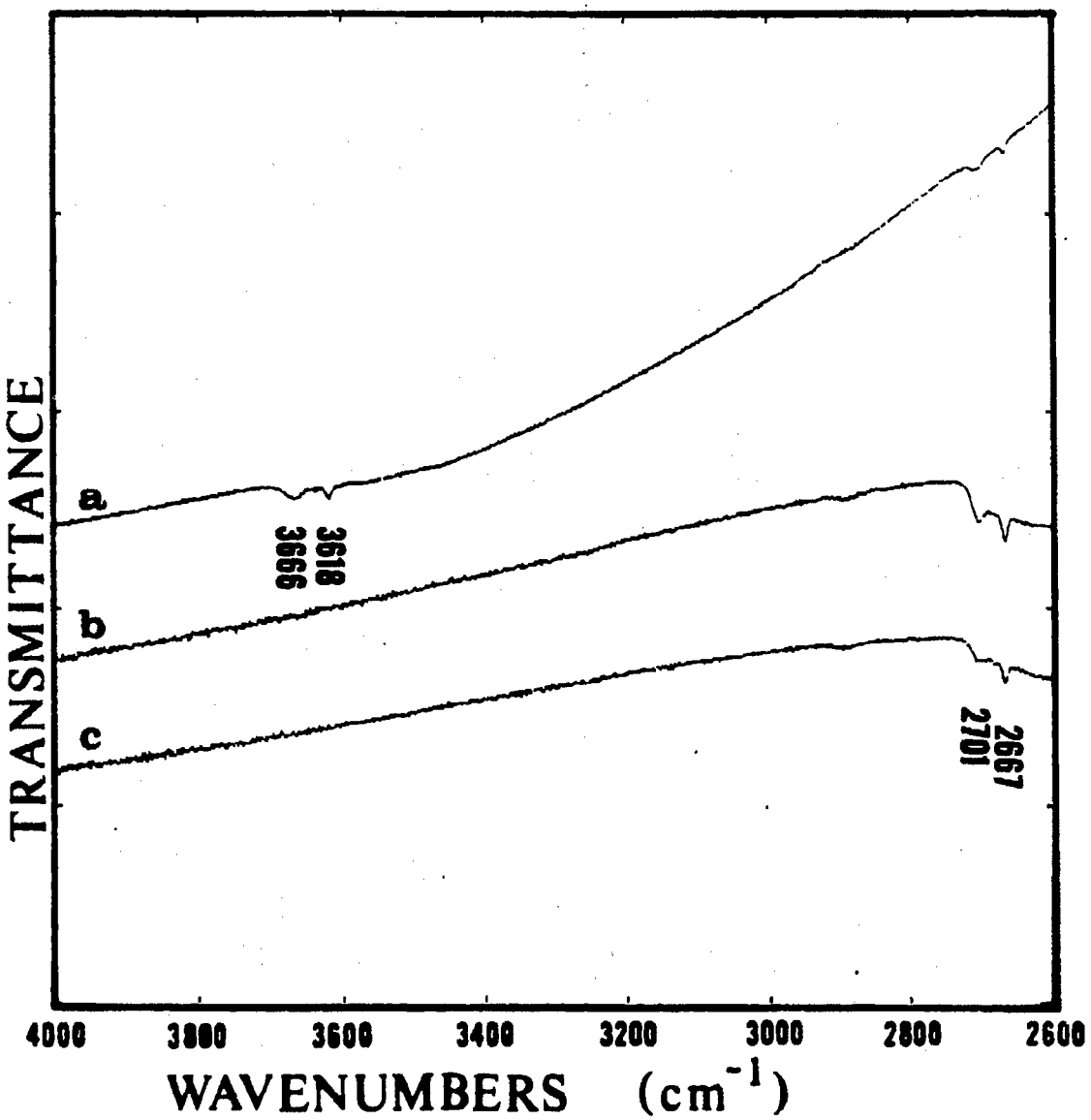
TRANSMITTANCE
a
b
c
3696
3618
2701
2667
4000
3800
3600
3400
3200
3000
2800
2600
WAVENUMBERS (cm^{-1})

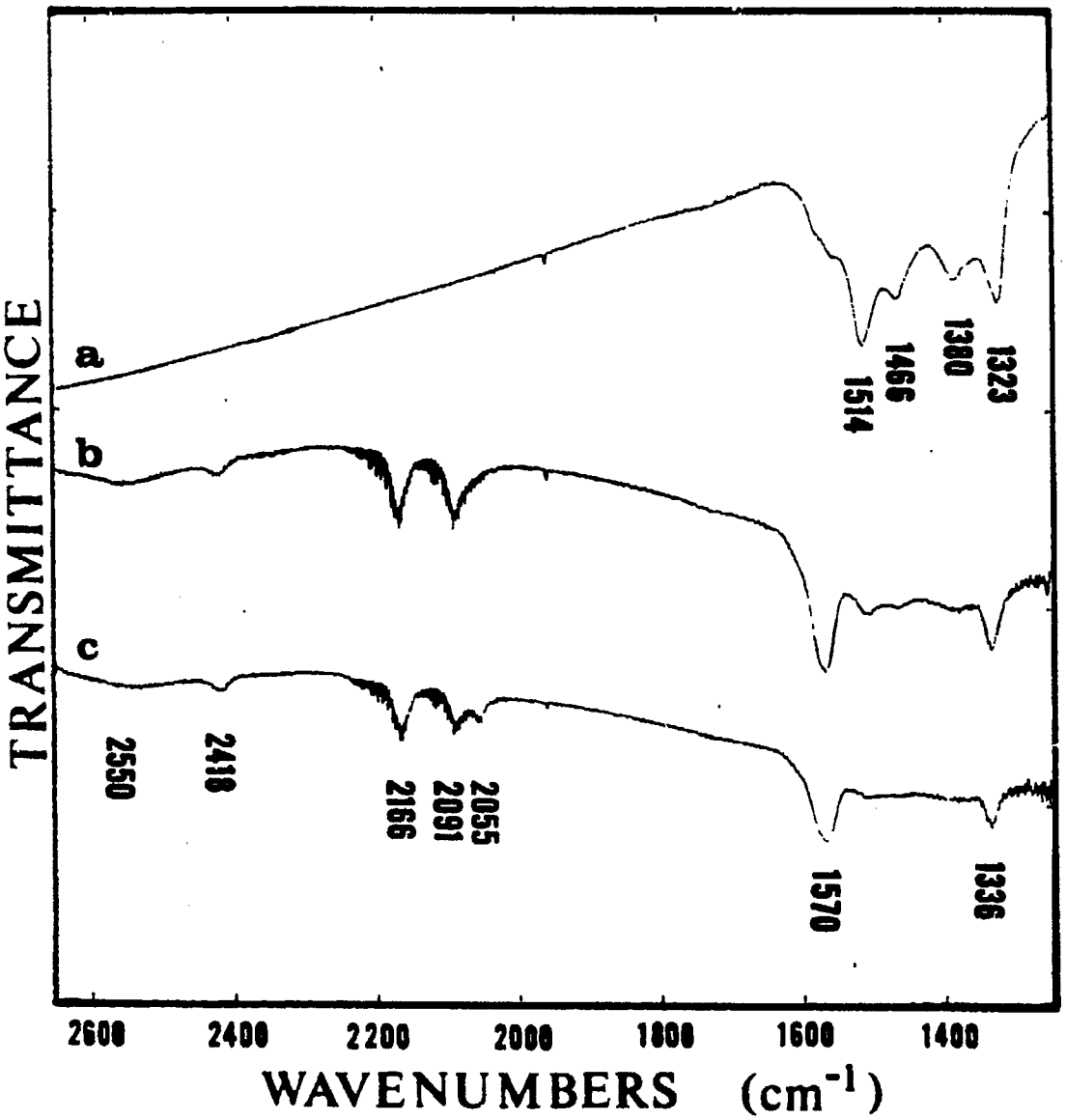

Figure 27. Continued

apparent) developed with the concurrent decrease in the OD group at 2701 cm^{-1}.

The adsorption of carbon monoxide on a reduced 90/10 Zn/Cu catalyst (pretreatment #3) at 200°C and 1 atmosphere, shown in Figure 28, was conducted to determine if the hydrogenation of surface species would be greater on a reduced rather than oxidized catalyst. A carbonyl species was formed at 2093 cm^{-1} and the unidentate carbonate (bands at 1469 and 1380 cm^{-1}) diminished. The formate (bands at 2972, 2880, 1576, 1379, and 1364 cm^{-1}) and bidentate carbonate (bands at 1516 and 1325 cm^{-1}) species were essentially unaffected by CO adsorption. The transmittance did decrease during adsorption, especially at the lower wavenumbers.

When a mixture of carbon monoxide and hydrogen (CO/H_2 = 1/2) was adsorbed on a reduced 90/10 Zn/Cu catalyst (pretreatment #3) at 200°C, the behavior of surface species was comparable to other studies with this mixture. Figure 29 shows that formate groups were hydrogenated to methoxy groups, accompanied by the decrease of the hydroxyl group at 3665 cm^{-1}.

A decrease in the temperature of CO hydrogenation to 100°C had the effect of lowering surface reaction rates and stabilizing a reaction intermediate. Adsorption of carbon monoxide and hydrogen (CO/H_2 = 1/2) on a reduced 95/5 Zn/Cu catalyst (pretreatment #3) is shown in Figure 30. Surface carbonate groups gradually decreased as formate groups increased. An adsorbed formaldehyde species (bands at 2935 and 2852 cm^{-1}) formed during an 8-hour period, possibly an intermediate between formate and methoxy species. At 100°C, the carbonyl species had a slightly

Figure 28. Carbon monoxide adsorption on reduced 90/10 Zn/Cu oxide at 200°C

a) reduced surface

b) exposure for 5 minutes.

c) exposure for 1 hour

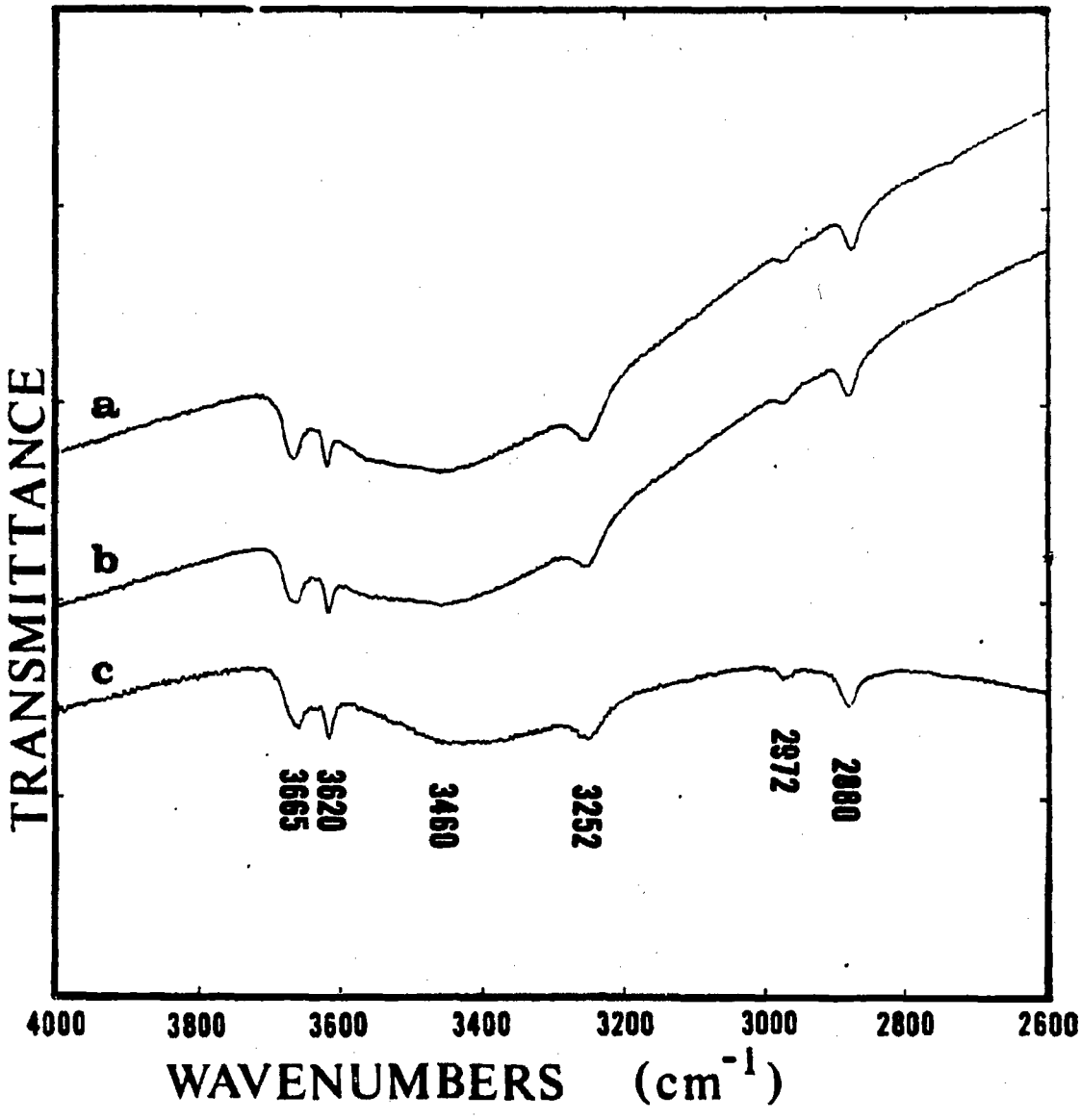
TRANSMITTANCE
a
b
c
3665
3620
3460
3252
2972
2880
4000
3800
3600
3400
3200
3000
2800
2600
WAVENUMBERS (cm-1)

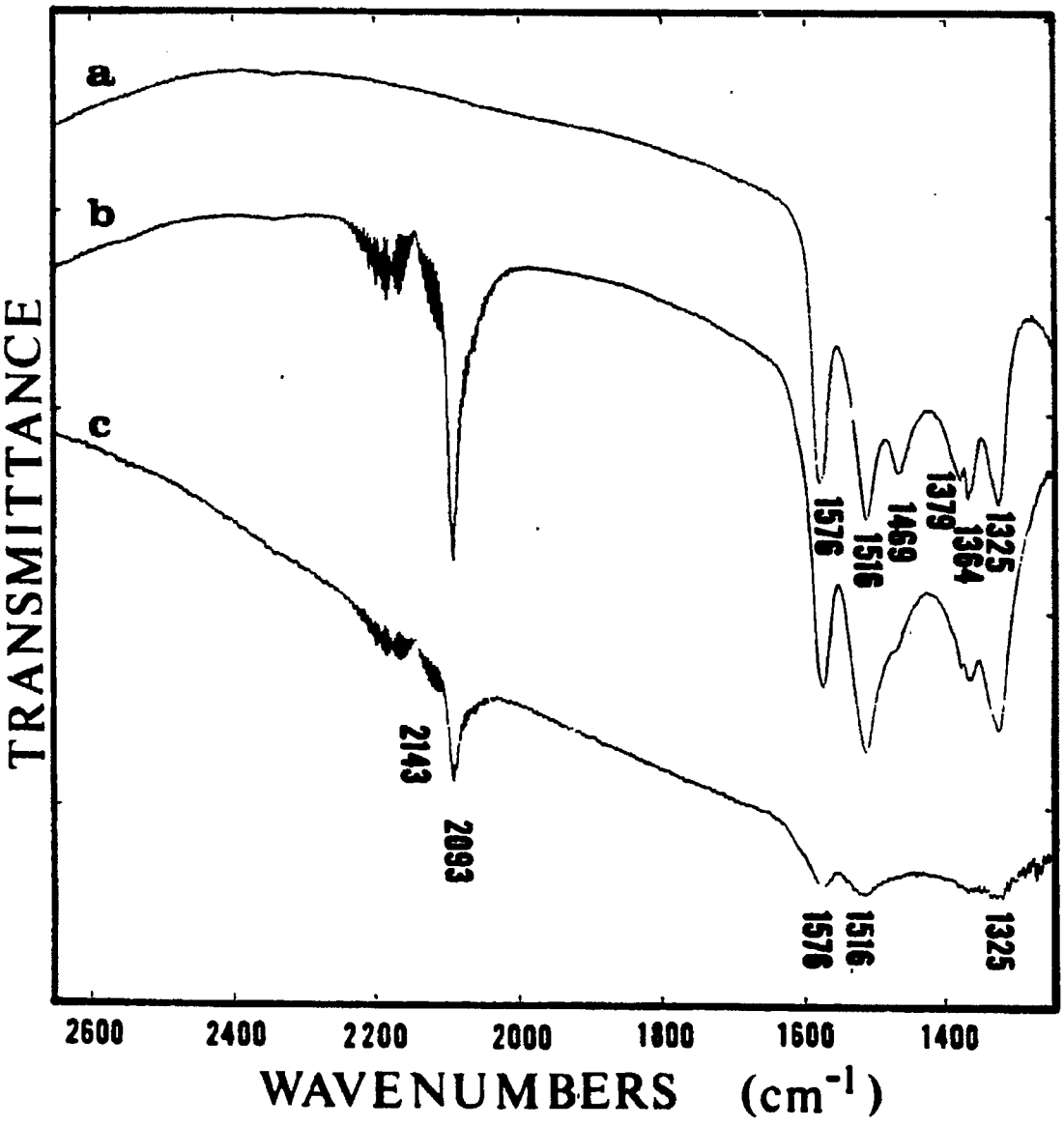

Figure 28. Continued

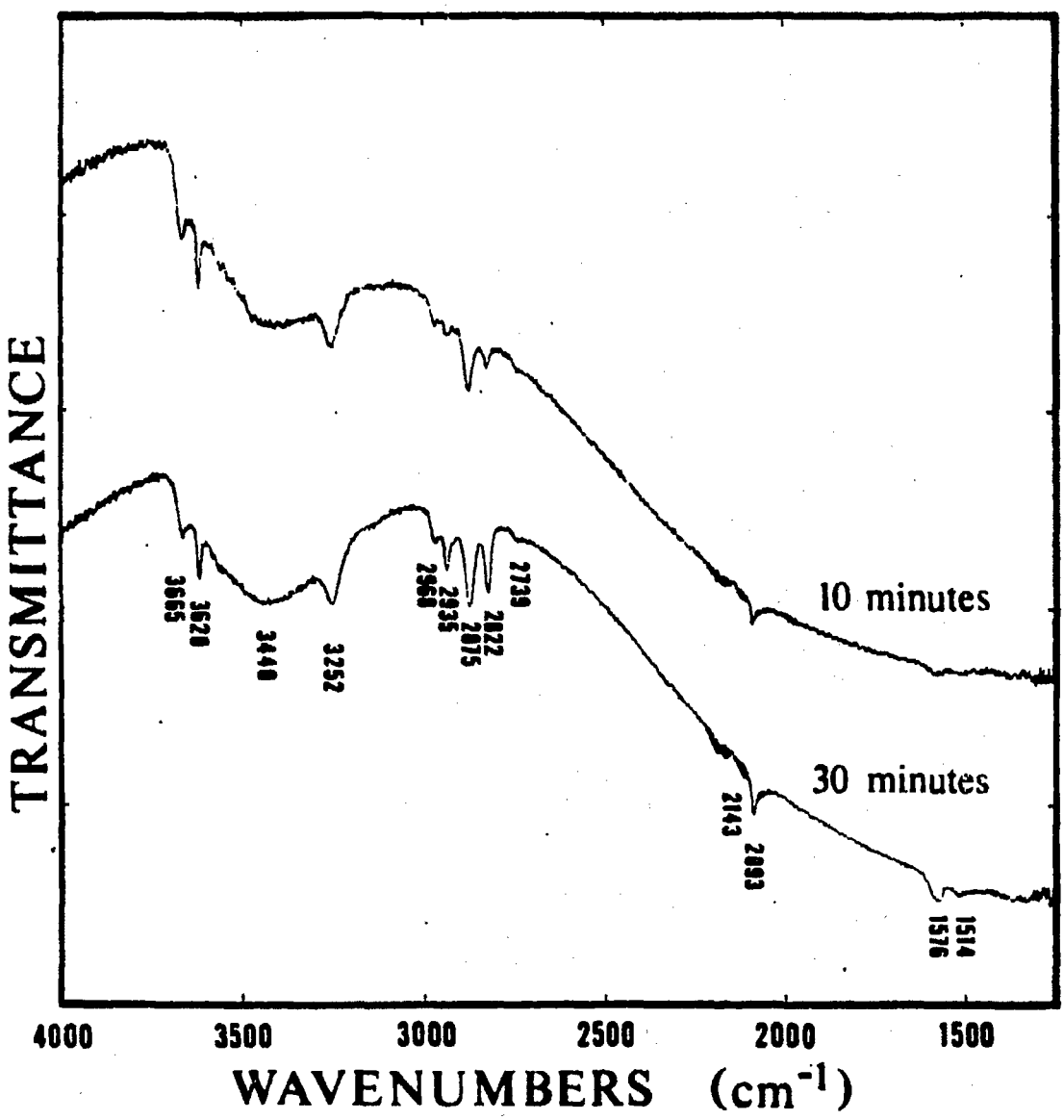

Figure 29. Adsorption of CO-H_2 mixture on reduced 90/10 Zn/Cu oxide at 200°C

Figure 30. Adsorption of CO-H_2 mixture on reduced 95/5 Zn/Cu oxide at 100°C

a) reduced surface

b) exposure for 5 minutes

c) exposure for 8 hours

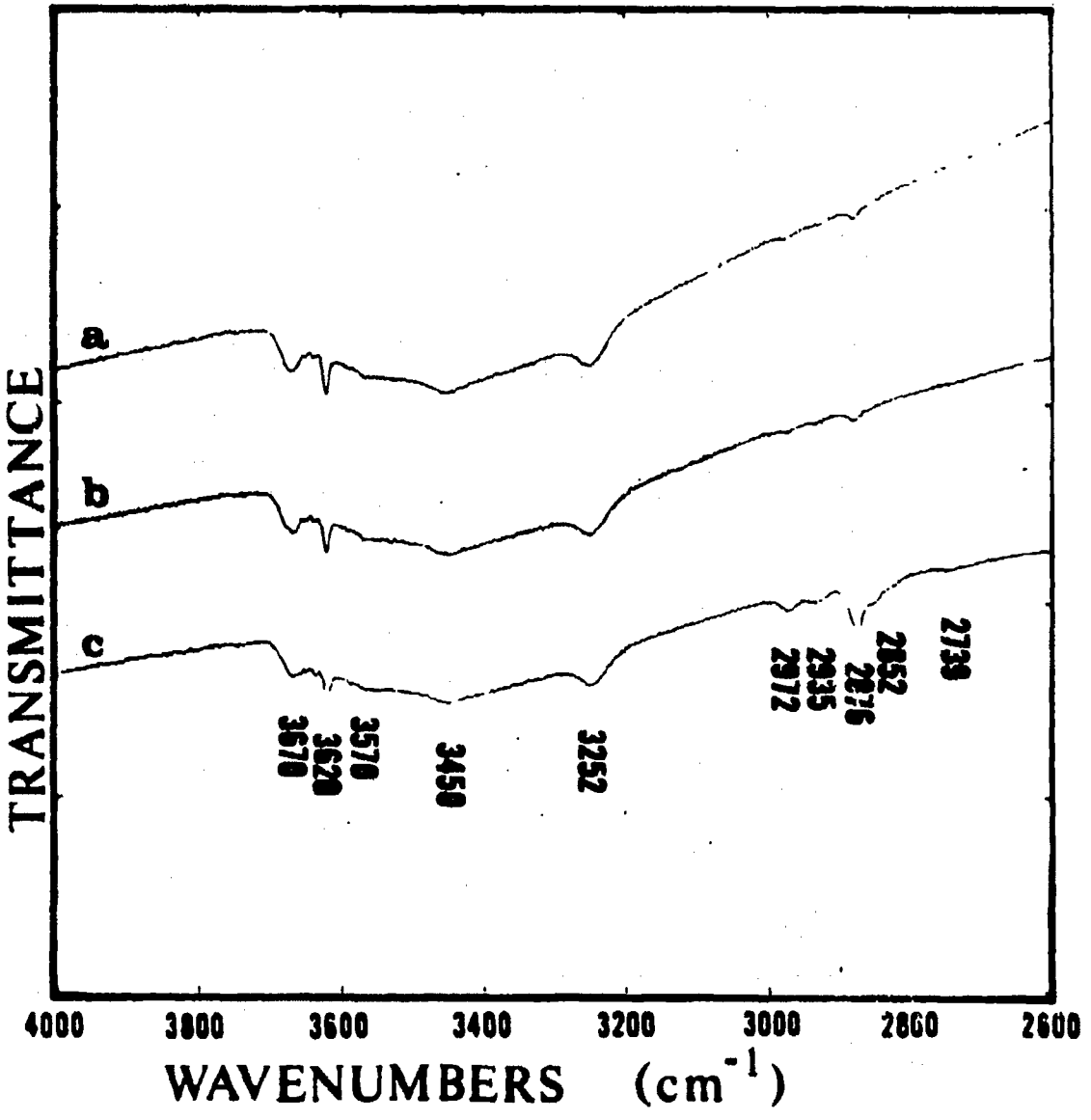
TRANSMITTANCE
a
b
c
3570
3520
3450
3252
2917
2852
2739
4000
3800
3600
3400
3200
3000
2800
2600
WAVENUMBERS (cm-1)

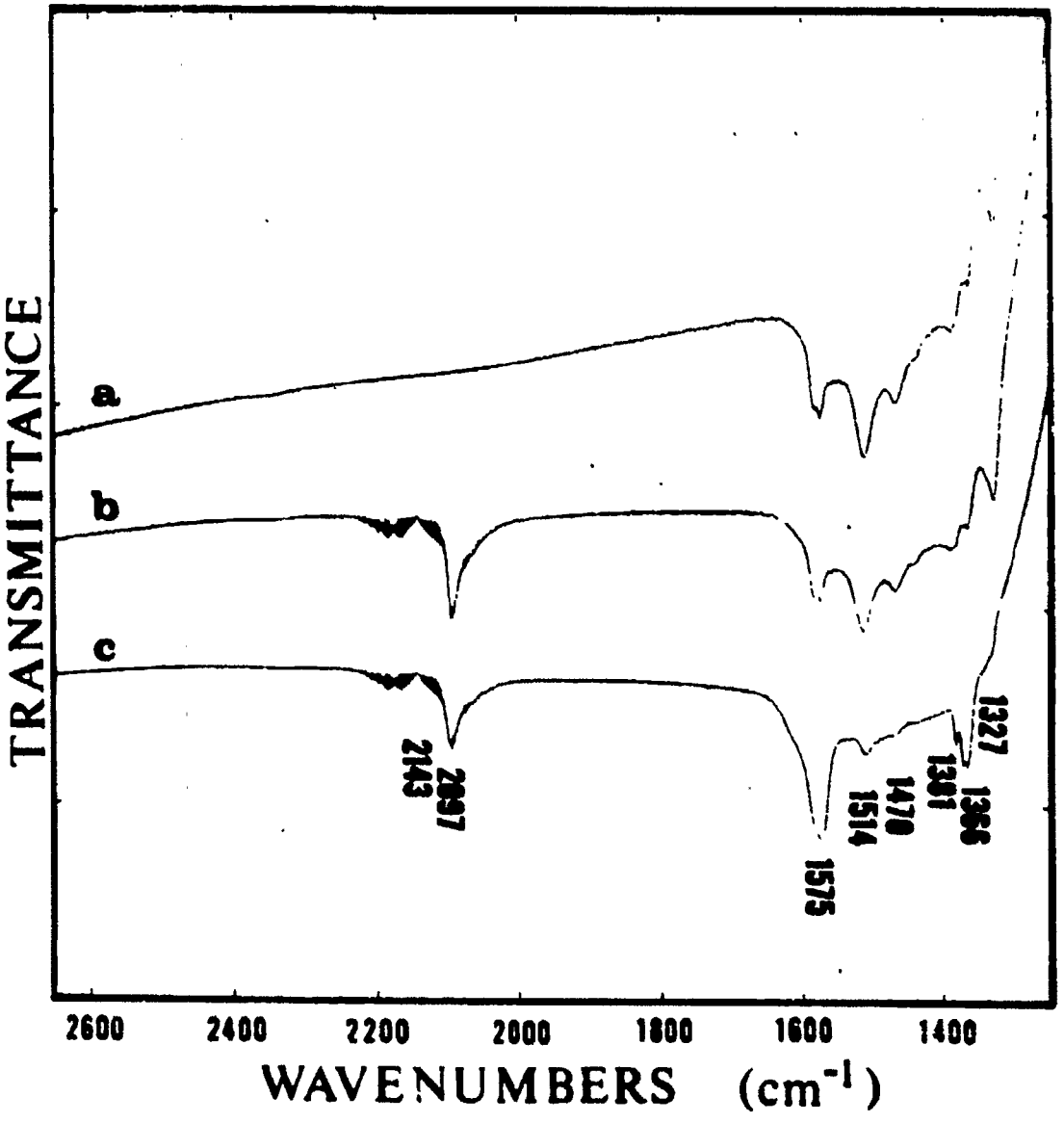

Figure 30. Continued

frequency (band at 2097 cm^{-1}), but the other bands occurred in the same positions found at 200°C.

The activity of a reduced 90/10 Zn/Cu catalyst (pretreatment #3) for the water-gas shift reaction at 200°C and 1 atmosphere was determined for a high CO/H_2O ratio (approximately 100/1). Figure 31 shows that carbonyl species and formate groups were quickly formed without any significant changes in the residual carbonate groups. The water-gas shift reaction occurred at these conditions as indicated by the presence of gaseous carbon dioxide (band at 2350 cm^{-1}) in the spectra. No methoxy groups were formed.

The hydrogenation of carbon dioxide (reverse water-gas shift reaction or methanol synthesis) would be expected to have surface species in common with both reactions. The concurrent adsorption of carbon dioxide and hydrogen (CO_2/H_2 = 1/1) on an oxidized 90/10 Zn/Cu catalyst (pretreatment #1) at 200°C and 1 atmosphere is shown in Figure 32. Formate (bands at 2970, 2872, 2737, 1572, and 1366 cm^{-1}) and adsorbed formaldehyde (bands at 2930, 2851, and 1620 cm^{-1}) groups developed quickly. The surface carbonate species diminished and the catalyst was reduced (development of 3252 cm^{-1} band). After 4 hours, the amount of methoxy groups formed was negligible. Substitution of the gas phase with pure hydrogen did not produce methoxy groups after an hour of hydrogen exposure.

Since formate groups were hydrogenated to methoxy groups in the presence of carbon monoxide but not in the presence of carbon dioxide, it appeared that the carbonyl species might enhance formate hydrogenation. To test this possibility, carbon monoxide was adsorbed on a

Figure 31. Adsorption of CO-H_2O mixture on reduced 90/10 Zn/Cu oxide at 200°C

a) reduced surface

b) exposure for 30 minutes

c) exposure for 4 hours

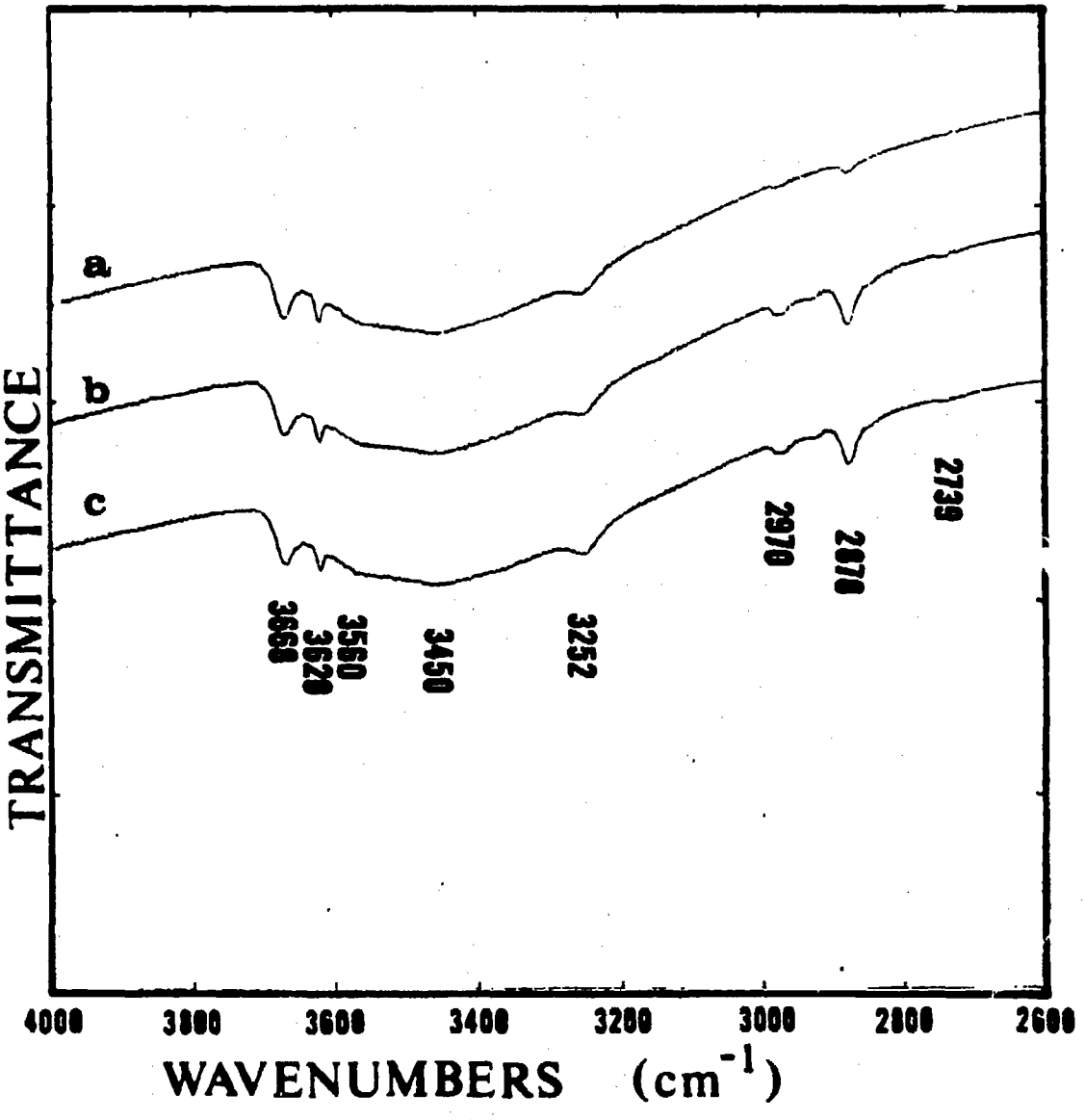
a
b
c
TRANSMITTANCE
3660
3620
3590
3450
3252
2970
2870
2739
4000
3800
3600
3400
3200
3000
2800
2600
WAVENUMBERS (cm-1)

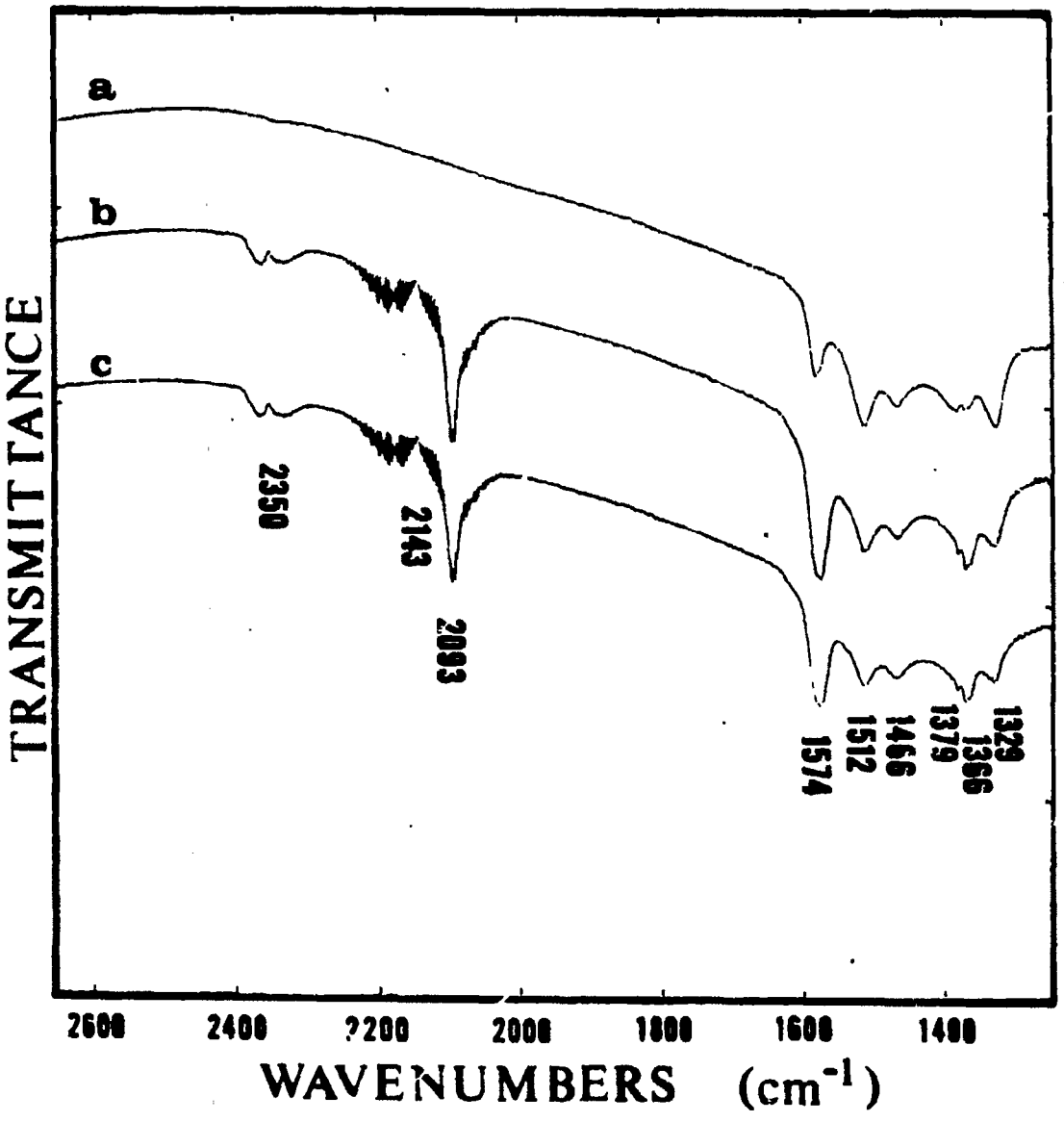

Figure 31. Continued

Figure 32. Adsorption of CO_2-H_2 mixture on 90/10 Zn/Cu oxide at 200°C

a) oxidized surface

b) exposure for 5 minutes

c) exposure for 4 hours

d) exposure to hydrogen for 1 hour

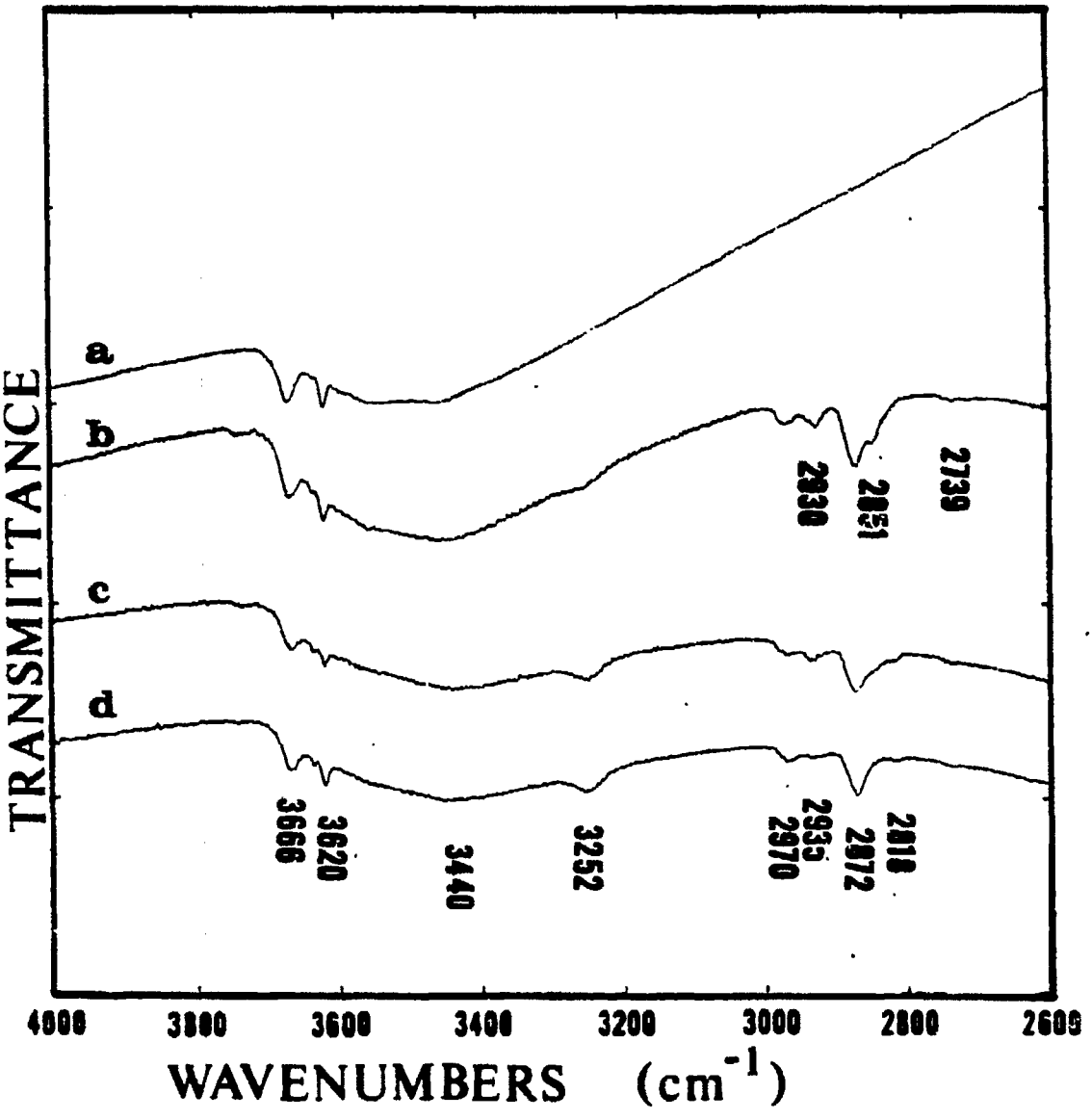
TRANSMITTANCE
a
b
c
d
2930
2851
2739
3666
3620
3440
3252
2933
2970
2872
2818
4000
3800
3600
3400
3200
3000
2800
2600
WAVENUMBERS (cm-1)

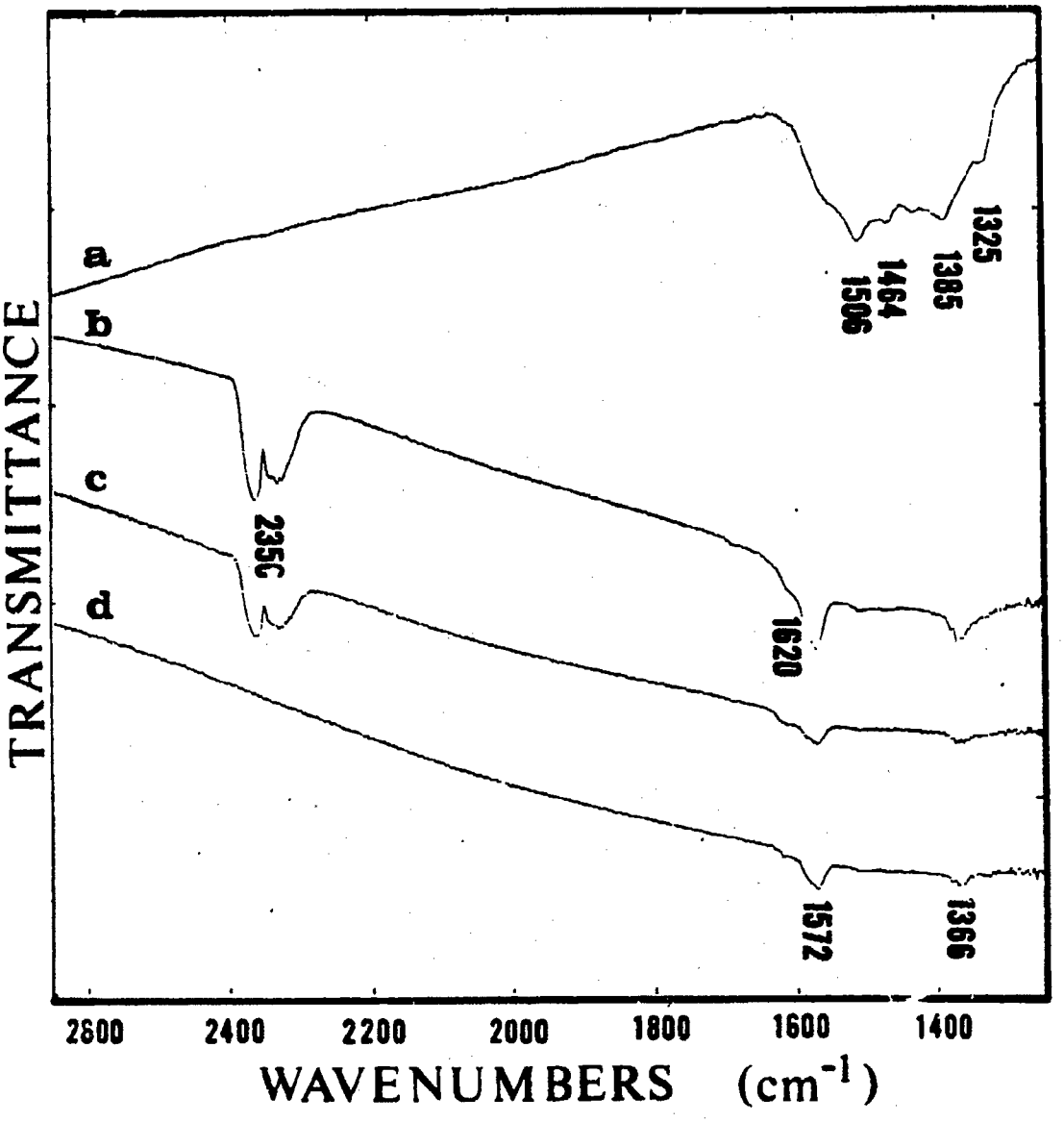

Figure 32. Continued

reduced 95/5 Zn/Cu catalyst (pretreatment #3) at 200°C and 1 atmosphere followed by carbon dioxide adsorption (Figure 33). The carbonyl species was weakly adsorbed, desorbing when the gaseous CO was flushed from the cell with nitrogen. The subsequent adsorption of carbon dioxide caused partial oxidation of the catalyst (a transmission increase and the 3252 cm^{-1} band decrease) and decreased formate groups, while the carbonate groups were increased. The addition of hydrogen to the carbon dioxide decreased carbonate groups and increased formate groups without any development of methoxy groups.

The adsorption of formic acid (88% HCOOH, 12% H_2O) on a reduced 95/5 Zn/Cu catalyst (pretreatment #3) at 165°C and 1 atmosphere is shown in Figure 34. Exposure of the acid to the catalyst was brief (5 minutes) because the acid severely decreased the transmittance through the sample. Spectra were taken in nitrogen after the transmission had increased to several percentage transmittance. Formic acid adsorption produced a formate species (bands at 2968, 2873, 2736, 1572, 1380, and 1366 cm^{-1}), methoxy groups (bands at 2935 and 2825 cm^{-1}), and a new hydroxyl group (band at 3524 cm^{-1}). This hydroxyl species disappeared as methoxy groups increased, and formate decomposition was indicated by the presence of carbon dioxide in the isolated cell. Methoxy groups formed without any gaseous hydrogen present because the cell was flushed with nitrogen after the initial exposure. Since it was possible that some hydrogen might have existed in the micropores, this experiment was repeated using a 50% nitrogen-50% hydrogen gas mixture. The development of methoxy groups occurred at essentially the same rate as that in nitrogen, indicating that gaseous hydrogen was not

Figure 33. CO_2 hydrogenation preceded by CO adsorption

a) exposure to CO

b) N_2 purge for 10 minutes.

c) exposure to CO_2 and N_2

d) exposure to CO_2, H_2, and N_2

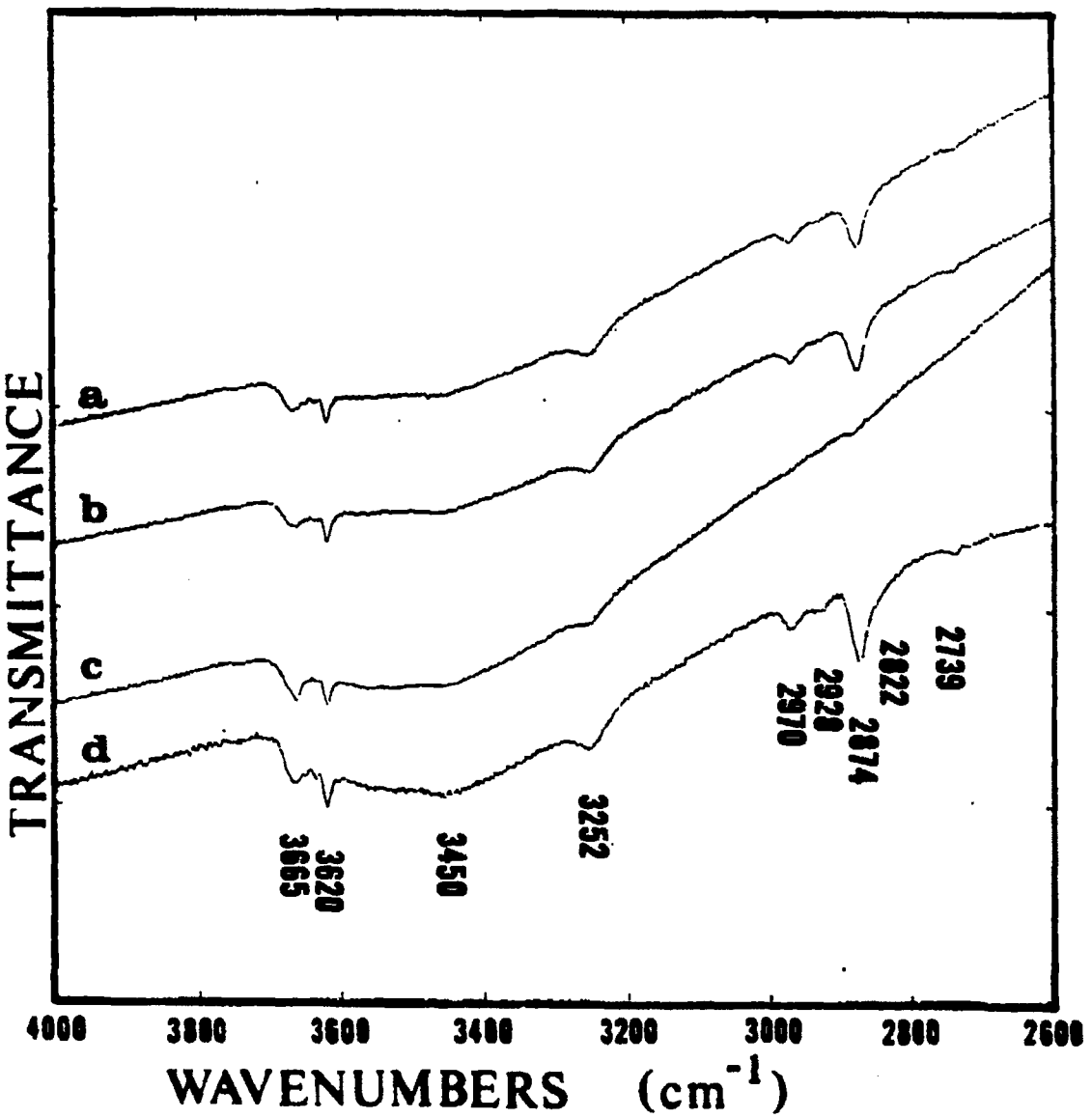
TRANSMITTANCE
a
b
c
d
3665
3620
3450
3252
2970
2920
2874
2822
2739
4000
3800
3600
3400
3200
3000
2800
2600
WAVENUMBERS (cm-1)

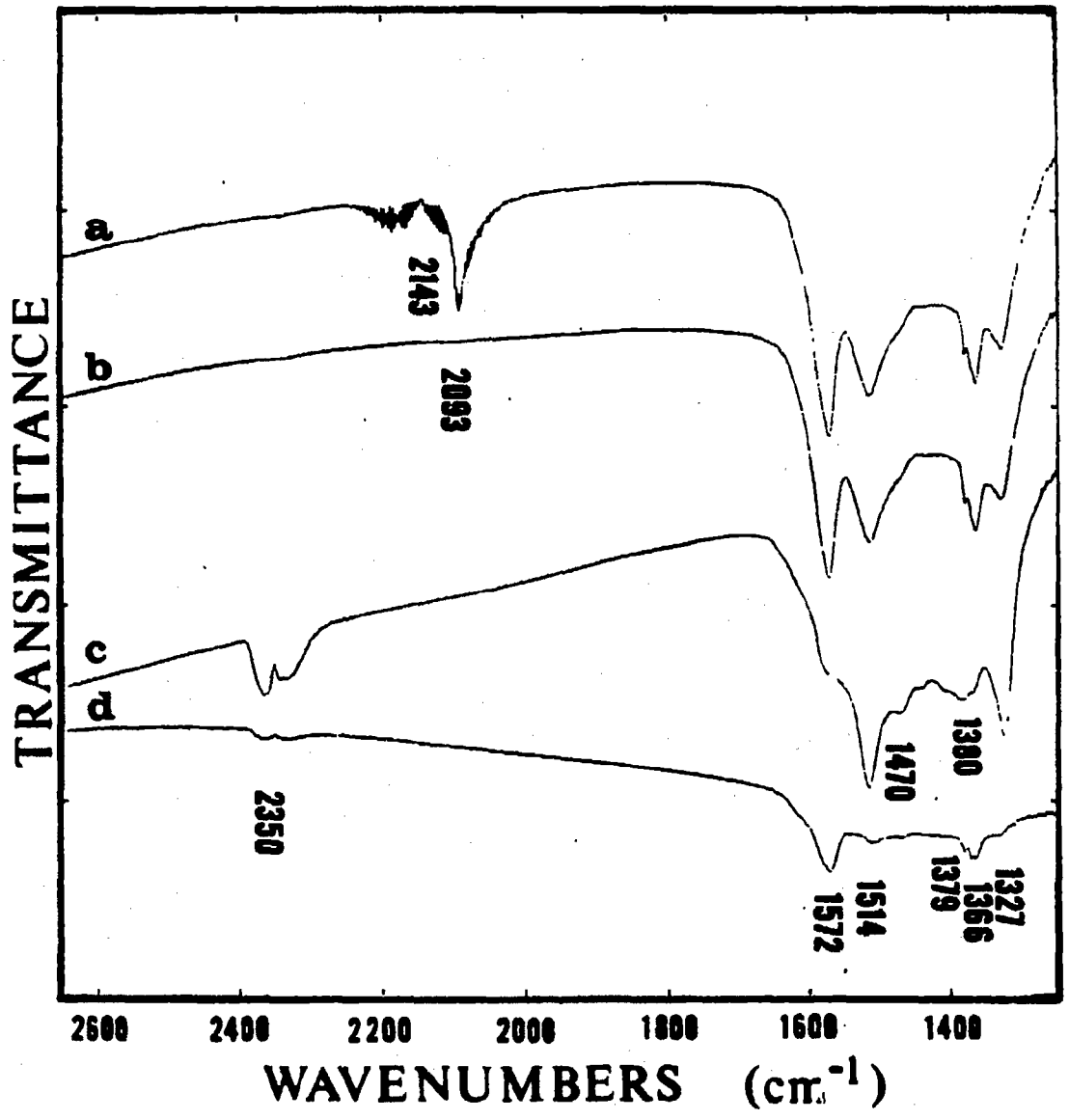

Figure 33. Continued

Figure 34. Adsorption of formic acid on 95/5 Zn/Cu oxide at 165°C

a) reduced surface

b) 30 minutes after exposure

c) 4 hours after exposure

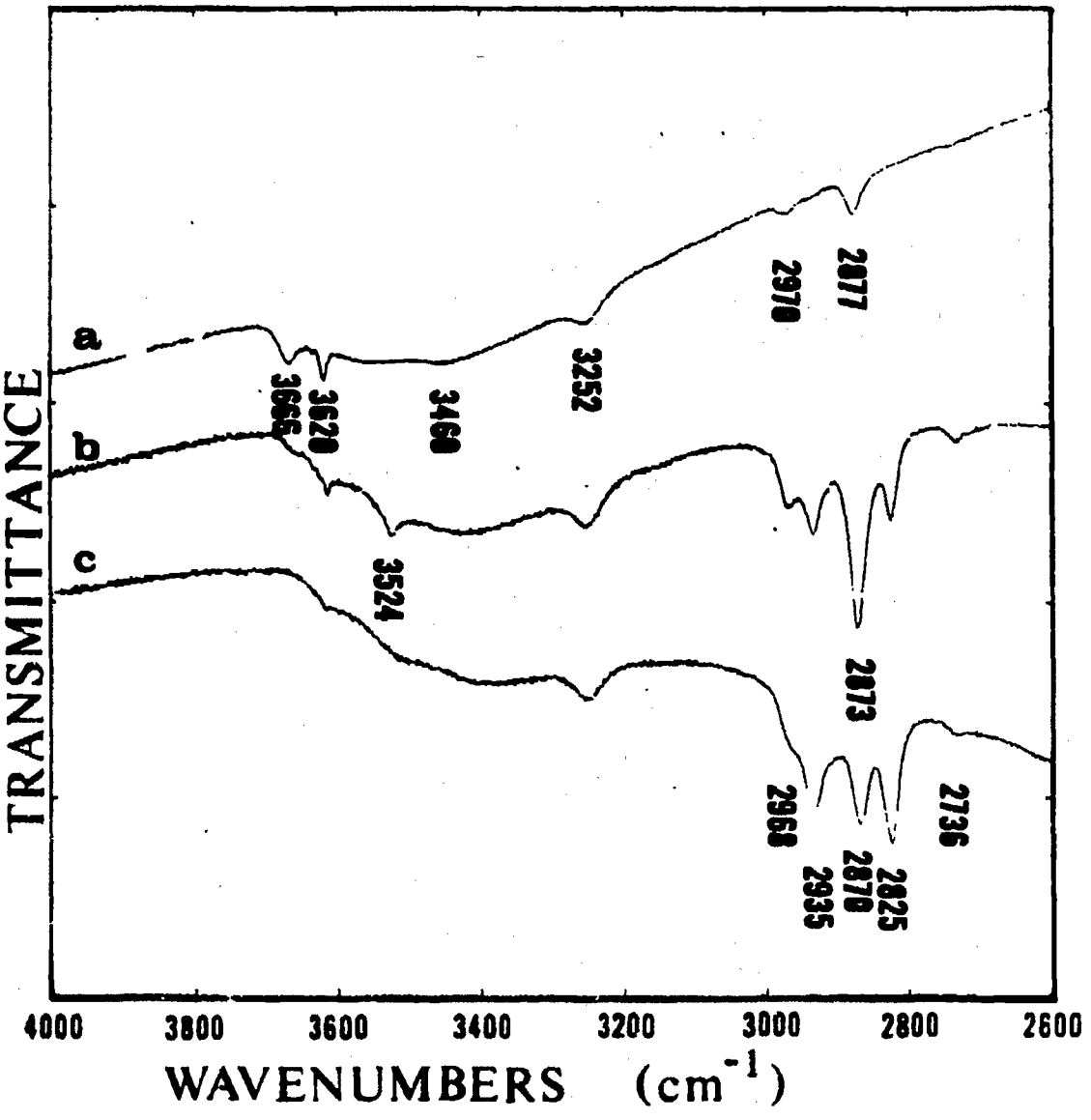
TRANSMITTANCE
a
b
c
3666
3620
3490
3252
2978
2877
3524
2973
2960
2935
2870
2825
2736
4000
3800
3600
3400
3200
3000
2800
2600
WAVENUMBERS (cm-1)

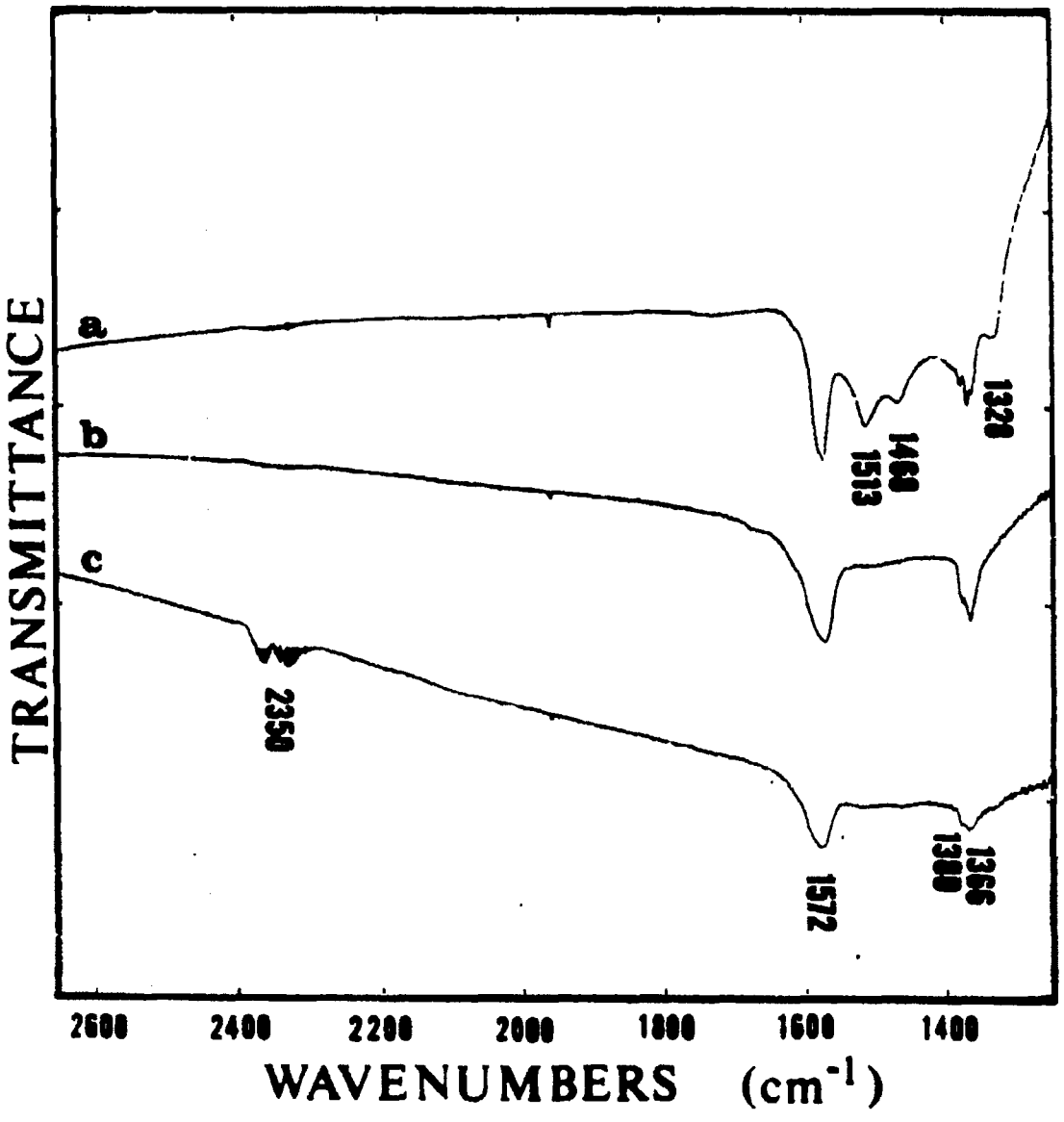

Figure 34. Continued

directly involved in methoxy formation. The development of methoxy groups led to the disappearance of the isolated hydroxyl groups at 3666 and 3620 cm^{-1}. The C-H stretching frequency of the formate species was shifted from 2877 to 2870 cm^{-1} as the amount of methoxy groups increased on the surface; the hydroxyl at 3620 cm^{-1} shifted to 3613 cm^{-1} as the band decreased.

Formaldehyde adsorption on a reduced 95/5 Zn/Cu catalyst (pretreatment #3) at 200°C and 1 atmosphere is shown in Figure 35. Formaldehyde vapor was briefly exposed to the surface (5 minutes) and the spectra were taken in nitrogen. Initially, formate (bands at 2970, 2875, 2739, 1578, 1379, and 1364 cm^{-1}) and methoxy (bands at 2934 and 2820 cm^{-1}) groups dominated the surface without any evidence of adsorbed formaldehyde. Both the methoxy and formate groups gradually decomposed, restoring the isolated hydroxyl groups (bands at 3668 and 3620 cm^{-1}) and increasing the amount of surface carbonates.

The surface of a reduced 95/5 Zn/Cu catalyst (pretreatment #3) was exposed to formaldehyde vapor at 100°C (Figure 36) to stabilize the surface formaldehyde groups. An adsorbed formaldehyde species (bands at 2935, 2860, 2739, 1700, and 1609 cm^{-1}) and formate groups (bands at 2976, 2880, 2739, 1578, 1381, and 1366 cm^{-1}) were formed, accompanied by the disappearance of the isolated hydroxyl groups (bands at 3670 and 3620 cm^{-1}). Because formate groups were known not to displace the isolated hydroxyls, it can be safely assumed that adsorbed formaldehyde occupied the same sites as isolated hydroxyls.

The adsorption of methanol on a reduced 95/5 Zn/Cu catalyst (pretreatment #3) at 190°C and 1 atmosphere is shown in Figure 37. Methanol

Figure 35. Adsorption of formaldehyde on 95/5 Zn/Cu oxide at 200°C

a) reduced surface

b) 5 minutes after exposure

c) 20 minutes after exposure

d) 1 hour after exposure

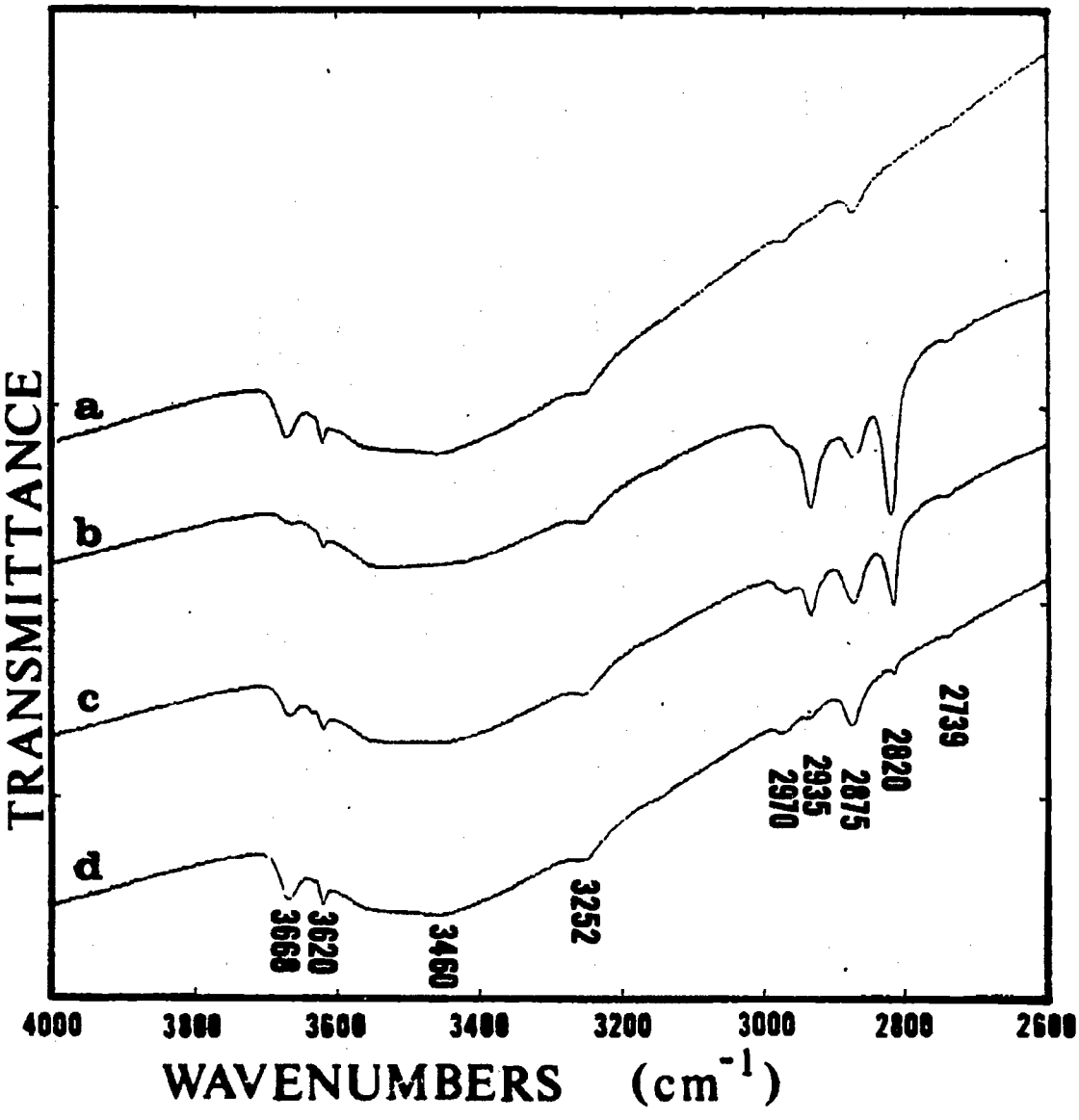
TRANSMITTANCE
a
b
c
d
3668
3620
3460
3252
2970
2935
2875
2820
2739
4000
3800
3600
3400
3200
3000
2800
2600
WAVENUMBERS (cm-1)

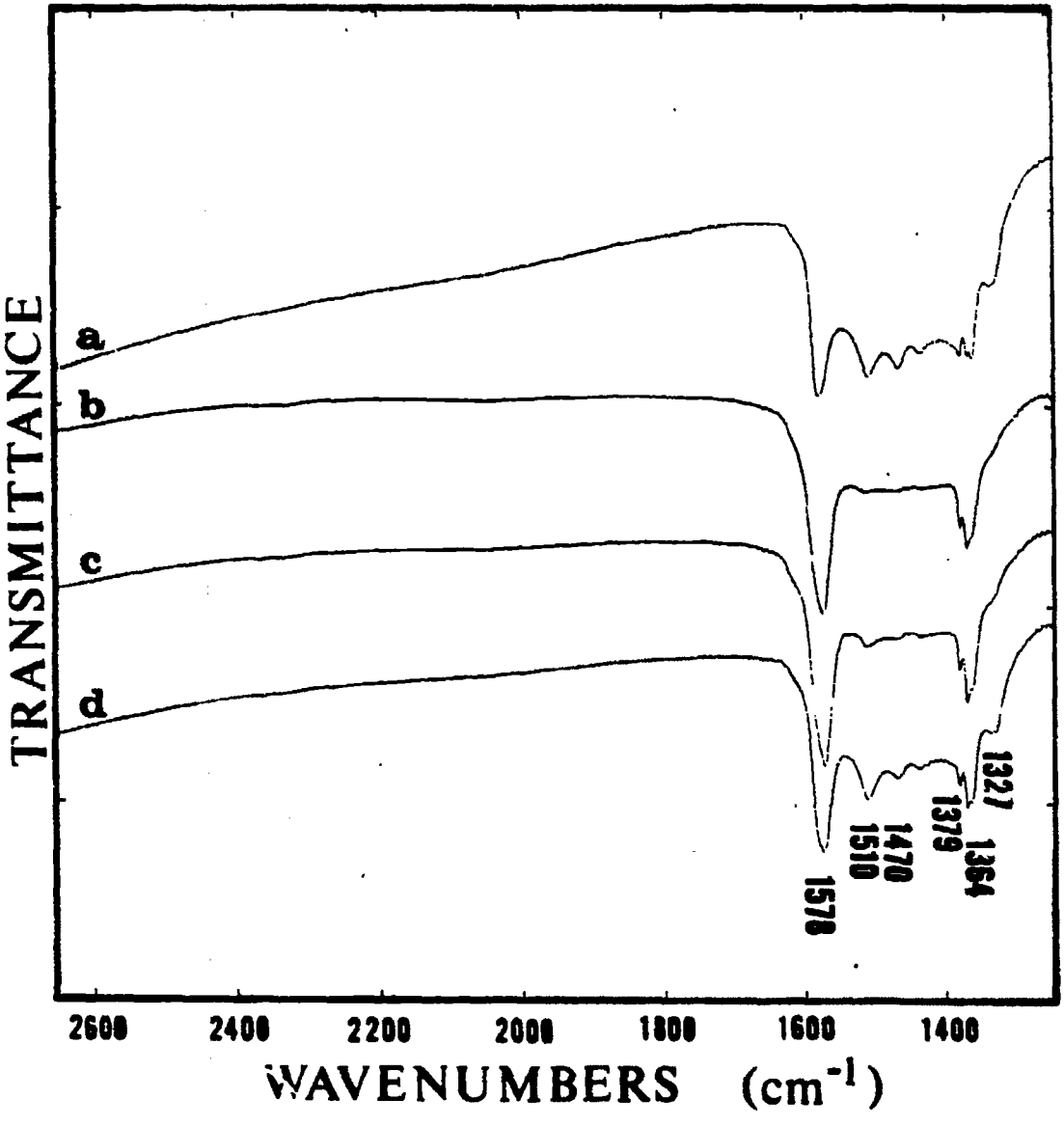

Figure 35. Continued

Figure 36. Adsorption of formaldehyde on 95/5 Zn/Cu oxide at 100°C

a) reduced surface

b) 30 minutes after exposure

c) after second H_2CO exposure

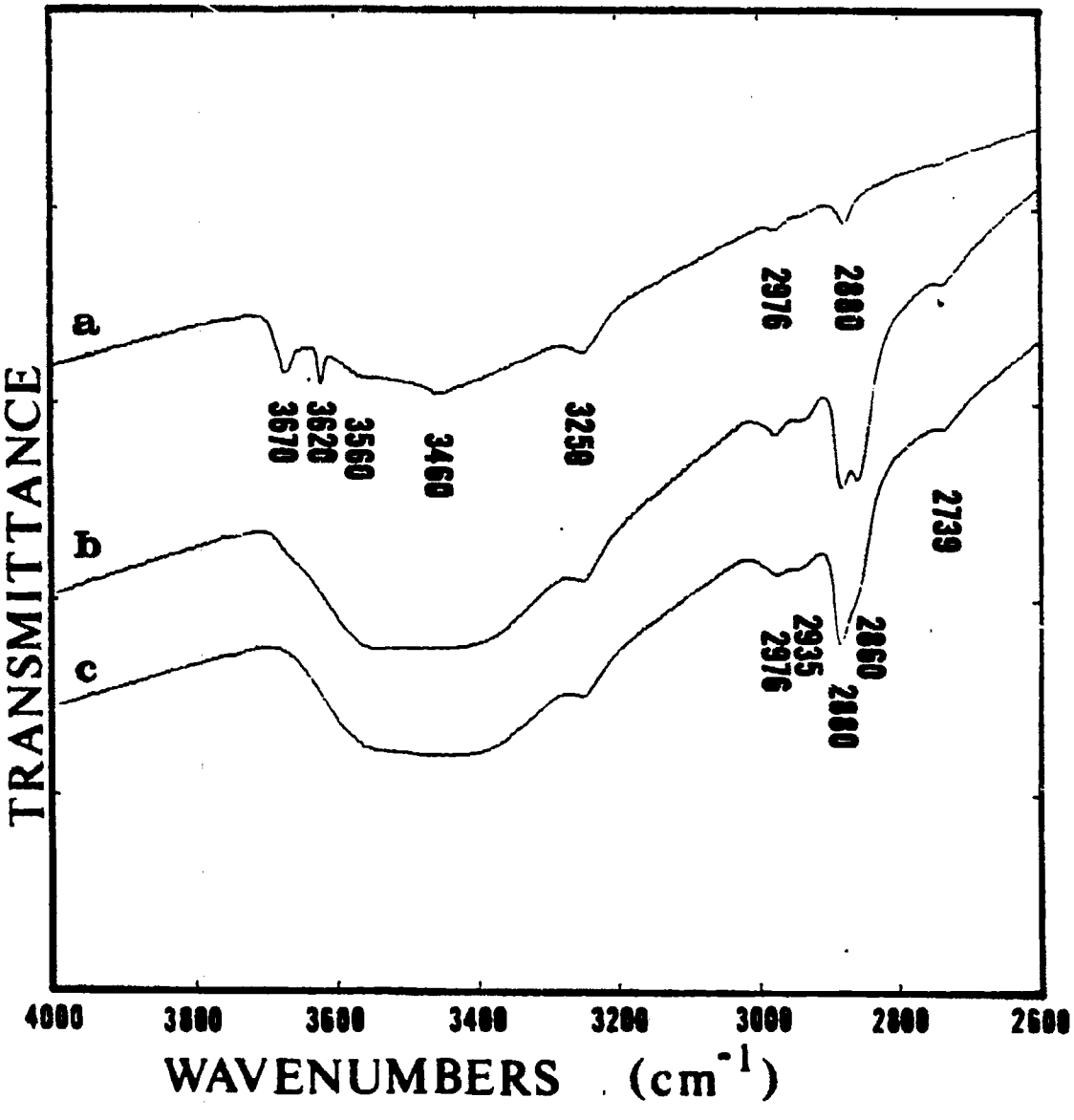
TRANSMITTANCE
a
b
c
3670
3620
3590
3460
3250
2976
2880
2739
2935
2976
2860
2880
4000
3800
3600
3400
3200
3000
2800
2600
WAVENUMBERS (cm-1)

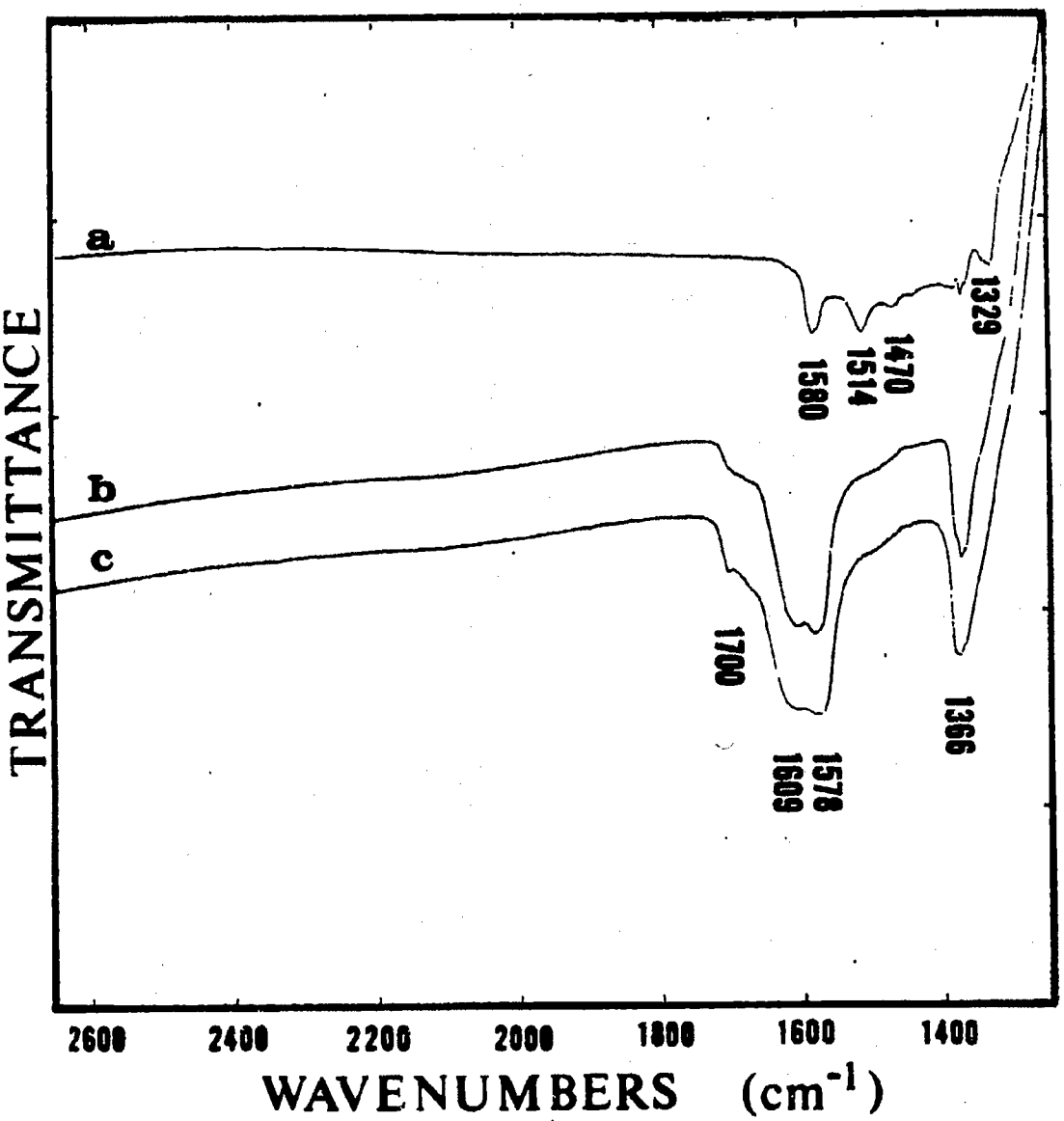

Figure 36. Continued

Figure 37. Adsorption of methanol on reduced 95/5 Zn/Cu oxide at 190°C

a) during exposure

b) 10 minutes after exposure

c) 4 hours after exposure

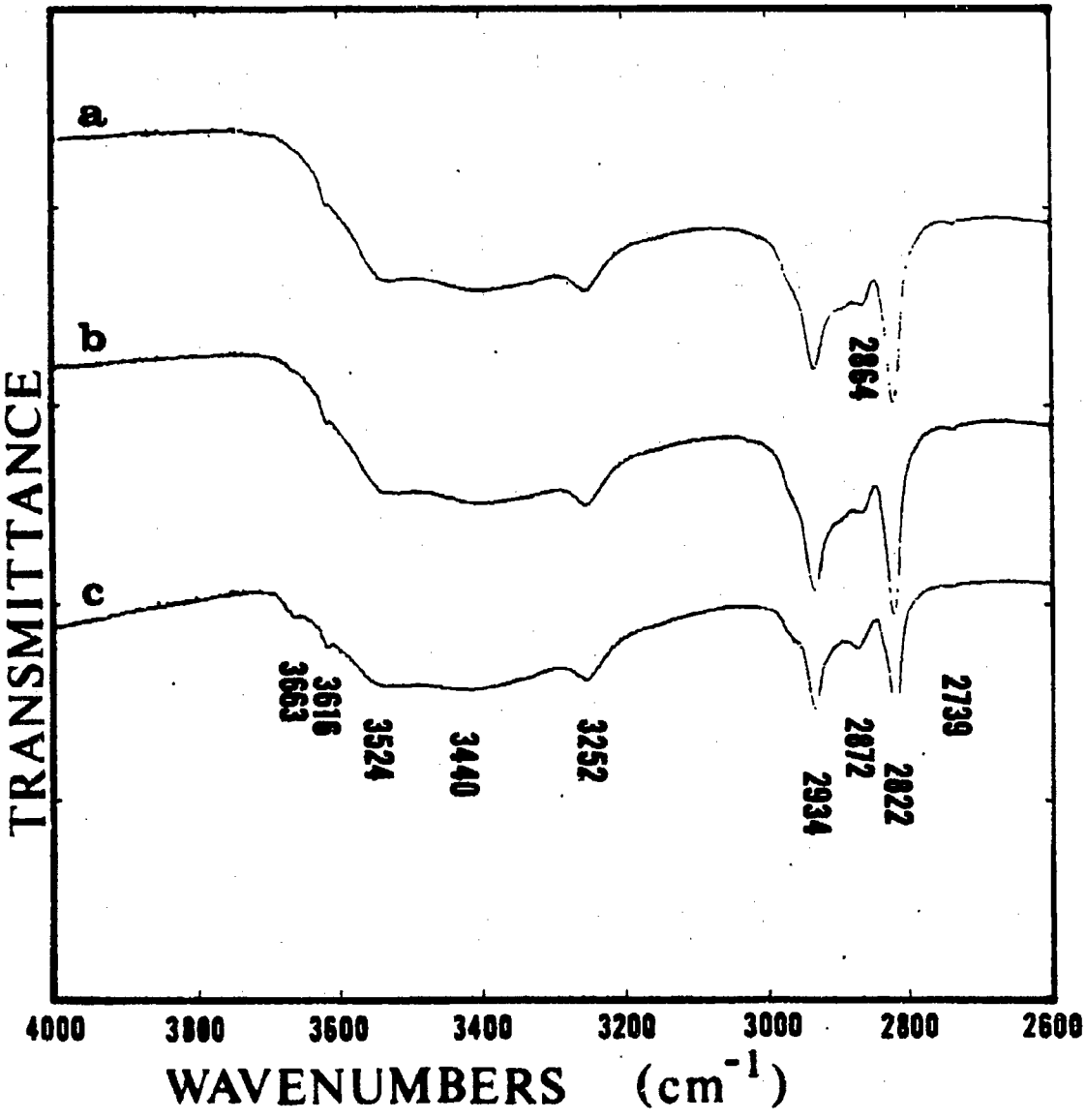
a
b
c
TRANSMITTANCE
3693
3618
3524
3440
3252
2934
2872
2822
2739
4000
3800
3600
3400
3200
3000
2800
2600
WAVENUMBERS (cm-1)

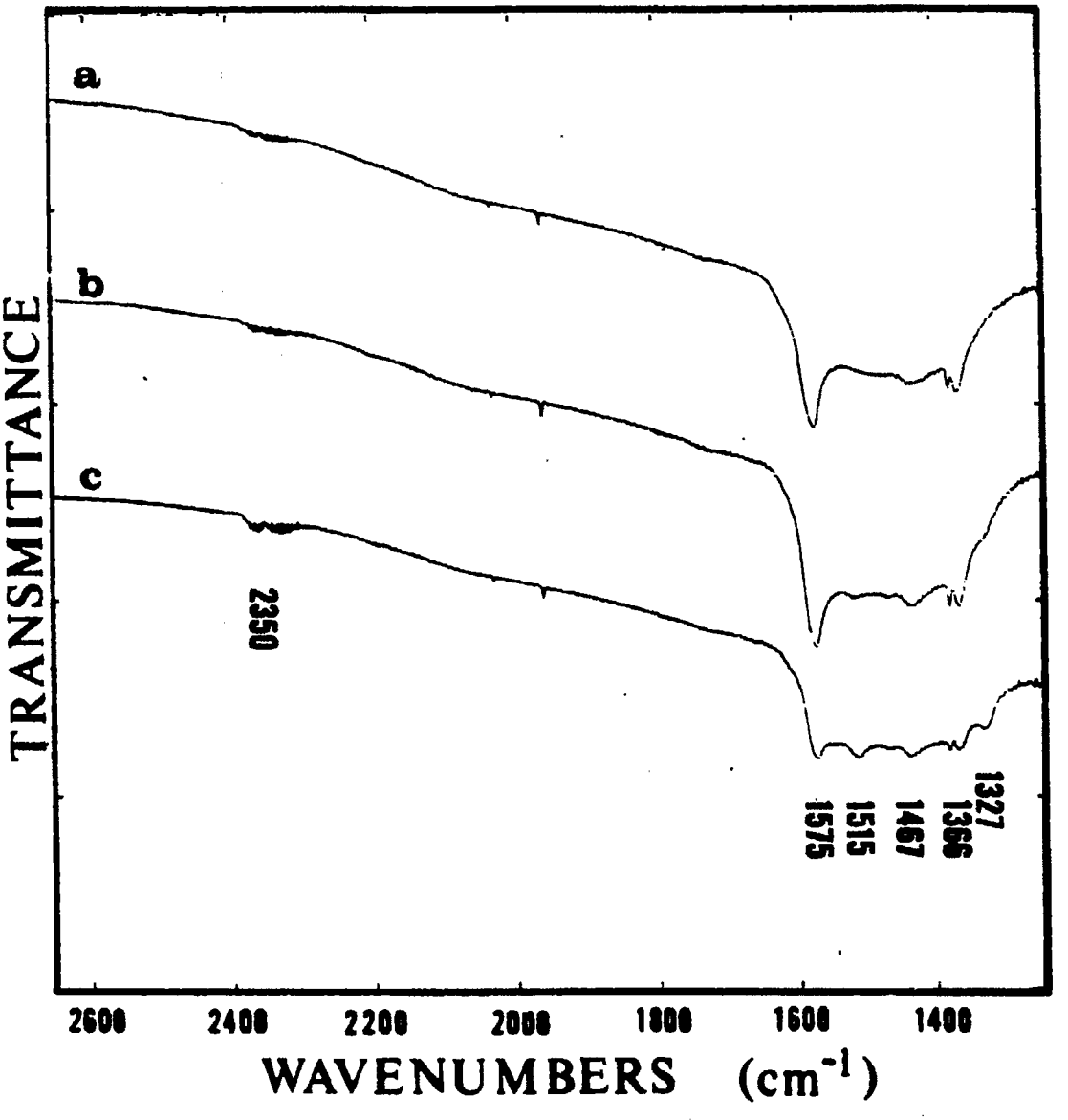

Figure 37. Continued

adsorption produced methoxy groups (bands at 2934 and 2822 cm^{-1}) and a new hydroxyl group at 3524 cm^{-1} while displacing the isolated hydroxyls (bands at 3663 and 3616 cm^{-1}). The slow decomposition of methoxy groups began to restore the isolated hydroxyl groups (bands at 3663 and 3616 cm^{-1}) while formate decomposition increased the amount of surface carbonates and produced some gaseous carbon dioxide.

Because the formation of a methoxy species from methanol would involve the dissociation of the hydroxyl hydrogen, a deuterated methanol (CH_3OD) was adsorbed on a reduced 90/10 Zn/Cu catalyst (pretreatment #3) at 130°C and 1 atmosphere to establish the adsorption sites of the dissociated hydrogen. The adsorption temperature of 130°C was used to inhibit methoxy decomposition which would increase isotopic mixing between adsorbed hydrogen and deuterium species. Figure 38 shows that methanol-d adsorption formed methoxy groups (bands at 2935 and 2824 cm^{-1}) and a new OD group (band at 2613 cm^{-1}). The residual hydroxyl groups (bands at 3670, 3620, and 3450 cm^{-1}) were displaced or shifted to OD groups whereas the hydroxyl group at 3252 cm^{-1} remained unchanged. No exchange was observed between OD groups and methoxy groups, and only a slight exchange occurred between OD groups and the formate species as indicated by the small band at 2152 cm^{-1} (the C-D stretch of deuterated formate).

The adsorption of CD_3OD on a reduced 90/10 Zn/Cu catalyst (pretreatment #3) at 130°C and 1 atmosphere is shown in Figure 39. These spectra were complex and harder to interpret because the initial surface had formate groups. Methanol-d_4 adsorption formed deuterated methoxy groups (bands at 2222, 2201, 2140, and 2058 cm^{-1}) and the new OD group (band at 2619 cm^{-1}). The hydroxyls except the band at 3252 cm^{-1}

Figure 38. Adsorption of CH_3OD on 90/10 Zn/Cu oxide at 130°C

a) reduced surface

b) exposure for 10 minutes

c) exposure for 1 hour

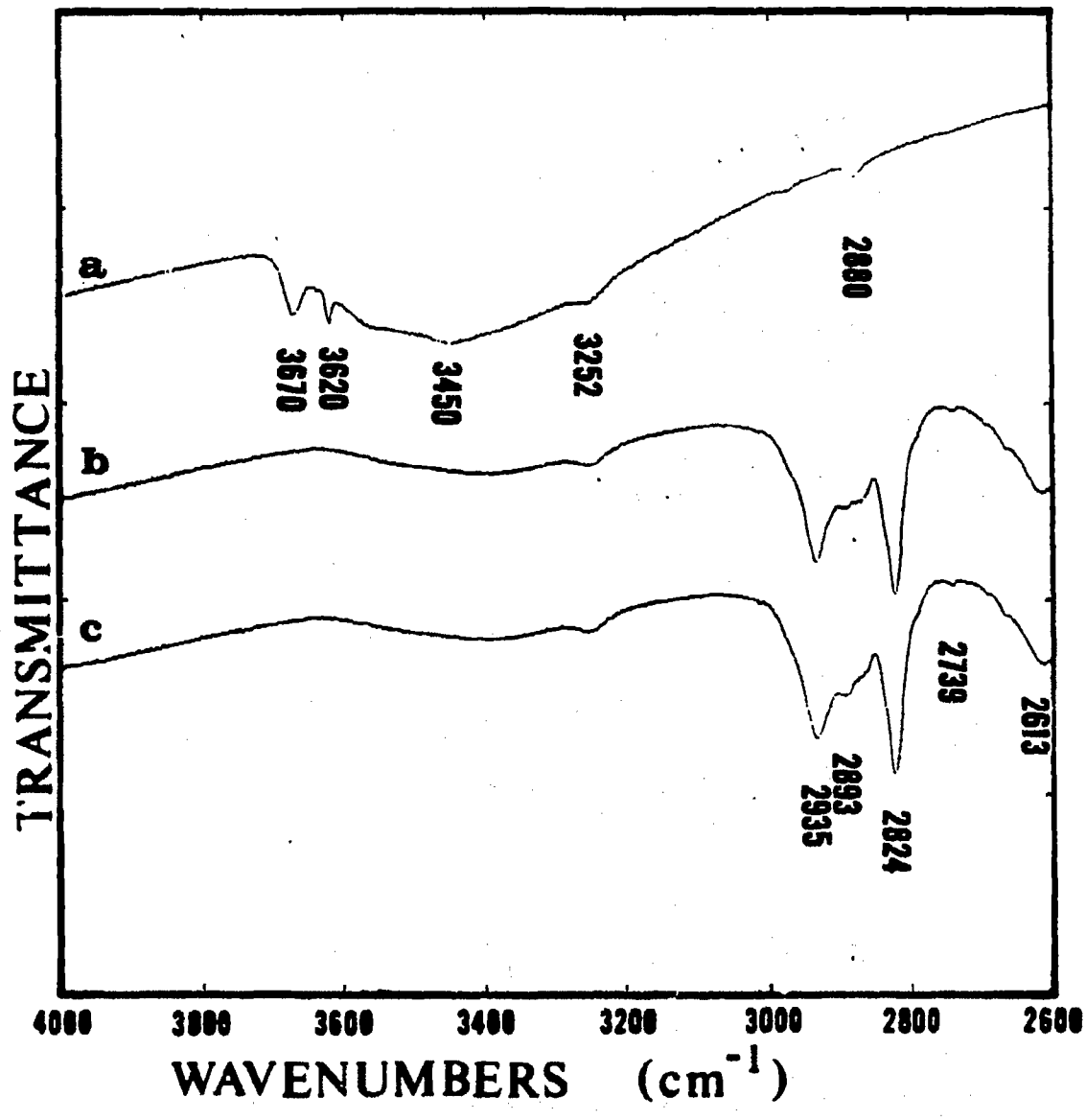
a
b
c
3670
3620
3450
3252
2880
2935
2893
2824
2739
2613
TRANSMITTANCE
4000
3800
3600
3400
3200
3000
2800
2600
WAVENUMBERS (cm-1)

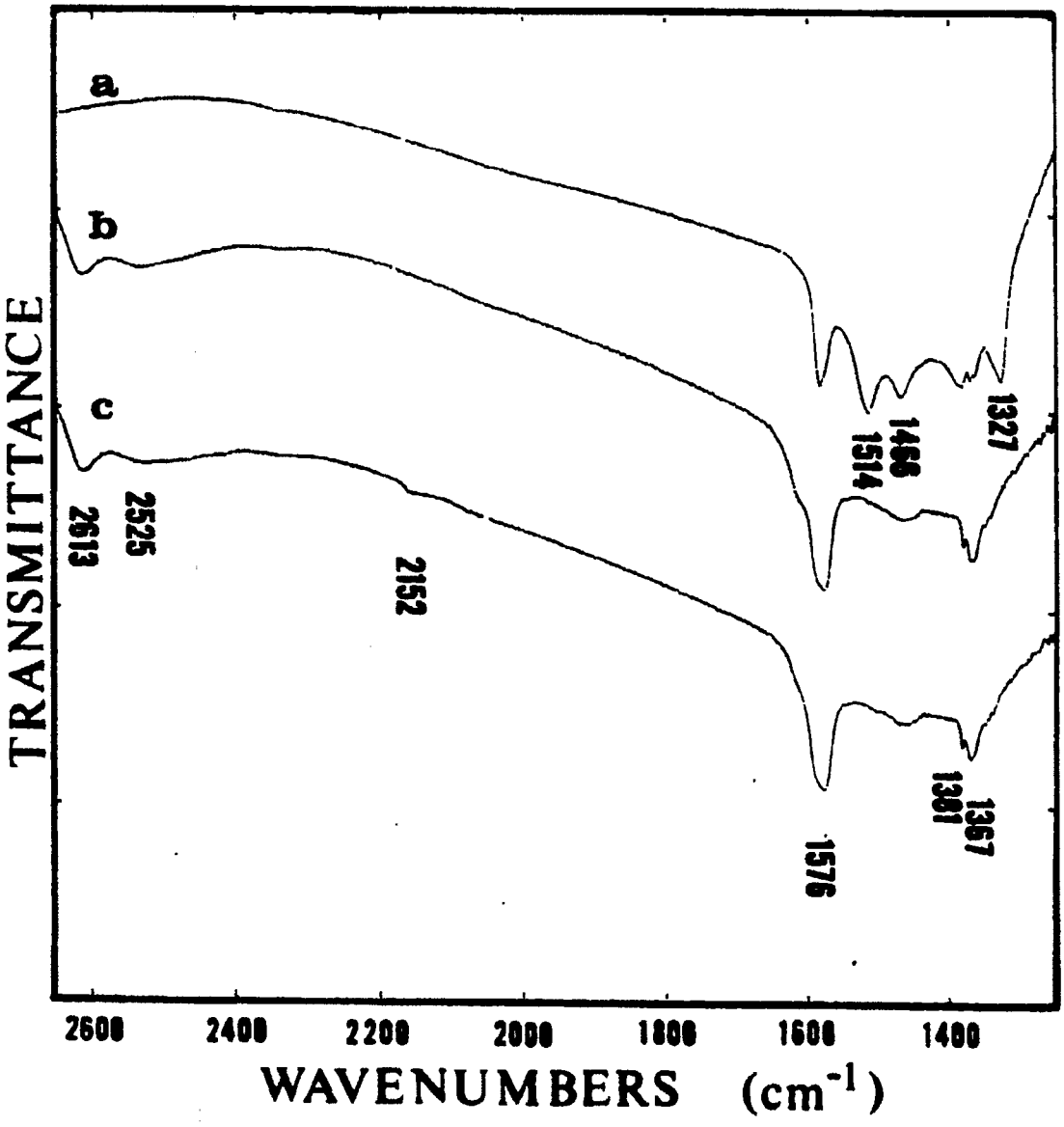

Figure 38. Continued

Figure 39. Adsorption of CD_3OD on 90/10 Zn/Cu oxide at 130°C

a) reduced surface

b) exposure for 5 minutes

c) exposure for 1 hour

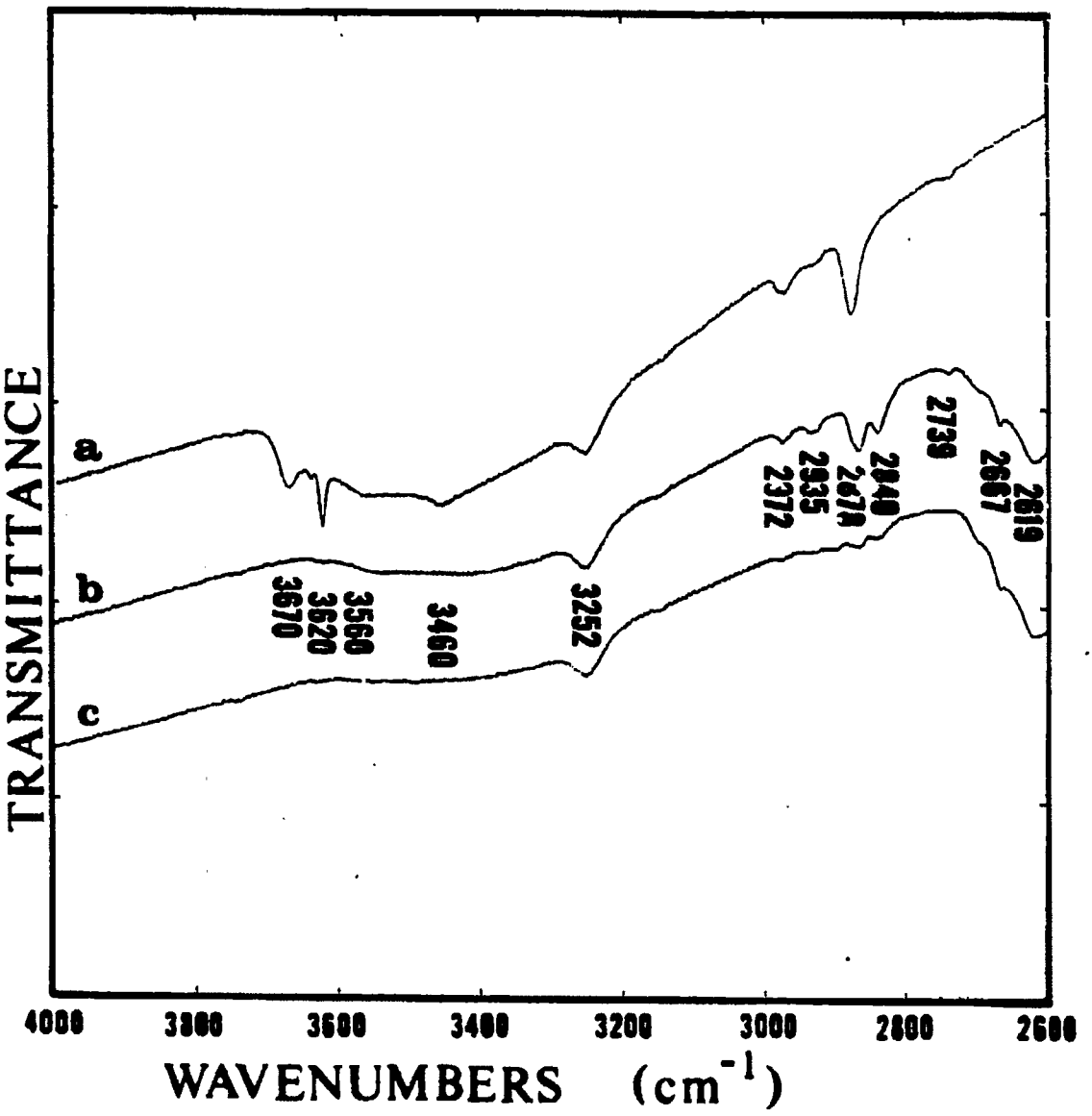
TRANSMITTANCE
a
b
c
3670
3620
3560
3490
3252
2372
2335
2278
2140
2739
2667
2610
4000
3800
3600
3400
3200
3000
2800
2600
WAVENUMBERS (cm-1)

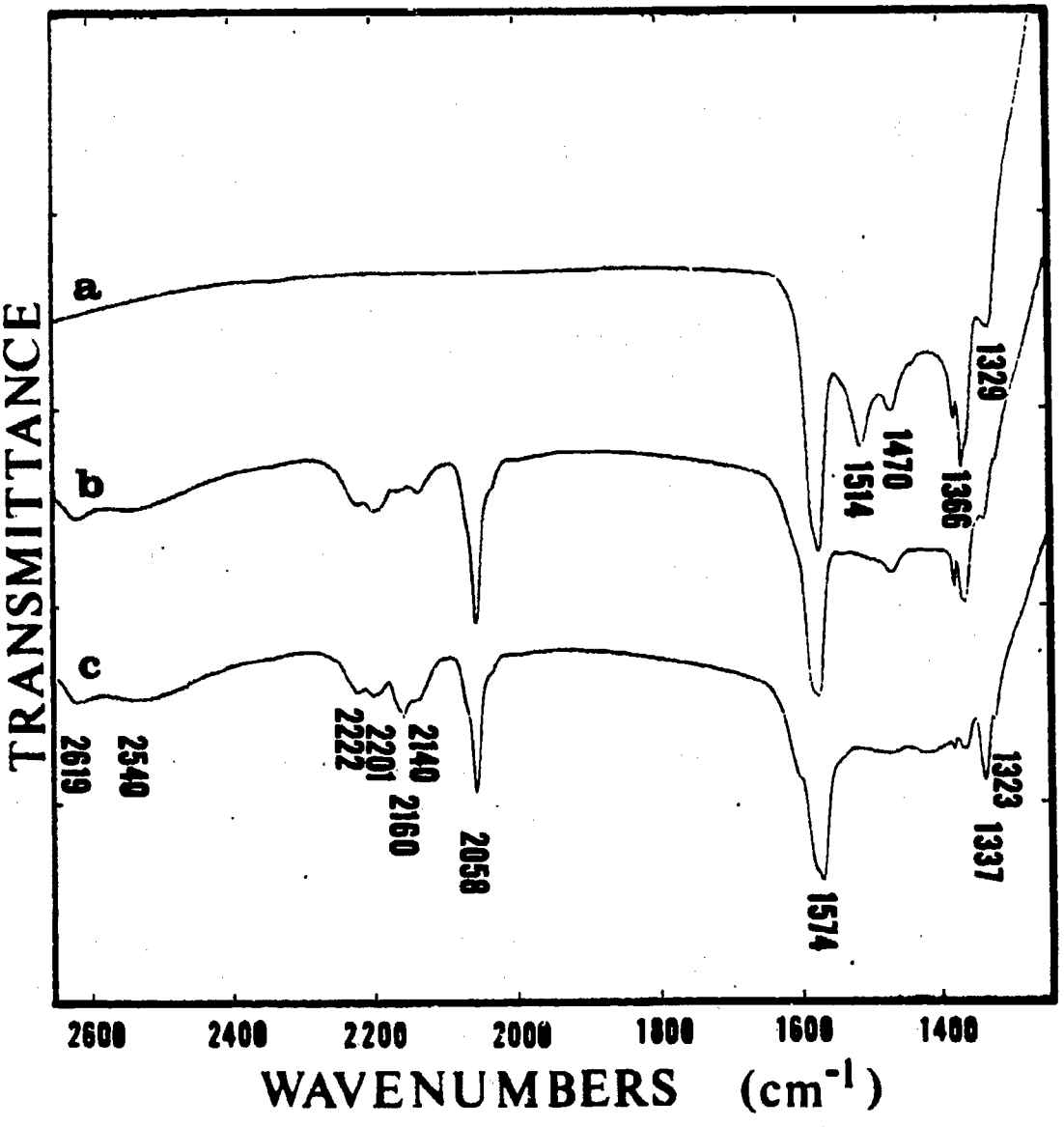

Figure 39. Continued

were shifted or displaced. The formate was diminishing while it appeared an adsorbed formaldehyde species (bands at 2935 and 2840 cm^{-1}) was temporarily formed. Both the formate and adsorbed formaldehyde species eventually disappear. Deuterated formate species (bands at 2160, 1574, and 1337 cm^{-1}) developed as the formate decreased, indicating that exchange between deuterated and hydrogenated species occurred readily.

The effect of methanol adsorption in an oxidizing environment was determined by exposing a reduced 95/5 Zn/Cu catalyst (pretreatment #3) to a methanol-water mixture (20% CH_3OH) at 150°C and 1 atmosphere (Figure 40). Initially, methoxy (bands at 2934 and 2818 cm^{-1}) and formate (bands at 2972, 2878, 1576, 1381, and 1364 cm^{-1}) groups developed with some indication of an adsorbed formaldehyde species (band at 2845 cm^{-1}) also present. The isolated hydroxyl groups (bands at 3666 and 3620 cm^{-1}) were greatly diminished but had not disappeared. After an hour, the surface species were essentially the same as the initial adsorbed species.

Adsorption on Ternary Oxides

The zinc-copper-aluminum oxide catalysts were satisfactory for transmission infrared studies in the fully oxidized state, but became nearly opaque when reduced in hydrogen. This class of catalysts could not be investigated. The zinc-copper-chromium oxide catalysts maintained good transmittance in both the oxidized and reduced states. Results obtained from this class of catalysts were better than some of

Figure 40. Adsorption of CH_3OH-H_2O mixture on 95/5 Zn/Cu oxide at 150°C

a) reduced surface

b) exposure for 5 minutes

c) exposure for 1 hour

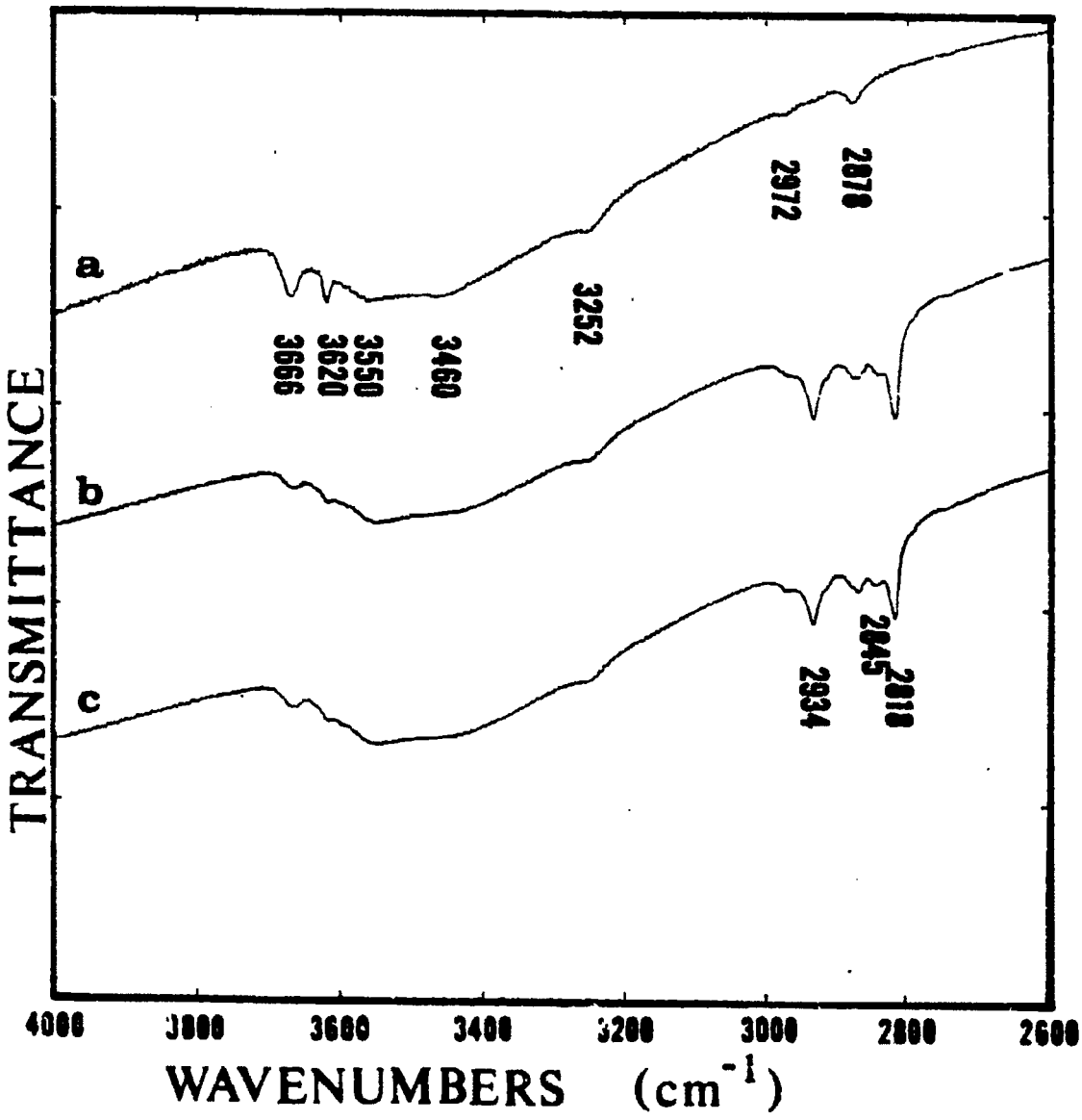
a
b
c
3699
3620
3550
3460
3252
2972
2878
2934
2845
2818
TRANSMITTANCE
4000
3800
3600
3400
3200
3000
2800
2600
WAVENUMBERS (cm-1)

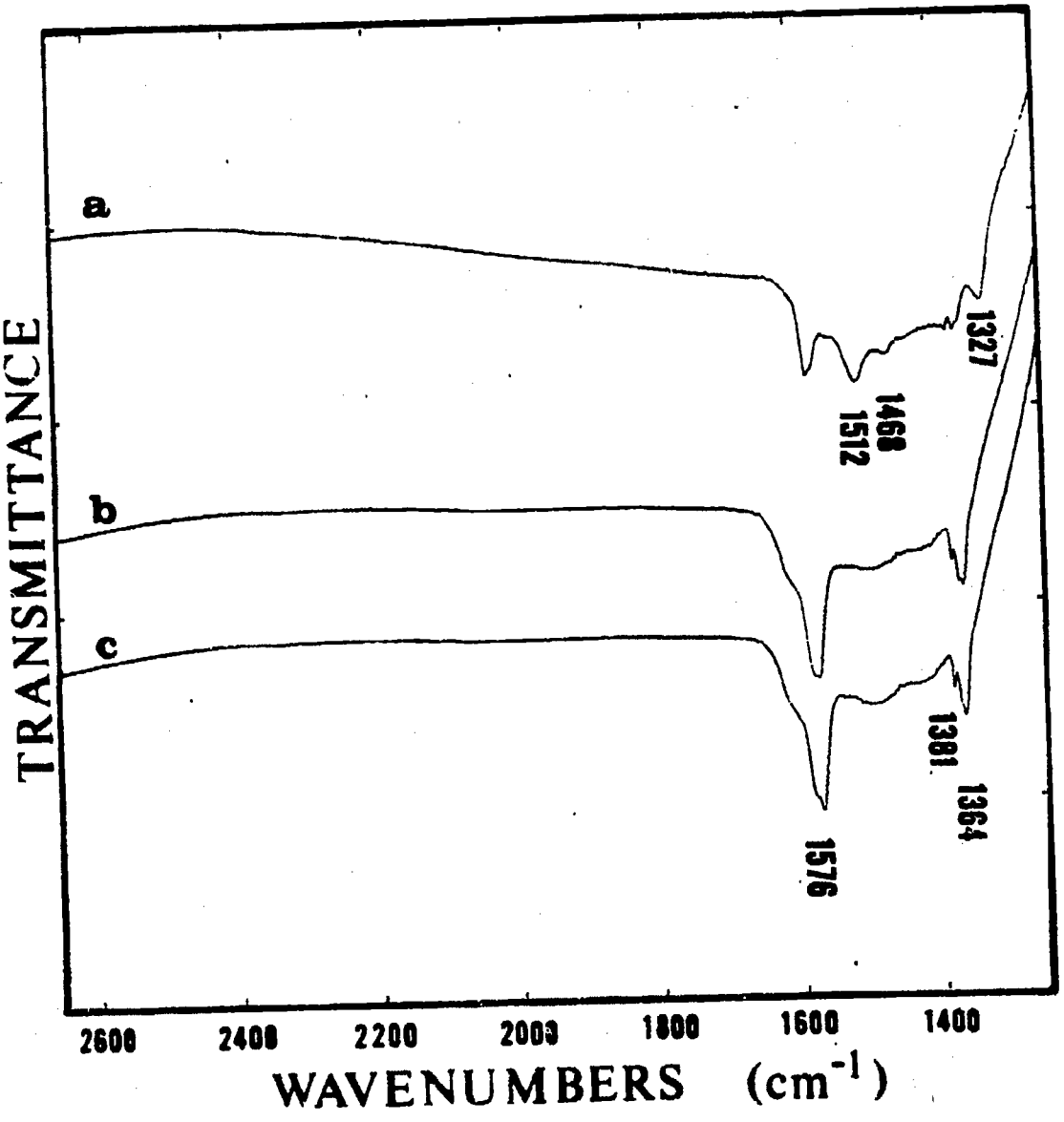

Figure 40. Continued

the information collected from the binary catalysts because the transmittance was always good over the entire wavenumber region. The catalysts used in this investigation had compositions of 90/5/5 and 80/10/10 Zn/Cu/Cr oxides which were reduced in a 5% H_2-95% N_2 mixture (pretreatment #3) prior to all adsorption studies.

The adsorption of carbon monoxide and hydrogen ($H_2/CO = 2/1$) on 90/5/5 and 80/10/10 Zn/Cu/Cr catalysts at 200°C and 1 atmosphere is shown in Figures 41 and 42, respectively. The residual hydroxyl groups (bands at 3666, 3620, and 3480 cm^{-1}) and the hydroxyl species at 3252 cm^{-1} were not very distinct on these ternary compositions; band intensity decreased with increasing chromium content. The behavior of adsorbed species on each catalyst was quite similar. The initial exposure to the mixture produced the carbonyl species (band at 2087 cm^{-1}) and a formate group (bands at 2964, 2872, 1576, 1381, and 1360 cm^{-1}). The surface carbonates (bands at 1510, 1433, and 1323 cm^{-1}) gradually disappeared. Methoxy groups (bands at 2932 and 2820 cm^{-1}) developed more quickly on the 90/5/5 Zn/Cu/Cr catalyst than the 80/10/10 Zn/Cu/Cr catalyst.

The transmittance of these ternary catalysts during the adsorption of formic acid solution (88% HCOOH, 12% H_2O) did not decrease sufficiently to prevent detection of adsorbed species, unlike the binary catalysts. Formic acid adsorption on 90/5/5 Zn/Cu/Cr and 80/10/10 Zn/Cu/Cr catalysts at 200°C and 1 atmosphere is shown in Figures 43 and 44, respectively. An adsorbed formate species (bands at 2964, 2872, 1576, 1381, and 1360 cm^{-1}) and gaseous carbon dioxide (band at 2350 cm^{-1}) can be seen in the spectra when formic acid was in the gas phase. A band in the 1985-1992 cm^{-1} region on 90/5/5 Zn/Cu/Cr oxide

Figure 41: Adsorption of CO-H_2 mixture on 90/5/5 Zn/Cu/Cr oxide at 200°C

a) reduced surface

b) exposure for 5 minutes

c) exposure for 1 hour

d) exposure for 8 hours

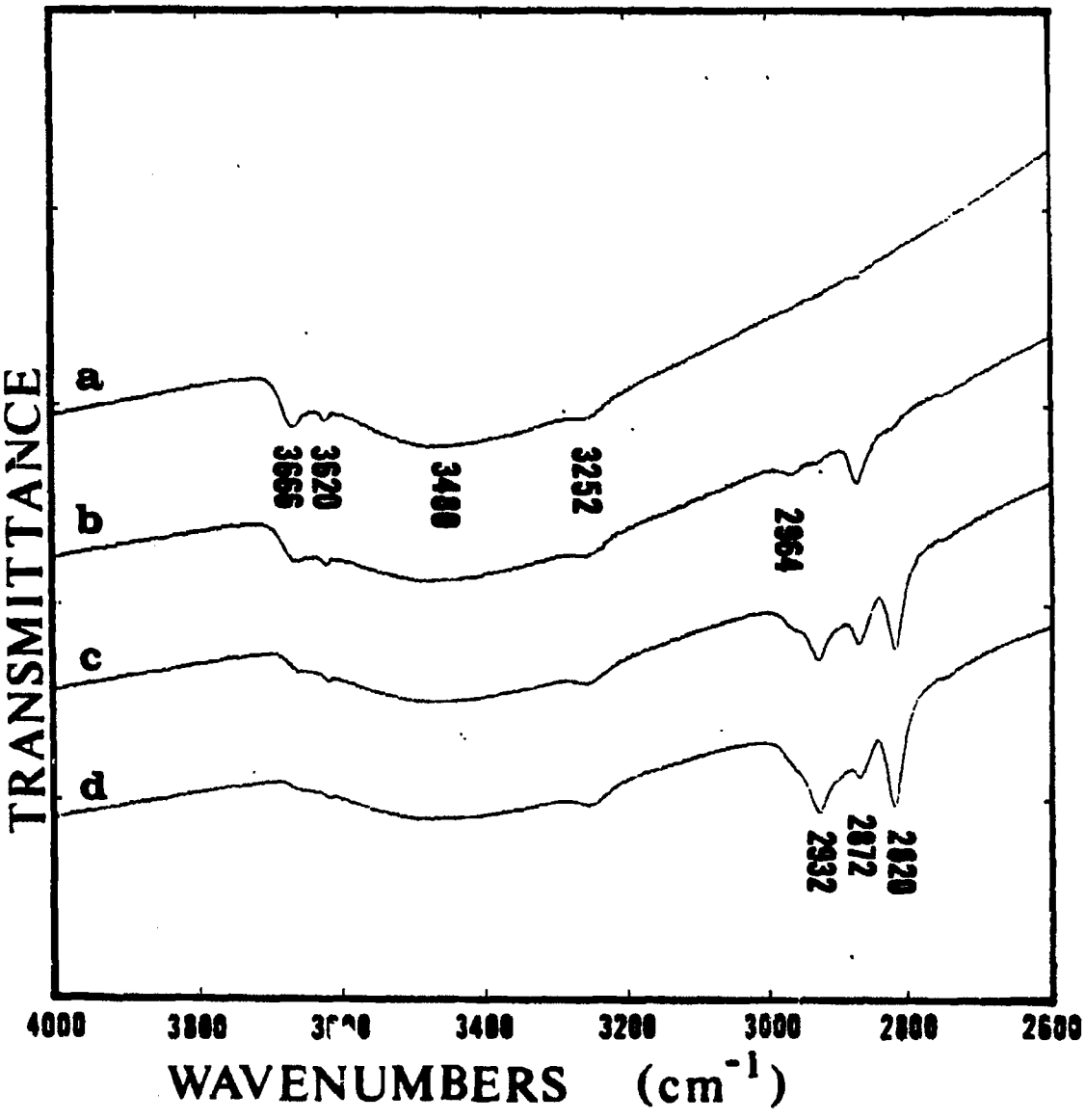
TRANSMITTANCE
a
b
c
d
3656
3520
3400
3252
2964
2932
2872
2820
4000
3800
3600
3400
3200
3000
2800
2600
WAVENUMBERS (cm-1)

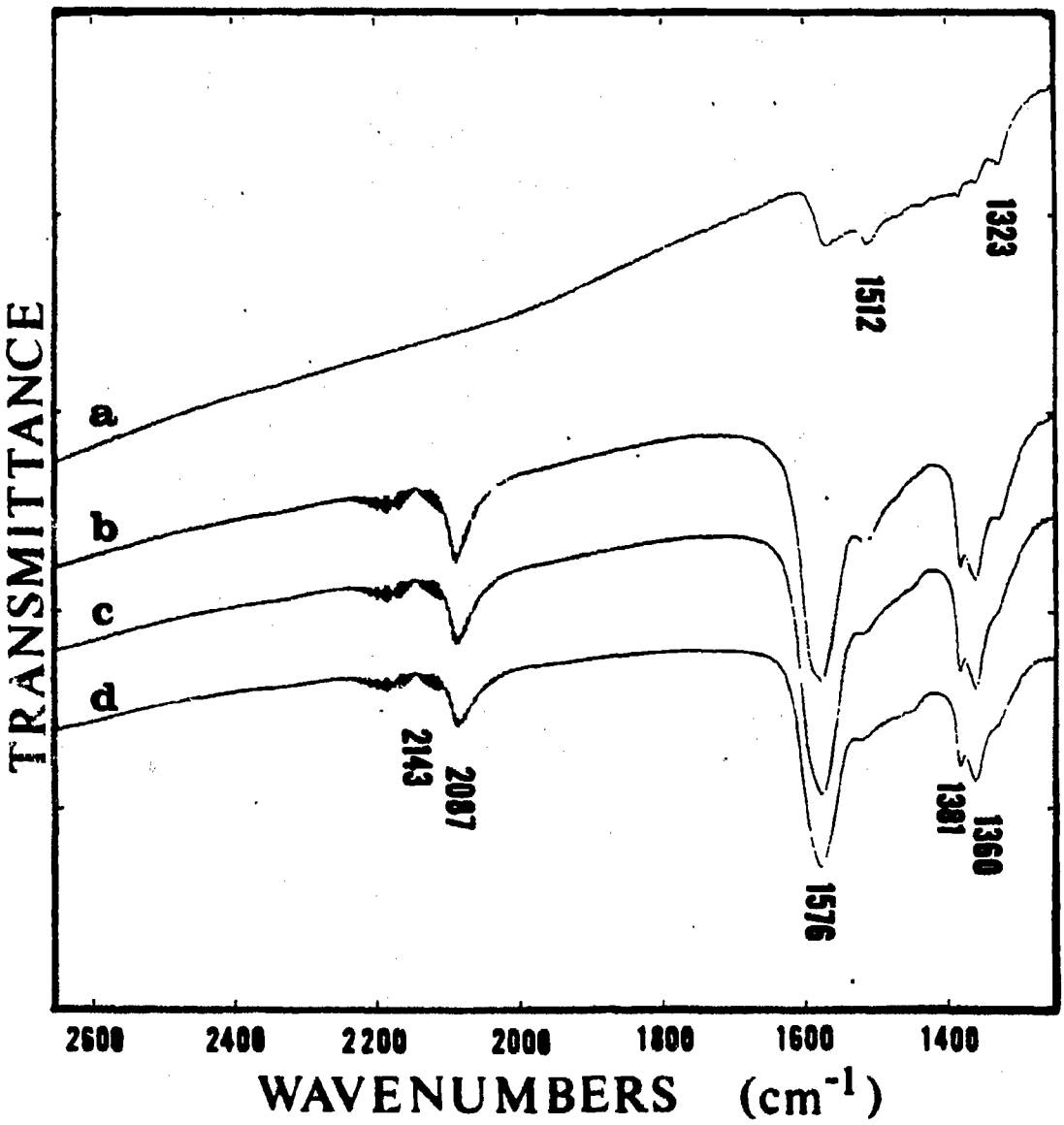

Figure 41. Continued

Figure 42. Adsorption of CO-H_2 mixture on 80/10/10 Zn/Cu/Cr oxide at 200°C

a) reduced surface

b) exposure for 5 minutes

c) exposure for 1 hour

d) exposure for 8 hours

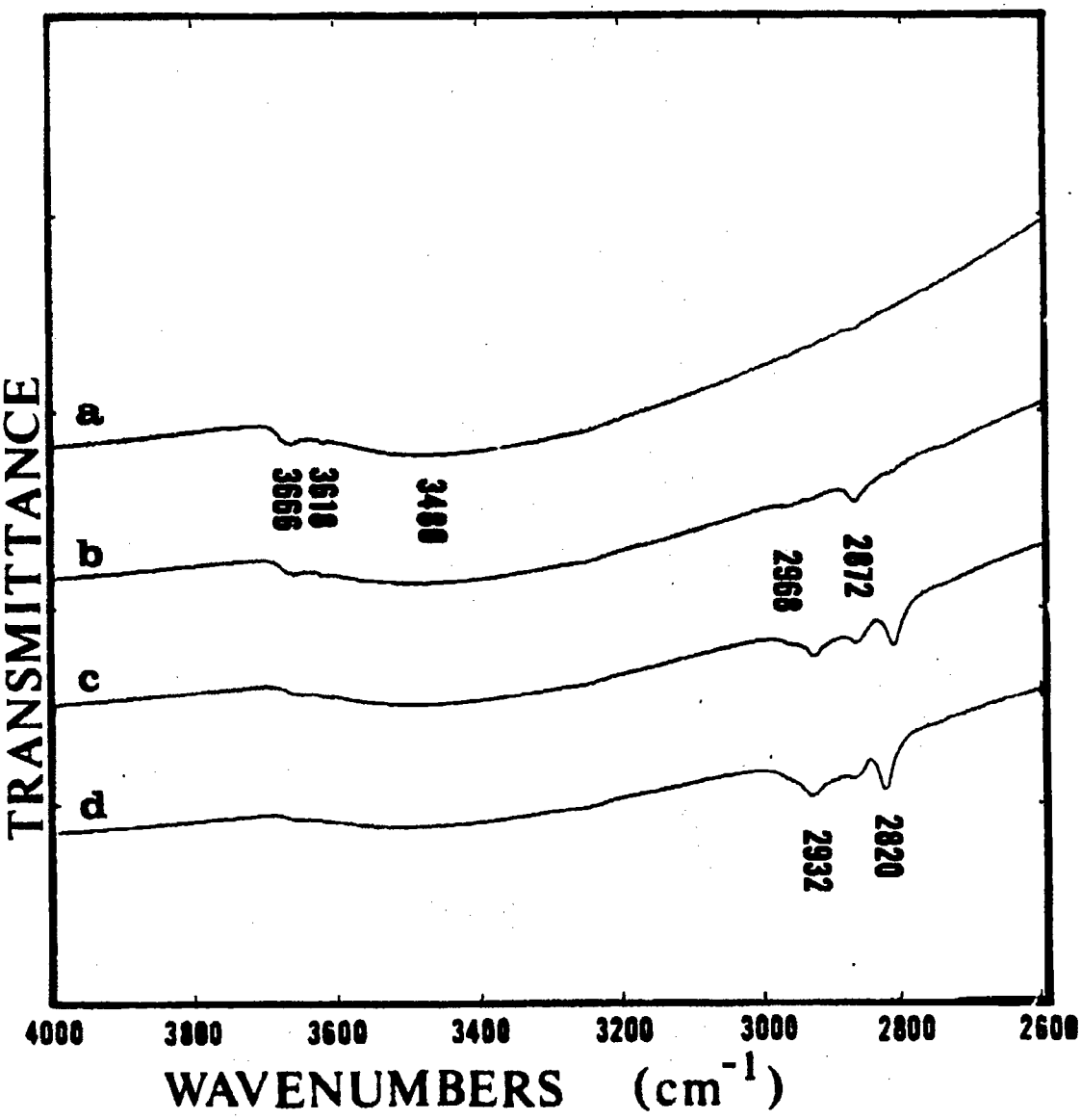
TRANSMITTANCE
a
b
c
d
3610
3666
3400
2968
2872
2932
2820
4000
3800
3600
3400
3200
3000
2800
2600
WAVENUMBERS (cm-1)

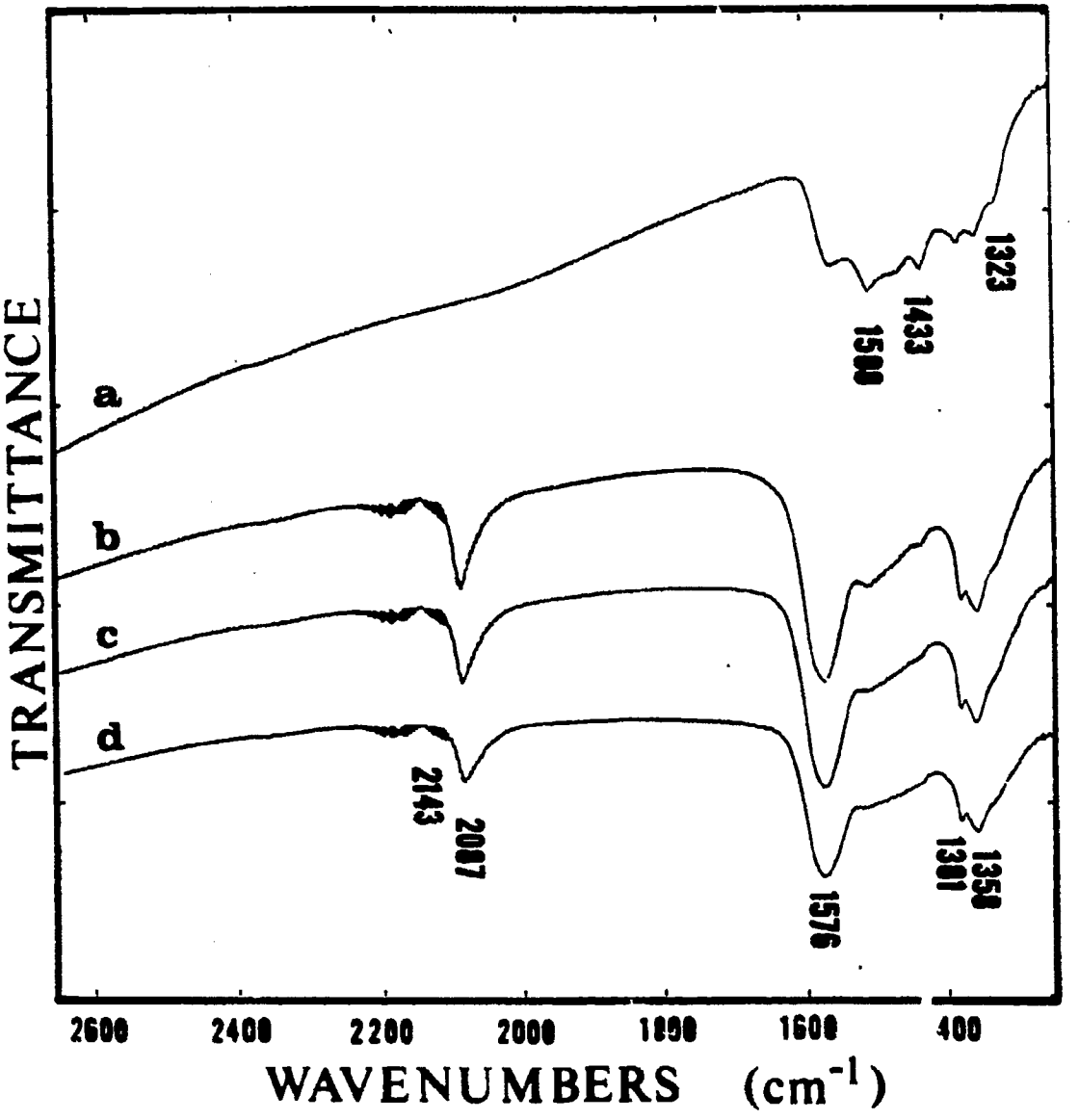

Figure 42. Continued